On the gas exchange and isofluxes of New Zealand mosses

A thesis

submitted in fulfilment

of the requirements for the degree

of

Master of Science (Research) in Ecology and Biodiversity

at

The University of Waikato

by

Tania Zi Xin Ng

2023

Abstract

The stable isotopic composition of plant tissue reflect biophysical and biochemical processes that occur during water uptake and cellulose synthesis. Stable isotope techniques in plant science have primarily focused on vascular plants; however, there is a growing interest in the stable isotopic composition of nonvascular plants, especially for paleoclimate reconstruction. The stable carbon isotopic composition of plant organic matter provides information of when a plant was photosynthetically active, while the stable oxygen isotopic composition can infer the environmental conditions that favoured photosynthesis. Presently, little is known about the relationship between the stable oxygen isotopic composition of moss tissue and the environment due to the complexity of the isotopic fractionation processes involved. This thesis offers insight on the oxygen isotopic composition of moss tissue and phyllid water through three separate studies and addresses the possible isotopic fractionation processes that may influence the stable isotopic composition observed.

The first study investigated the oxygen isotopic composition of evaporated water from two species of moss: *Ptychomnion aciculare* and *Dawsonia superba*. Measurements of on-line gas exchange and the isotopic composition of vapour water from the mosses were taken. Two oxygen isotope theories were applied to explain the observed oxygen isotopic composition of evaporated water. The first isotope theory was Rayleigh's distillation theory, often used to describe the oxygen isotope variation observed in the global hydrological cycle. The second theory was the modified Craig–Gordon model, often applied to isotopic enrichment in vascular leaves. The results highlighted how the anatomical differences of the phyllid structure influences the isotopic composition of evaporated and transpired water.

The second study interpreted the stable carbon and oxygen isotopic composition of *D. superba* stems. This involved taking 10 mm transverse sections along the stem and analyzing the isotopic composition of each section. The results from the carbon isotope analysis indicated that the carbon isotopic composition was more depleted at the base of stem compared to the tip, suggesting soil respiration, rather than atmospheric CO_2, was the primary factor influencing the isotopic composition of the stem. Additionally, analyses of the stable oxygen isotopic composition of *D. superba* stem indicated seasonal

variations that coincided with the seasonal shifts in the oxygen stable isotopic composition of precipitation.

The final study investigated the relationship between the isotopic composition of *Sphagnum cuspidatum* bulk tissue and the oxygen isotopic composition of source water was investigated under laboratory settings. The oxygen isotopic composition of moss tissue is theorized to reflect the oxygen isotopic composition of source water, offset by the biochemical fractionation constant. Four sealed growth chambers were set up and the mosses were watered with different isotopically labelled water for 6 months. *S. cuspidatum* was harvested, dried, and analyzed for the stable isotopic composition. The results indicated that oxygen isotopic composition of moss tissue increased by 0.17‰ for every 1‰ increase in source water, a relationship much lower than predicted by the theory. This suggested that the isotopic composition of moss tissue reflects an equilibrium process between source water and the vapour from atmospheric air.

These studies contribute theoretical and practical advancements in understanding the relationship between moss stable isotopes and the environment. The research here demonstrated the relationship between the oxygen isotopic composition of moss bulk tissue to the oxygen isotopic composition of precipitation and water sources, in both field and laboratory settings. They also provide insight into how the physiology and anatomy of moss phyllids influence the observed isotopic composition fixed in organic material.

Acknowledgements

序言

致妈妈，爸爸，婆婆，姨妈，姨丈。我的论文写完了！！

感谢姨媽和姨丈，感谢你们帮忙带大我，感谢你们在我成长过程中教给我所有人生的课程。谢谢你们和我一起庆祝我每一次成功的时刻。

致婆婆，感谢您从中国搬到新西兰带大我和我的兄弟姐妹。谢谢你为我做的每一餐饭菜。您一生致力于抚养我们，并为我们提供了我们所希望的最美好的童年。

最后，送给爸爸妈妈。感谢您们为确保我们过上美好的生活而做出的所有牺牲。你们努力工作给了我们所有你在成长过程中没有的机会。你们把所有的重担都扛在肩上，所以我们都不必面对任何困难。因为你，我们过上了奢华的生活。感谢您们对我的信任并鼓励我继续深造。由于您们的辛勤工作、爱、支持和奉献，我们现在都取得了成功。是时候停止工作了，我们会照顾您的！

我的根基建立在你的牺牲之上。

This thesis reflects not only the wonderful physiology of mosses, but also the love and support from everyone around me.

First, I would like to thank my supervisor, Prof. Margaret Barbour. I am so grateful for the opportunity to work with you and learn from you. Your knowledge and passion for plant science is truly inspiring! Thank you for your endless encouragement, enthusiasm, and for believing in me, even when I doubted myself. I appreciate the time you've taken out of your very busy schedule to explain complicated isotope theories to me, and for going over my results and drafts with me. And most importantly, thank you for fostering and nurturing my newly found interest in mosses and stable isotopes!

I wish to extend my gratitude to Mike Clearwater, for introducing me to the wonderful world of plants and for providing me with the first stepping stones towards my career as an aspiring plant scientist. Without you, I probably wouldn't be where I am today.

To Dani Le Lierve, for her knowledge around the lab, and making sure I had what I need to finish this thesis. Thank you for coming out onto the field with me and for driving the ute. I am thankful that you were so organised and eager to hunt down *Dawsonia superba* with me.

This thesis would not be what it is today without the students from the Plant Physiology lab at the University of Waikato – Stevie Noe, Joana Unteregger, and Moari West. I thank each of you for all the stories and quick walks down the hall to the tea room. It's been a blast combining brains and solving problems together. And I would not have finished this thesis without the friendship from Milena Janke, and René Devenish. I could not thank them enough for all the laughter and mental meltdowns we've gone through together while finishing our theses. What a wild ride.

To Matija Đurić, Reza Sajeed, and Tyller McCulloch for letting me just be me and for providing the best source of laughs. I would like to specially thank Nemanja Poznanović, for not only being a good friend, but for explaining all the random maths questions I ask, even when I don't give context. You have singlehandedly saved me from many hours of confusion and headaches.

To my dear friend, Emma Appleton. I truly appreciate all the love and support you've given me over the years. Thank you for celebrating every success and for listening to all the minor inconveniences I get myself into. I'm so proud of the woman you've become and I know you're going to do big and meaningful things in the future! I look forward to growing old with you.

To Mead Blackmore, for all the dinners you've cooked and for letting me choose the movie and then go home just as things were getting interesting. I promise to stay for a whole movie one day!

To Sayuri Pomare, Darren Pomare, and Kun-Ka Leger-Yoshihara. Thank you for welcoming me into your family with wide open arms. To Shokei Leger-Yoshihara, your love and support has kept me sane in my frantic moments. Thank you for your unconditional love, words of encouragement, and providing me a safe place to just exist. I am undoubtedly a better person because of you.

I want to thank my family for their support. To Jamie Ng, for his patience and understanding. To Ada Lin, Cherry Lin, and Sarah Ng. I thank the three of you for always picking up my phone calls at the most random times and just having a conversation with me.

And to my little brother, Brandon Ng. Your work ethics were the inspiration behind this thesis. You have a heart of gold, and you are definitely the light of the family. I am forever grateful to have you by my side. Thank you for never doubting me for a moment. I thank you for all that you've done, not only for me, but for everyone you love. My achievements – past, present, and future, will always be yours.

Lastly, to my parents Ng Yue Yee and Ng Muk Fat, and my grandparents Shen Qi Zhi and Tang Yao Hang, for raising and shaping me into who I am today. They provided me with the opportunities they could have only wished for growing up. I am where I am today because of all the sacrifices each of you have made.

Table of Contents

List of Figures

List of Tables

List of Symbols and Abbreviations

α^+	Effective temperature fractionation factor ($\alpha^+ > 1$)
a_κ	kinetic fractionation factor ($\alpha_\kappa > 1$)
Δ	Isotopic discrimination (‰)
$\delta^{13}C$	Carbon isotopic composition (‰)
$\delta^{13}C$	Carbon isotopic composition (‰)
$\delta^{13}C_{BULK}$	Carbon isotopic composition of organic bulk tissue (‰)
$\delta^{13}C_{BULK}$	Carbon isotopic composition of organic bulk tissue (‰)
$\delta^{13}C_P$	Carbon isotopic composition of the plant (‰)
$\delta^{18}O_{BULK}$	Oxygen isotopic composition of organic bulk tissue (‰)
$\delta^{18}O_P$	Oxygen isotopic composition of the plant (‰)
$\Delta^{18}O_v$	Oxygen isotopic composition of atmospheric vapour, relative to source water (‰)
$\delta^{18}O$	Oxygen isotopic composition (‰)
$\delta^{18}O_C$	Oxygen isotopic composition of cellulose (‰)
$\delta^{18}O_e$	Oxygen isotopic composition at the leaf evaporative site (‰)
$\delta^{18}O_E$	Oxygen isotopic composition of transpired water (‰)
$\Delta^{18}O_{es}$	Oxygen isotopic composition of leaf water at the sites of evaporation, relative to source water (‰)
$\delta^{18}O_L$	Oxygen isotopic composition of leaf water (‰)
$\delta^{18}O_{PRECIP}$	Oxygen isotopic composition of precipitation (‰)
$\delta^{18}O_{SW}$	Oxygen isotopic composition of source water (‰)

$\delta^{18}O_v$	Oxygen isotopic composition of vapour (‰)
δD	Deuterium isotopic composition (‰)
ε^+	Kinetic fractionation factor (= $\alpha^+ + 1$)
ε_{bio}	Biochemical fractionation factor (‰)
ε_k	Equilibrium fractionation factor (= $\alpha_k + 1$)
Γ^*	CO_2 compensation point in the absence of dark respiration (μmol mol^{-1})
A_L	Transpiring leaf surface (m^2)
C_A	Concentration of water in ambient air flowing into leaf chamber (mol m^{-3})
C_C	Concentration of bulk water vapour in the leaf chamber (mol m^{-3})
C_M	Concentration of water in mixed air entering the oxygen vapour analyser (mol m^{-3})
E	Leaf transpiration rate (mol m^{-2} s^{-1})
e_a	Water vapour of ambient air (mol fraction)
e_i	Water vapour of intercellular space (mol fraction)
$e_{s(T)}$	Saturation vapour pressure with temperature (kPa)
f	Proportion of water remaining after removal by phase change
g_b	Boundary layer conductance (mol m^{-2} s^{-1})
g_s	Stomatal conductance (mol m^{-2} s^{-1})
h	Humidity at leaf temperature (= w_a/w_i)
k	Carboxylation efficiency (= V_C/C_C)
l_b	Relative biochemical limitations to photosynthesis (%)
l_m	Relative mesophyll limitation to photosynthesis (%)

p_a	Atmospheric CO_2 pressure (μmol mol^{-1})
p_i	Intercellular CO_2 pressure (μmol mol^{-1})
q_A	Flow rate of ambient air into leaf chamber (m^3 s^{-1})
q_M	Flow rate of mixed air entering oxygen vapour analyser (mol m^{-3} s^{-1})
R	Isotopic ratio
R_A	$^{18}O/^{16}O$ isotopic ratio of ambient air
R_C	$^{18}O/^{16}O$ isotopic ratio of water vapour inside the leaf chamber
R_d	Day respiration rate (μmol mol^{-2} s^{-1})
R_{ev}	$^{18}O/^{16}O$ isotopic ratio at the evaporative site
R_L	$^{18}O/^{16}O$ isotopic ratio of transpired leaf water
R_M	$^{18}O/^{16}O$ isotopic ratio of well-mixed water vapour
R_{sample}	Isotopic ratio of the sample
$R_{standard}$	Isotopic ratio of the standard
T	Leaf temperature (°C, unless stated otherwise)
t	Time (seconds, unless stated otherwise)
V_C	Volume of bulk water inside the leaf chamber (m^3)
w_a	Ambient humidity (mol fraction)
w_i	Humidity inside the leaf at the site of evaporation (mol fraction)
C–G	Craig–Gordon model
PDB	Pee Dee Formation
RH	Relative humidity (%)
RubDP	Ribulose 1,5-diphosphate

RuBisCO	Ribulose-1,5-bisphosphate carboxylase/oxygenase
PGA	3-phosphoglyceric acid
VPD	Vapour pressure deficit
VSMOW	Vienna Standard Mean Ocean Water
WCC	Water conducting cells

Chapter 1
General introduction

The research here addresses how stable isotopes are used to understand the water-use strategy of mosses and how past water environments are resolved by analysing the oxygen stable isotope composition of moss bulk tissue. This study primarily investigates the use of stable oxygen isotopes, with a secondary analysis of stable carbon isotopes.

This chapter provides background information on the general morphological and physiological characteristics of mosses, with emphasis on how these traits relate to water use and uptake. In addition, definitions of stable isotopes will be described, along with the stable isotope theories that are relevant to plant science. Lastly, the aim and objectives, and thesis layout will be described at the end of this chapter.

1.1 Uniqueness of Bryophytes

Bryophytes were among the first plants to successfully colonise land 450-551 million years ago (Budke *et al.*, 2018; Turberville *et al.*, 2021), and are hypothesised to closely resemble the anatomical, morphological, and physiological characteristics of ancient terrestrial plants (Shaw & Renzaglia, 2004). Traditionally, the term “bryophytes” is used to describe a paraphyletic group of three distinct phyla — Anthocerotophyta (hornworts), Marchantiphyta (liverworts), and Bryophyta (mosses) (Shaw et al., 2011). Bryophytes are functionally different from vascular plants as they are dominant in the gametophyte generation, short in stature, and lack: a well-developed vascular system, a true root system capable of drawing water from the surrounding soil, and true leaves with mechanisms to regulate gas exchange and water loss (Proctor, 1982; Atala, 2011).

Like all plants, the life cycle of mosses are characterised by the alternation of generation (Fig. 1.1). The dominant life stage of mosses are the haploid gametophyte generation, which are long-lived and the more photosynthetically active generation (Hedderson & Longton, 1996). Mosses start their life cycle as spores with well-developed chloroplasts, capable of photosynthesis from the onset of emergence (Valanne, 1984). The spores bud and develop into filamentous complexes known as protonema comprised of chloronema cells, that then elongate to form caulonema cells (Schofield, 1981). The caulonema bud and differentiate into phyllids and give rise to leafy photosynthesising gametophores (Mishler, 2001). The moss sporophyte generation, on the other hand, are short-lived and produce spores only once (Hedderson & Longton, 1996). The sporophytes are attached to gametophytic shoots and depend on them for water and nutrients (Vitt, 1981). The sporophyte generation begins as a fertilized egg and eventually produces spores via meiosis in a terminal sporangium (Harrison & Morris, 2018). Eventually the sporophyte ceases to be photosynthetically active, and dries (Vitt, 1981). The spores of mosses are primarily dispersed through water (Hedderson & Longton, 1996), although some species may disperse their spores through insect dispersal (Lewis *et al.*, 2014).

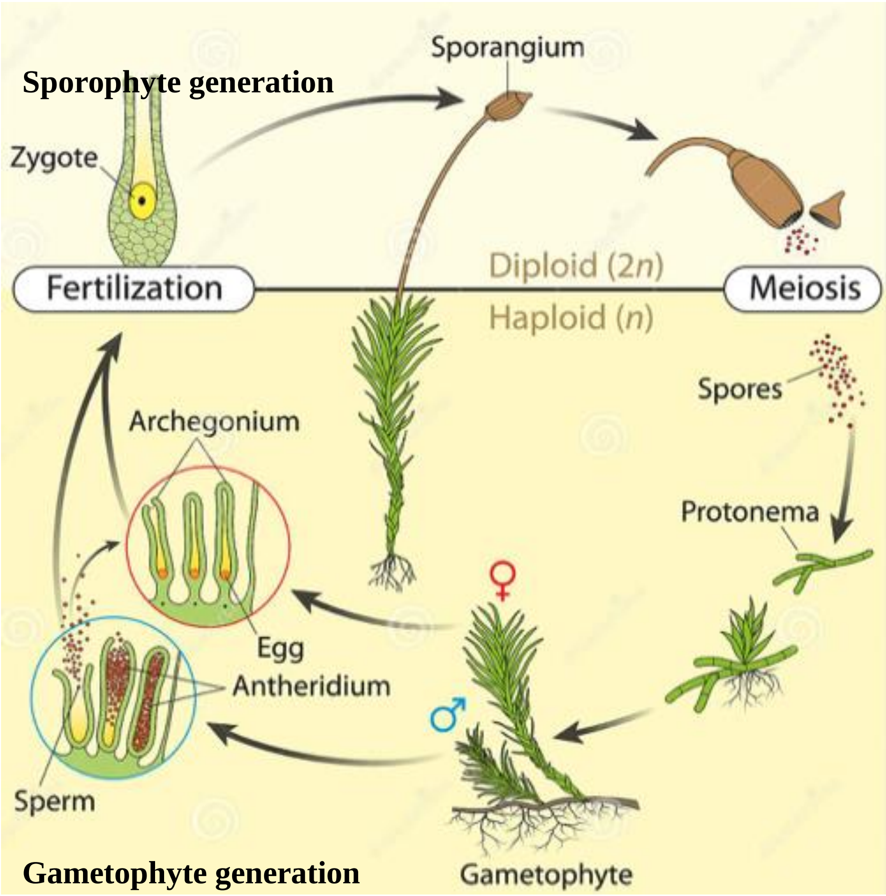

Figure 1.1. Illustrative diagram of the life cycle of a moss. The diploid sporophyte generation is short-lived and produces spores. In the gametophyte generation, the spore develops into filamentous complexes known as protonema. The protonema develops and differentiate into leafy photosynthetic gametophores (Image sourced from: https://www.britannica.com/science/alternation-of-generations).

Due to the physiology and life strategies of bryophytes, they can colonise environments with little soil and/or nutrients, low air temperatures, and irregular or unpredictable water avialablity – environments where vascular plants are commonly excluded from (Proctor et al. 2007). The simple life form of bryophytes enables them to survive in the harshest conditions, with extreme winds, temperature and droughts (Mishler, 2001).

1.2 The morphology of mosses

Bryophytes generally lack complex morphological and physiological structures (e.g, roots and stomata) that limit their active interactions with the environment. The body plan of mosses are organised into branching stem-like tissues (caulids), with leaf-like structures (phyllids) arranged spirally (Hedderson & Longton, 1996). Additionally, some mosses have filamentous rhizoids. The rhizoids' role is yet to be resolved, but the general consensus is that they function as an anchor to the substrate (Turberville *et al.*, 2021).

There are five main life forms mosses display: cushion, turf, mat, dendroid, and weft (Reski, 1997). Cushion mosses are most common in well-drained habitats where relative humidity is low, while dendroid mosses are found in habitats where relative humidity is high. Turf and mat (or carpet) mosses are not environmentally restricted and weft mosses are typically found on outcrops or on rock surfaces (Schofield, 1981; Reski, 1997; Huttunen *et al.*, 2018). Mosses are morphologically adapted to specific habitats, however studies have shown through experimental manipulation that mosses are to some degree phenotypically plastic, with the ability to alter their growth form to suit their environment (Schofield, 1981; Buryová & Shaw, 2013; Oke *et al.*, 2020). For example, a study by Oke et al (2020) investigated the wide range of morphological changes displayed in the carpet moss *Sphagnum magellanicum* in response to two major influences on life forms (Huttunen *et al.*, 2018): moisture and light availability. *S. magellanicum* are found both in hollows (where moisture availability is high) and in hummocks (away from the water table and often exposed to high irradiance). Oke et al (2020) observed the greatest change in hollow-originated plants transplanted to hummocks. Here, the hollow-originated plants changed from green to reddish pink and remained shorter in height (Oke *et al.*, 2020) However, genetic evaluations of *S. magellanicum* are required to conclude the changes Oke et al (2020) observed were changes driven by the environment, rather than local adaptations. The environment may fluctuate from a high water table to low multiple times over the life time of a moss (Greenwood *et al.*, 2019). The degree of plasticity partially determines the survival of an organism in a changing environment.

Since there are no regulatory systems in mosses to control water uptake and loss, their cellular water status is controlled by diffusion and surface absorption. Therefore, there are evolutionary pressures for moss organs to remain small and thin, and lignin is not necessary for support against gravity or the negative pressures generated during transpiration (Brodribb *et al.,* 2020).

1.3 Moss water relations

One of the greatest challenges for life in the above-ground environment is the availability of water. Water is essential for metabolism and reproduction for mosses, but often available in limited and sporadic supplies (Proctor, 1982). To maintain the positive water balance required for photosynthesis and growth, bryophyte tissues readily absorb water in the forms of precipitation, dewfall, or atmospheric water vapour when under conditions of high humidity (Royles *et al.*, 2014).

Mosses are often described as "poikilohydric" or "endohydric" (Budke *et al.,* 2018) based on their adaptations to water availability (Proctor & Tuba, 2002). The term "poikilohydric" is used to define mosses with no regulatory mechanisms against water loss, which results in leaf water often being equilibrated with the environments' water status (Proctor *et al.*, 1998; Xia *et al.*, 2020). In contrast, the term "endohydric" describes mosses with physiological adaptations that allow for some degree of water regulation (Thomas *et al.*, 1996). Endohydric mosses may be structurally complex, often having anatomical features analogous to the water related characteristics of vascular plants. However, it is important to view the adaptations to water supply on a scale, with different degrees of water regulation (Proctor & Tuba, 2002). Nevertheless, the ability or inability to regulate water largely determines the habitat mosses are found in, and their growth form (Mishler, 2001; Proctor, 2010).

1.3.1 Poikilohydric mosses

Poikilohydric mosses are generally simple in structure. The phyllids of poikilohydric mosses are typically composed of small narrow cells, with dense cellular contents and small vacuoles (Proctor *et al.*, 2007). The phyllids of poikilohydric mosses are readily wetted, and can expand within minutes from their dried state to their normal moist appearance on the addition of water (Proctor, 2000).

As a well-developed vascular system is absent in the poikilohydric moss body form, the movement of water must predominately rely on external capillary action (Proctor, 1982). The water conducting system of mosses is poorly developed (Valanne, 1984), and most of the water taken up by mosses occurs as dew, precipitation, or drops from the vascular canopy. Mosses can use facilitative interactions such as lateral movement of water externally across space, or vertical movement of water through their litter matrices as a means of responding to changes in their moisture environment (Oke *et al.*, 2020).

Additionally, poikilohydric mosses are often desiccation tolerant and can survive drying to a point where no liquid water remains in the cells, and where the water content decreases down to 5-10% (Green *et al.*, 2011; Dilks & Proctor, 2013). But upon remoistening, essentially normal metabolism returns within minutes or hours. This phenomenon is well documented in the highly desiccation-tolerant desert moss species *Tortula ruralis* (Proctor, 2000). *T. ruralis* has been recorded to remain desiccated for up to six years and recover to normal activity and growth within hours of rehydration (Proctor & Pence, 2002; Oliver *et al.*, 2005).

1.3.2 Endohydric mosses

The phyllids of endohydric mosses can be structurally complex (Thomas *et al.*, 1996; Proctor, 2013). An example of an endohydric moss family is the Polytrichaceae. Here, the phyllids consists of a broad midrib that makes up most of the phyllid width with closely spaced longitudinal rows of green mesophyll-like lamellae on the upper surface (Proctor, 2013). The whole structure is covered with a waxy cuticle that is hypothesized to keep water out, optimizing CO_2 diffusion and therefore increasing the photosynthetic capacity (Clayton-Greene *et al.*, 1985; Proctor, 2013). The waxy cover and ventilated lamellae of Polytrichaceae phyllids are the closest functional parallels to the leaves of vascular plants (Clayton-Greene *et al.*, 1985).

Furthermore, there are a few species of mosses that have convergently evolved alongside vascular plants, where some species can reach heights of 60 cm to ca. 1 m (Atala, 2011). In the tall moss genera such as *Dawsonia* and *Polytrichum*, water is internally conducted through water-conducting cells (hydroids) in the central strand (Brodribb *et al.*, 2020), and can move externally through the capillary spaces in the leaves (Proctor, 2000). Like tracheids and vessel elements of tracheophytes, the water conducting cells (WCCs) of mosses undergo programmed cytoplasmic lysis and lack cytoplasmic contents at maturity, but do not deposit lignin in their cell walls (Ligrone *et al.*, 2022). These WCCs have been regarded as analogous to the xylem of vascular plants as they function in transporting water around the plant (Proctor *et al.*, 1998).

These structural characteristics are frequently cited as the closest functional parallels of vascular plants (Clayton-Greene *et al.*, 1985), and are presented as evidence of parallel evolution of photosynthetic tissues of Polytrichaceae and higher plants (Thomas *et al.*, 1996). Furthermore, these characteristics have been concluded to contribute to the faster carbon assimilation and photosynthetic rates observed in Polytrichaceae (Clayton-Greene *et al.*, 1985; Brodribb *et al.*, 2007; Proctor, 2013).

1.4 Photosynthesis is strongly limited by water availability in mosses

There are potential limitations associated with carbon assimilation and the moss's adaptations to water loss (Proctor *et al.*, 2007). Rice and Giles (1996) demonstrated that CO_2 diffusion is four times slower through water than through free air. Because of the anatomical constraints of mosses, they are widely known to have low productivity and low photosynthetic capacity (Valanne, 1984). For poikilohydric mosses with thin phyllids, it is intuitive that they would be best adapted to function under low radiation as high irradiance leads to high evaporation (Proctor & Tuba, 2002). The response of photosynthesis to water content has been published for a number of species, from a wide range of habitats, including *Sphagnum acutifolia* (Williams & Flanagan, 1996), *Torula ruraliformis* (Seel *et al.*, 1992), and *Polytrichum commune* (Seel et al., 1992). Under environmental conditions where a high tissue-to-air vapour pressure deficit is established, surface water evaporates first, and the diffusive supply of CO_2 (and therefore photosynthetic rate), increases (Rice & Giles, 1996; Williams & Flanagan, 1996). As the evaporation of surface water continues, the tissues become desiccated and metabolism slows and eventually becomes inactive until water is available once again (Royles *et al.*, 2013a).

However, the rate of carbon assimilation and evaporation differs depending on the mosses' morphological features. Williams and Flanagan (1996) compared how changes in water content affected photosynthesis in two boreal moss species: *Sphagnum acutifolia* and *Pleurozium schreberi*. The results confirmed the general pattern of variation in net photosynthesis and water content, but found *Sphagnum* had a higher overall assimilation rate than *P. scheberi* as the tissues of *Sphagnum* were denser. Additionally, Krupa (1984) showed that moss phyllids with surface lamellae generally had higher photosynthetic rates than those without. It is suggested that the separation of lamellae rows allow for rapid diffusion of water vapour and CO_2 between the surface area of photosynthetic cells and the atmosphere (Brodribb *et al.*, 2020). These results emphasise the trade-off and relationship between moss physiology and water use strategy.

It has been debated whether moss photosynthesis is limited by the biochemical reactions (l_b), or by mesophyll conductance (g_m) (Perera-Castro *et al.*, 2022). The recent study by Perera-Casrro et al. (2022) explored the photosynthetic limitations in bryophytes. Using gas exchange measurements, g_m and l_b were estimated from curve-fitting models and the electron transport rate to compare whether mesophyll conductance or the biochemical reactions were the limiting factor. Measures of total chlorophyll concentration, total soluble protein and Ribulose-1,5-bisphosphate carboxylase/oxygenase (RuBisCO) content were taken to investigate the nature of biochemical limitations to photosynthesis (Perera-Castro *et al.*, 2022). Although there were some discrepancies with their results, biochemical limitations were likely to be the main limiting factor in moss photosynthesis.

1.5 Stable isotopes

Stable isotopes are atoms of the same number of protons and electrons, but with different number of neutrons (therefore different in atomic mass), and that do not decay or change over time. In nature, the two stable isotopes of carbon are ^{12}C and ^{13}C (Farquhar *et al.*, 1989b), where ^{12}C is the most abundant, making up 98.9% of the carbon and the remaining 1.1% being ^{13}C (Farquhar et al. 1989b). For oxygen, the naturally occurring stable isotopes are ^{16}O, ^{17}O, and ^{18}O. The most abundant oxygen isotope is ^{16}O, occurring in approximate concentrations of 99.74%, while ^{16}O and ^{18}O exist in approximate concentrations of 0.05% and 0.21% respectively (Barbour, 2007). Due to the uneven distribution within and among different compounds, investigating isotope ratios reveal details about the chemical, physical and metabolic processes involved in natural cycles (Peterson & Fry 1987; Farquhar et al. 1989a).

The isotopic composition (δ) is measured in units of parts per thousand (‰), relative to a known standard composition. δ ιs calculated as (Vogel, 1980; O'Leary, 1981):

$$\delta_X = [(R_{sample}/R_{standard}) - 1] \times 1000, \qquad [1.1]$$

where X is the element of interest (e.g., ^2H or D, ^{13}C, or ^{18}O), and R represents the abundance ratios of the heavy to light isotopes (e.g., D/H, $^{13}C/^{12}C$, and $^{18}O/^{16}O$) in the sample and the standard, respectively (Dawson et al. 2002).

The isotope composition of a sample is typically compared against a standard, as the absolute isotope composition is often difficult to measure directly (Farquhar et al. 1989b). For $^{13}C/^{12}C$, the standard is commonly the carbon dioxide produced from the reaction of Pee Dee Belemnite (PDB) with H_3PO_4, with the isotope ratio (R) of 1.124 x 10^{-2} (Craig, 1954). Since organic matter is always depleted in ^{13}C compared to PDB, the $\delta^{13}C$ values of organic samples are negative (O'Leary, 1981). A less negative value means the sample is richer in ^{13}C. The standard for $^{18}O/^{16}O$ is commonly Vienna-Standard Mean Oceanic Water (VSMOW) (Craig, 1957), where R is 2.0052 x 10^{-3} (Barbour, 2007).

Another way to express isotope effects is through the isotopic discrimination (Δ). Isotopic discrimination or enrichment represents the isotopic difference between a source and product (O'Leary, 1993). In the case of plants, the isotopic enrichment of plant tissue ($\Delta^{18}O_p$) above source water is understood as (Barbour, 2007):

$$\Delta^{18}O_p = \frac{\delta^{18}O_{SW} - \delta^{18}O_p}{1 + \delta^{18}O_{SW}}, \qquad [1.2]$$

Where $\delta^{18}O_{SW}$ is the oxygen isotopic composition of source water and $\delta^{18}O_p$ is the oxygen isotopic composition of the plant.

Stable isotopes provide natural markers for the environmental control of metabolic reactions (Farquhar *et al.*, 1989a; Dawson *et al.*, 2002). Analyses of the stable isotope composition preserved in tree rings (Poussart *et al.*, 2004) and peat cores (Ménot-Combes *et al.*, 2002; Royles *et al.*, 2012a) are widely used as environmental tracers that provide information about past growth conditions. More recently, the stable isotope composition of cellulose and source water have been used to quantify responses of mosses in remote areas to climate change (Royles *et al.*, 2013b; Royles & Griffiths, 2015).

1.5.1 Fractionation

Variation in the isotopic ratios are products of "isotope effects" (Farquhar *et al.*, 1989a). The isotope effect or isotope fractionation are the result of a physical, chemical, or biological change that alters the isotopic composition (O'Leary *et al.*, 1992). These processes are a mass-dependent phenomenon, caused by the physical and chemical processes that influence each isotope in a particular phase (Peterson & Fry, 1987). Isotope fractionations are often categorised as being kinetic or equilibrium/thermodynamic.

Kinetic fractionation occurs in unidirectional reactions and depends on differences in reaction rates and diffusion co-efficients of the molecule (Farquhar & Lloyd, 1993; O'Leary, 1993; Dawson *et al.*, 2002). For example, the kinetic fractionation for stable carbon isotopes can be expressed as (Farquhar & Lloyd, 1993):

$$a_k = \frac{k^{12}}{k^{13}}\ , \qquad [1.3]$$

where *k* is the diffusion coefficient for C^{12} and C^{13}.

In biological systems, the kinetic fractionation are usually catalysed by an enzyme that discriminates among the isotopes in a mixture, so that the substrate and product are isotopically distinct from one another at the end of the reaction (Dawson & Brooks, 2001). Since the chemical bonds formed with lighter isotopes are more readily broken, they tend to be more reactive and are likely to be concentrated in the product faster and more readily than the heavier isotope.

Equilibrium fractionation, on the other hand, occurs during the isotopic exchange between two separate phases (e.g., liquid to vapour) (Farquhar & Lloyd, 1993; O'Leary, 1993; Dawson *et al.*, 2002; Ellehoj *et al.*, 2013). Equilibrium fractionation describes the unequal distribution of isotopes between co-existing phases or molecules, explained by the quantum mechanical effect on the partition factors for the molecule/phase of interest (Dawson *et al.*, 2002; Gat, 2005; Ellehoj *et al.*, 2013). Equilibrium fractionation is often defined as the ratio between the forward and backwards reaction (Farquhar & Lloyd, 1993):

$$\alpha^{+} = \frac{R_A}{R_B}, \qquad [1.4]$$

This reaction represents the balance of two kinetic fractionation processes at a chemical equilibrium and is generally smaller than individual kinetic effects (Farquhar *et al.*, 1989a). All equilibrium fractionation are temperature dependent, while only some kinetic fractionations depend on temperature (Farquhar *et al.*, 1982).

1.6 ^{13}C fractionation during photosynthesis

During photosynthetic gas exchange, the carbon isotope ratio ($^{13}C/^{12}C$) in plant organic matter differs to the carbon isotope ratio of source CO_2 (O'Leary, 1988; Farquhar *et al.*, 1989a). The two greatest fractionation factors that influence the total carbon discrimination of organic plant material occur during the biochemical fixation of atmospheric CO_2 by Ribulose-1,5-bisphosphate carboxylase/oxygenase (RuBisCO), and the bidirectional diffusional fractionation of CO_2 between the chloroplast and the atmosphere (Vogel, 1980). These two processes discriminate against the heavier CO_2 ($^{13}CO_2$), resulting in plants containing less ^{13}C than the atmosphere (O'Leary, 1988).

The fractionation that influences the carbon isotope ratio of plants can be further broken down and described as (Vogel, 1980; Lloyd & Farquhar, 1994)

i. The diffusion of $^{13}CO_2$ across the boundary layer to the leaf surface
ii. Diffusion through the stomatal apertures and the intercellular spaces to the boundary of mesophyll cells

iii. Diffusion through mesophyll plasma membrane and cytoplasm to the chloroplasts

iv. Initial step of carboxylation in the stroma where $^{13}CO_2$ is fixed to ribulose 1,5-diphosphate (RubDP) to yield 3-phosphoglyceric acid (PGA)

Since diffusion of CO_2 are driven by concentration gradients from the air to the intercellular space, the isotopic discrimination for C_3 plants can be expressed as (O'Leary, 1993):

$$\Delta^{13}C = [a + (b - a) \cdot p_i/p_a - d], \quad [1.5]$$

where α represents the discrimination due to diffusion, *b* is the discrimination caused by carboxylation, p_i is the intercellular gas-phase pressure of CO_2, p_a is the atmospheric CO_2 pressure, and *d* includes the fractionation associated with photorespiration and respiration, and carbon export included in the fractionation factor *b* (O'Leary, 1993).

The isotopic fractionation processes that occurs during CO_2 diffusion are fundamentally different for mosses compared to vascular plants due to the lack of stomata. Hence, fractionations associated with ii above are absent in mosses. The total resistance to CO_2 diffusion is the sum of the atmospheric boundary layer resistance and the internal resistance (Proctor, 1982). However, moss $\delta^{13}C$ values are comparable to those found in C_3 vascular plants (see Proctor (1992) for table of values), indicating broadly similar diffusive (i and iii above) and biochemical limitations on the rate of carbon uptake (Proctor *et al.*, 1992).

As indicated above, ^{13}C is discriminated against during carboxylation by RuBisCO because of the lower reactivity of ^{13}C relative to ^{12}C (Farquhar *et al.*, 1982). This is expressed in C_3 plants as having a $\delta^{13}C$ approximately 20‰ more negative than atmospheric CO_2 (O'Leary, 1981). The degree of discrimination of ^{13}C by RuBisCO may vary depending on the pH, temperature, and metal ion concentrations within the photosynthetic cells (O'Leary, 1988). The variation of discrimination against ^{13}C in mosses reflect the changes in balance between carboxylation and diffusion limitations (Royles *et al.*, 2012b). Rice and Giles (1996) showed that discrimination of $^{13}CO_2$ and assimilation rate increased when the thickness of the external water film was reduced.

Interpretations of moss stable carbon isotope composition provide insight into periods when environmental conditions favoured photosynthesis (Royles *et al.*, 2014). Identifying conditions where mosses are photosynthetically active, especially during periods of net assimilation is crucial to interpreting preserved proxy signals and predicting responses of moss to changing environment.

1.7 δ^{18}O of plant material and climate

Without roots and with a limited conduction system, mosses are dependent on external water availability (Royles *et al.*, 2013b). However, relatively little is known about the relationship between δ^{18}O in moss tissue and the climate (Royles & Griffiths, 2015). This is partially due to the scarcity of data (Royles *et al.*, 2013b), but also because of the complexity of the isotope fractionation processes involved (Saurer *et al.*, 1997). Due to the simple physiology of mosses, δ^{18}O in plant tissues are expected to reflect δ^{18}O of the water source, offset by the biochemical fractionation constant (Zanazzi & Mora, 2005; Royles *et al.*, 2013b; Xia *et al.*, 2020).

1.7.1 Evaporation–condensation of water in hydrological cycles

Both kinetic and equilibrium isotope effects of H and O that are associated with the evaporation-condensation and phase changes of water are fundamental to quantitatively understand and model the dynamic processes of water cycles (Horita *et al.*, 2008). The spatiotemporal patterns of D/H and ^{18}O/^{16}O ratios in precipitation are well understood to be caused by the discriminatory rainout of isotopically heavier water molecules during condensation and result in a relatively well defined distribution of atmospheric D/H and ^{18}O/^{16}O at multiple scales (Jouzel & Merlivat, 1984; Good *et al.*, 2015; Gonfiantini *et al.*, 2018). Understanding the factors that govern the evaporation of water from the ocean is essential, as the ocean regulates the climate of the earth's system (Dar *et al.*, 2020). The fractionation factors that partition water isotopologues depend on the temperature and the rate of reaction (Dansgaard, 1964). This process results in an unequal distribution of isotopes in different phases within a system and can be explained by either the quantum mechanical effects on the partition factor of the molecules of concern (Rayleigh, 1905; Gat, 2005), or the kinetic effects of diffusion (Craig & Gordon, 1965).

The mathematical description of the change in isotopic composition was first described by Lord Rayleigh (1905), henceforth known as the Rayleigh distillation equation (Eqn. 1.6). This equation describes the curve of the equilibrium relationship between a liquid and vapour in a binary mixture for a closed distillation system. The composition of liquid to vapour depends on the pressure and temperature of the system (Rayleigh, 1905). Rayleigh's equation has been applied to the global hydrological cycle to quantify and model the fluxes between various parts of the cycle (Jouzel & Merlivat, 1984; Gat, 2000; Yoshimura, 2003). This model predicts that as the air mass cools, precipitation is formed in isotopic equilibrium with the vapour, resulting in a depletion of the heavy isotopes in the residual air (Fig. 1.2) (Gat, 2000). The modified Rayleigh's equation describes the fractionation of water vapour during evaporation from a water source (Gat, 2000; Dawson *et al.*, 2002):

$$\delta = \varepsilon^{*}\left(1 + \frac{\delta}{10}\right) dlnf, \qquad [1.6]$$

where ε^{*} is the liquid–vapour isotope fractionation factor at the ambient temperature and *f* is the fraction of water in the air mass relative to its initial value.

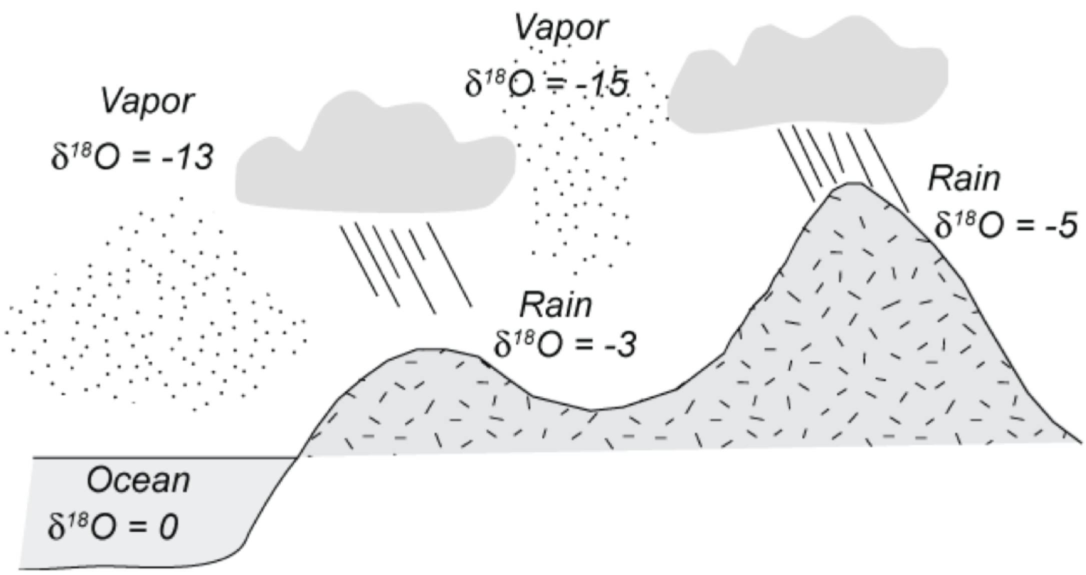

Figure 1.2: Illustrative diagram depicting the process of Rayleigh's distillation in the hydrological cycle. As water from the source (ocean) evaporates, the isotopic composition of water vapour is more depleted in ^{18}O compared to source water. When water vapour condenses and rainfall occurs, the isotopic composition of rainwater is more isotopically enriched compared to the vapour. The isotopic composition of rain becomes more enriched as it moves inland. From *Isotope tracers in catchment hydrology* (p. 221), by C. Kendall and E. A. Caldwell, 1998, Amsterdam: Elsevier Science B.V.

A limitation to Rayleigh's equation in understanding the hydrological cycle is its simplistic nature (Dansgaard, 1964; Gat, 2000; Yoshimura, 2003). Rayleigh's theory neglects to account for the kinetic fractionation processes that breaks the bonds between hydrogen and oxygen molecules in water (Dansgaard, 1964). Therefore, hydrologists have applied another model to understand the complexity of isotope fractionation during evaporation and condensation in the hydrological cycle. The Craig–Gordon model integrates kinetic and equilibrium fractionation processes and proposes a two-layer model to represent the isotopic composition of evaporation from the ocean's surface (Craig & Gordon, 1965). The isotopic composition of vapour generated on the surface of the ocean depends on the isotopic composition of the ocean's surface water, the isotopic composition of the water vapour in the ambient atmosphere and the relative humidity (Dar et al., 2020). The Craig–Gordon equation can be expressed in terms of isotopic ratios as (Craig & Gordon, 1965):

$$R_{ev} = \alpha_k \cdot \frac{R_L \cdot a^+ - RH \cdot R_A}{1 - RH}, \qquad [1.7]$$

where R_L is the isotope ratio of liquid water, R_A is the isotope ratio of atmospheric moisture, RH is the relative humidity and α_k and α^+ is the kinetic and equilibrium fractionation factor, respectively.

Understanding how isotopes behave in the hydrological cycle strengthens our knowledge behind using mosses as a proxy for past climates as mosses and water are intimately linked.

1.7.2 Plant leaf water enrichment

In plants, leaf water becomes more enriched in the heavier isotope molecules as water vapor molecules containing the lighter isotopes are transpired more readily compared to water vapor molecules containing the heavier isotopes (Flanagan & Ehleringer, 1991). Although the traditional Craig–Gordon model is applied to explain evaporative enrichment of hydrological cycles, some parameters of the Craig–Gordon model have been modified to fit the evaporative enrichment of a leaf surface, expressed as an enrichment above source water as (Farquhar *et al.*, 1993; Barbour, 2007):

$$\Delta^{18}O_{es} = \varepsilon^{+} + \varepsilon_k + (\Delta^{18}O_v - \varepsilon_k)e_a/e_i, \qquad [1.8]$$

where $\Delta^{18}O_{es}$ is the leaf water enrichment above source water, e_a and e_i is the ambient and intercellular water vapour mol fraction, ε^{+} is the proportional depression of water vapour pressure by the heavier $H_2{}^{18}O_2$ molecule, and ε_k is the kinetic fractionation during diffusion through the stomata and the leaf boundary layer. The model expands from the traditional Craig–Gordon model as it includes the isotopic exchange between the water vapour in the atmosphere and leaf water (ε_k) (Flanagan, 1993).

1.8 Biochemical fractionation during cellulose synthesis

Organic plant materials are generally 27 ± 3‰ more enriched in ^{18}O compared to the water source (De Niro & Epstein, 1979; Sternberg *et al.*, 1986). It was previously hypothesised that the fractionation constant of 27 ± 3‰ was caused by one oxygen atom from water and two from CO_2 equilibrated with ambient water towards carbohydrate synthesis (Sternberg, 2009). However, tests for this hypothesis failed to show temperature effects (Sternberg *et al.*, 2006). Strong evidence suggests that the overall biochemical enrichment factor is associated with the reversible hydration of carbonyl intermediates that occurs during cellulose synthesis (Sternberg *et al.*, 1986).

$$H_2O + R_2CO \leftrightharpoons R_2C(OH)_2, \qquad [1.9]$$

Sternberg and De Niro (1983) tested the magnitude of the oxygen isotope fractionation between carbonyl oxygen and water for the carbonyl hydration reaction in acetone and found a fractionation factor of ~27‰, like that observed during cellulose synthesis.

1.8.1 Organic isotope composition in moss cellulose reflects the environmental water condition

Understanding how carbon and oxygen isotopes fractionate during photosynthesis has allowed researchers to use organic cellulose for paleoclimate reconstruction (Sauer *et al.*, 2001; Schubert & Jahren, 2012; Royles *et al.*, 2013a; Royles & Griffiths, 2015; Royles *et al.*, 2016; Street-Perrott *et al.*, 2018). This method of environmental reconstruction is typically applied to tree rings (McCarroll & Loader, 2004). However, a growing amount of research has been conducted on ombrotrophic (rain-fed) peat mosses. In stable environments like the polar regions, ombrotrophic mosses have accumulated cellulose for up to 5000 years, making them an invaluable tool for paleoclimate reconstruction.

The stable carbon isotope ratio of terrestrial plant organic matter varies among species and environmental factors (Cernusak *et al.*, 2013). Since cellulose is one of the most abundant and resistant organic compounds found in plants (Skrzypek *et al.*, 2007), cellulose preserves information about the climate in which the carbon molecules were fixed during photosynthesis. By analysing the organic cellulose of plants, researchers are able to reconstruct the timeline of environmental variations (Belmecheri & Lavergne, 2020).

Currently, the research into mosses as a proxy for past climates are based on peat mosses (Sauer *et al.*, 2001; Kaislahti Tillman *et al.*, 2010; Bramley-Alves *et al.*, 2015; Jassey & Signarbieux, 2019), or aquatic submerged mosses (Sauer *et al.*, 2001; Skrzypek *et al.*, 2007). By coupling the knowledge about the patterns of isotope composition in hydrological cycles and moss photosynthesis, researchers are able to reconstruct past environmental conditions since mosses are only metabolically active during periods where the environmental conditions are suitable for photosynthesis. When oxygen is fixed into carbohydrates such as cellulose, the oxygen isotope ratio is controlled by the isotopic composition of cellular water (Sauer *et al.*, 2001). Because the $^{18}O/^{16}O$ ratio of meteoric water is directly related to climate temperature, the ratio of $^{18}O/^{16}O$ of cellulose in plants therefore also relates to climatic temperature (Epstein *et al.*, 1977).

1.9 Aims and objectives

Our current understanding of the carbon and oxygen isotope composition of moss bulk tissue relies on comparing the isotopic composition with meteorological and microclimatic conditions (Royles *et al.*, 2016). However, this technique relies on general assumptions on the fractionation processes that occurs during cellulose synthesis and does not take into account species– and life-form– influences on the composition of stable isotopes. The purpose of this research is to understand the fractionation processes that occur in response to drying in poikilohydric and endohydric moss species and to explore the fractionation processes that occur during growth and cellulose synthesis. To understand these processes, the stable isotope composition of moss tissue and transpired water vapour will be analysed.

The aim and objectives of this thesis is to explore three different applications of stable carbon and oxygen isotopes, with respect to mosses. The key objectives of the study are:

1. To compare the oxygen isotope of evaporated leaf water from a poikilohydric and endohydric moss species and to investigate water enrichment in the Polytrichaceae family
2. To present a novel method of reconstructing the past water environment recorded along *Dawsonia superba* (Polytrichaceae) stems
3. To address the current knowledge gap in the reconstruction of past climates based on $\delta^{18}O_{BULK}$ moss tissues.

1.10 Thesis layout

This thesis consists of five chapters. The layout of chapters two, three, and four are formatted as scientific articles, each with their own introduction, methods, results, and discussion. Therefore, some information in this general introduction may be repeated in each chapter's introduction.

Chapter one is a general introduction describing the physiology of mosses and how their water relations differ from the well-studied vascular plants. It also includes definitions and current literature of the use of stable isotopes, namely, carbon and oxygen, as a method to understand the physiological constraints of mosses.

Chapter two examines the $\delta^{18}O$ of evaporated and transpired moss phyllid water of two widely contrasting mosses to determine how the physiological differences influence evaporation and transpiration. Two oxygen isotope models were used to explain the observed patterns in $\delta^{18}O$ of evaporated moss leaf water: The Rayleigh's s distillation theory, and the modified Craig-Gordon model.

Chapter three uses $\delta^{18}O_{BULK}$ of *D. superba* (Polytrichaceae) as a novel method to reconstruct $\delta^{18}O$ variations of precipitation and climatic conditions. As *D. superba* has been recorded to grow up to lengths of ca. 50 cm, there is potential environmental information stored within the stems. This chapter sampled *D. superba* from a single site in Central North Island, New Zealand, and the stable oxygen and carbon isotopic composition was analysed from 10mm transverse sections of the stems.

Chapter four addresses the current gap in our knowledge of using mosses as a proxy for past climate. This chapter offers a laboratory investigation of how $\delta^{18}O$ of source water is reflected in $\delta^{18}O$ of *Sphagnum* bulk tissue. *Sphagnum* was grown in growth chambers over 6 months and watered with isotopically labelled water. Samples were dried and bulk tissue was used for stable isotope analysis.

Lastly, Chapter five summarises the main findings of each chapter and discusses the areas of improvement and ideas for future research in studying moss physiology through the use of stable isotopes.

Chapter 2
$\delta^{18}O$ of transpired water and the isotopic enrichment of moss phyllid water: a reflection of contrasting moss phyllid physiology

2.1 Introduction

The use of stable isotopes in ecological research has increased tremendously in recent decades (Hobson, 2007). The $^{18}O/^{16}O$ composition of leaf water ($\delta^{18}O_L$) and transpired leaf water ($\delta^{18}O_E$) have been used to explore primary productivity, ecophysiological influences on water use efficiency, and paleoclimate reconstruction, to name a few (Dawson *et al.*, 2002; Barbour, 2007; Wang *et al.*, 2012).

$\delta^{18}O_L$ and $\delta^{18}O_E$ reflect the oxygen isotope composition ($\delta^{18}O$) of the water taken up by the plant (Barbour *et al.*, 2004) and leaf evaporative conditions, which are dependent on relative humidity and temperature of the surrounding environment (Farquhar *et al.*, 2007). Additionally, the conditions for leaf water evaporation involve complex interactions that occur between liquid water at the site of evaporation, water vapour in ambient air, and the environmental conditions, both in and around the leaf (Farquhar *et al.*, 2007). $\delta^{18}O_L$ in vascular plants are generally more enriched in ^{18}O compared to the soil water taken up by the plant because: 1) the vapour pressure of $H_2{}^{18}O$ is less than $H_2{}^{16}O$, and 2) $H_2{}^{18}O$ vapour diffuses more slowly than $H_2{}^{16}O$ (Farquhar *et al.*, 2007). (Yakir *et al.*, 1989). $\delta^{18}O_L$ is of interest when using biological paleoclimate proxies as it influences the oxygen isotope composition of cellulose, with an offset due to the equilibrium fractionation between organic molecules and water (27±3‰; (De Niro & Epstein, 1979). This offset allows for the interpretation of cellulose $\delta^{18}O$ as a proxy for paleoclimate reconstruction.

Mosses are invaluable biological proxies for past environmental conditions, especially when meteorological data is limited (Valanne, 1984; Royles *et al.*, 2013b). Given the extreme conditions of some ecosystems, such as Antarctica, nonvascular plants dominate the vegetative communities. Mosses in this region rely on water from ice-melt, which is influenced by temperature and seasonal changes. Given that water moves passively into moss tissues, and that mosses are only metabolically active when free water is available, understanding $\delta^{18}O$ of surrounding water plays a crucial role in interpreting the $\delta^{18}O$ of moss cellulose (Royles *et al.*, 2013b; Royles *et al.*, 2016). Interpretation of the oxygen isotope composition of moss cellulose thus relay information on the micro-environmental conditions that influence plant growth.

The current understanding of the observed variation in $\delta^{18}O$ of plant cellulose is that the variation are influenced by $\delta^{18}O$ of source water and the evaporative enrichment of leaf water that occurs during transpiration (Barbour *et al.*, 2004). As mosses lack mechanisms to regulate water loss, and are often in equilibrium with the water status of the environment (Green *et al.*, 2011; Bell *et al.*, 2021), it is assumed that $\delta^{18}O$ of moss cellulose is a direct reflection of source water (Sauer *et al.*, 2001; Royles *et al.*, 2013b; Xia *et al.*, 2020).

A strong mechanistic understanding of variation in $\delta^{18}O$ of the environment and leaf water is required to exploit the potential environmental proxy present in mosses. However, despite the major advances in $\delta^{18}O_L$ studies, the study of moss leaf water has been overshadowed by vascular plant leaf water research. Additionally, most of the studies on moss leaf water have focused on *Sphagnum* species (Nichols & Brown, 1980; Verma, 1996; Price *et al.*, 2009; McCarter & Price, 2014). As mosses are a functionally diverse group, studying one species does not capture the full complexity of the processes involved during moss water evaporation.

With around 20,000 species of mosses, their structure and physiology vary greatly (Waite & Sack, 2010; Thielen *et al.*, 2021). Some of these variations are reflected in the moss phyllid structure, which is closely linked to moss water relation strategies. The structure of moss phyllids are often considered “primitive” as they are hypothesized to reflect early terrestrial plants (Shaw *et al.*, 2011). However, despite their primitive structure, moss phyllids exhibit certain differences in morphology, as well in their anatomical structure. For example, the phyllid blade of poikilohydric mosses are a single cell layer thick, where the only differentiating cells are at the midrib of the leaf (Krupa, 1976). In contrast, the phyllids of the Polytrichaceae family are structurally complex. The upper surface consists of closely spaced longitudinal rows of green mesophyll-like lamellae (Proctor, 2013). Additionally, the surface of the lamellae are covered with granular wax, and most of the surface of young shoots are water-repellent (Proctor *et al.*, 1998). The lamellae are proposed to increase the surface area for CO_2 exchange, and the waxy surface is hypothesized to keep water out – optimizing photosynthesis. The influence the lamellae have on photosynthesis and carbon dioxide uptake is well studied (Proctor, 2013; Brodribb *et al.*, 2020). However, little is known about how they affect leaf water enrichment.

The present study aimed to investigate the evaporation rate and isoflux in mosses of contrasting hydric strategies, as a first step in understanding variation in the processes determining phyllid water isotope enrichment. Additionally, given that the lamellae of Polytrichaceae phyllids act as 'pseudo-mesophylls' (Proctor, 2013), the transpiration rates and the leaf water enrichment were examined to understand the role of lamellae in water regulation.

2.2 Materials and methods

2.2.1 Theoretical considerations

Throughout this study, concepts from Rayleigh's theory, the Craig Gordon model and plant transpiration were tested and applied.

2.2.1.1 Rayleigh's distillation theory

The isotope ratios found in the global hydrological cycle are determined by the isotope fractionation that accompanies evaporation from the ocean and terrestrial water bodies (Gat, 2000; Gonfiantini *et al.*, 2018). The exchange of water vapour between a raindrop and its environment plays an important role in the interpretation of oxygen of rain water (Friedman, 1962). When water evaporates and forms clouds, the isotopically heavier water tends to remain in the liquid phase: therefore, the water vapour is more depleted in ^{18}O compared to the liquid phase (Gat, 2000). When water condenses and forms precipitation, the heavier water tend towards the aqueous phase, so the precipitation is isotopically enriched relative to residual water vapour (Dansgaard, 1964). As this process is temperature dependent, precipitation becomes progressively more isotopically depleted at higher latitudes due to the preferential rainout of the heavier water as clouds move poleward (Dansgaard, 1964; Noone, 2008).

Mosses, which lack mechanisms to regulate water uptake and water loss, take up water passively via diffusion. Therefore, the isotope fractionation that occurs during evaporation of both the hydrological cycle and poikilohydric mosses may be represented by Raleigh's distillation equation, which follows (Rayleigh, 1905; Gat, 2000):

$$R = R_0 f^{\alpha^{+}-1}, \qquad [2.1]$$

where R_o is the initial isotope ratio of the water droplet, f denotes the proportion of water remaining after the removal by the phase change, and α^{+} is the effective temperature fractionation factor. Under Rayleigh conditions, the condensed water is removed from the vapour immediately after formation (Dansgaard, 1964).

As the phase change between liquid and vapour water is temperature dependent, α can be explained as the equilibrium fractionation ε^{+}, where the relationship between α^{+} and ε^{+} is $\varepsilon^{+} = (\alpha + 1)$ (Kendall & Caldwell, 1998; Farquhar & Gan, 2003). Therefore, the effective temperature fractionation factor can be expressed in terms of ε^{+}as (Bottinga & Craig, 1969; Barbour, 2007):

$$\varepsilon^{+}(‰) = \left[exp\left(\frac{1.137}{(273+T)^2} \times 10^3 - \frac{0.4156}{273+T} - 2.0667 \times 10^3\right) - 1\right], \qquad [2.2]$$

where T_1 denotes temperature in Kelvin.

The depletion of $^{18}O/^{16}O$ in precipitation is a function of the temperature dependent isotopic fractionation that occurs during evaporation, and the subsequent condensation of cloud moisture (Farquhar *et al.*, 1989b). Based on Rayleigh's theory, the oxygen isotope ratio of water in liquid and vapour phases are represented as an inverse logarithmic relationships as the volume of source water is reduced (Dansgaard, 1964). (Gat, 1996).

As moss phyllid water is often observed to be in equilibrium with environmental water conditions, Rayleigh's theory is assumed to explain the oxygen isotopic composition of evaporated moss phyllid water.

2.2.1.2 Leaf water enrichment at the site of evaporation

The difference between $\delta^{18}O_L$ and source water depends on the fractionation processes that occurs during transpiration (Flanagan & Ehleringer, 1991). At isotopic steady state, the transpired water is isotopically equivalent to source water to satisfy mass balance (Cernusak *et al.*, 2016). But under non-steady state conditions, the evaporative environment will influence the isotopic composition of transpired water (Farquhar & Cernusak, 2005). Water is more isotopically enriched at the site of evaporation as heavier $H_2{}^{18}O$ molecules tend to diffuse slower and have a lower vapour pressure than the lighter $H_2{}^{16}O$ (Barbour *et al.*, 2004). The theoretical basis for leaf water enrichment in vascular plants was developed from Craig and Gordon's (1965) model (C–G model) for the evaporative enrichment that occurs over the surface of a water body. This model has been modified to include influences of the isotopic exchange between the water vapour in the atmosphere and leaf water, expressed as (Flanagan *et al.*, 1991; Farquhar *et al.*, 1993; Barbour, 2007):

$$\Delta^{18}O_{es} = \varepsilon^{+} + \varepsilon_k + (\Delta^{18}O_v - \varepsilon_k)e_a/e_i, \qquad [2.3]$$

where ε_k represents the kinetic fractionation that occurs during diffusion through the boundary layer and stomata, ε^{+} represents the proportional depression of the heavier water vapour pressure compared with the lighter water vapour pressure, $\Delta^{18}O_v$ is the difference in oxygen isotope composition of the atmospheric vapour compared to source water, and e_a and e_i are ambient and intercellular vapour pressures, respectively (Barbour & Farquhar, 2003; Barbour, 2007). As e_a and e_i are the ratio of water vapour between air and intercellular space, e_a/e_i can simply be expressed as the relative humidity, if leaf temperature is equal to air temperature (Song *et al.*, 2013; Cernusak *et al.*, 2016). e_a/e_i depends on the saturation vapour pressure of water ($e_{s(T)}$), which increases exponentially with temperature. The saturation vapour pressure of water at 25° is expressed as (Horita *et al.*, 2008):

$$e_{s(T)} = f\left(a \cdot \exp\frac{bT}{c+T}\right), \qquad [2.4]$$

where a is 6.14, b is 18.56, c is 255.57 at 25°C, based on the exponential relationship between vapour pressure and temperature (Horita *et al.*, 2008).

As $\Delta^{18}O_v$ is the difference between the oxygen isotope composition of atmospheric vapour and source water, it can simply be expressed as (Farquhar & Gan, 2003):

$$\Delta^{18}O_v = \frac{\delta^{18}O_v - \delta^{18}O_s}{1 + \delta^{18}O_s}, \qquad [2.5]$$

where $\delta^{18}O_s$ and $\delta^{18}O_v$ is the isotopic composition of source water and atmospheric vapour respectively. However, in open, well-mixed conditions $\Delta^{18}O_v$ is often close to $-\varepsilon^+$ (Barbour, 2007), so that $\Delta^{18}O_e$ is approximately proportional to $1 - e_a/e_i$.

In the modified C–G model (Eqn. 2.3) there are two isotope effects that occur during evaporation: an equilibrium effect that results from the liquid to vapour phase change (ε^+), and a kinetic effect caused by the different diffusion rates of the light and heavier isotopes in the water vapour of air (Flanagan *et al.*, 1991).

The kinetic fractionation factor is defined as (Farquhar *et al.*, 1989b):

$$\varepsilon_\kappa = \frac{28g_s^{-1} + 18.7g_b^{-1}}{g_s^{-1} + g_b^{-1}}, \qquad [2.6]$$

where g_s is the stomatal conductance which the diffusivity of $H_2{}^{16}O$ in air is 25‰ more than the diffusivity of $H_2{}^{18}O$, and g_b is the boundary layer conductance (approximately 18.9‰) (Farquhar *et al.*, 1993). However, it should be noted that mosses are astomatic, so g_s should be adjusted accordingly.

As ε^+ is temperature dependent (Bottinga & Craig, 1969; Horita & Wesolowski, 1994), equation 2.2 can be applied to determine the equilibrium fractionation that occurs in this model.

As the hydroids replenish evaporated phyllid water in Polytrichaceae mosses, the closed system of the Rayleigh distillation model is unlikely to be useful for these mosses, compared with poikilohydric mosses. Further, the lamellae of Polytrichaceae mosses are observed to curl and reduce surface area in response to increasing evaporative demands, potentially allowing some regulation of water loss, analogous to stomata in vascular plants. The Rayleigh model will be used to assess isotopic enrichment of transpired water during evaporation in the poikilohydric moss, and the Craig-Gordon model will be used to assess transpired water and to predict leaf water enrichment in the endohydric moss.

2.2.2 Plants and materials

The two moss species chosen for this experiment represent widely contrasting water interaction strategies due to the physiological constraints of their leaf structure. *Ptychomnion aciculare* phyllids are one cell layer thick and were selected to test Rayleigh's theory in mosses, and *Dawsonia superba* was chosen as the representative species for the Polytrichaceae family, as they are hypothesized to express leaf water enrichment more similar to that of vascular plants. A transverse hand-section was performed on the phyllid of each species to compare the anatomical features (Fig. 2.1).

P. aciculare samples were obtained from the shade house at the University of Waikato, New Zealand, where they were kept well hydrated with regular misting with tap water twice a day. *P. aciculare* used in this study were selected from green, healthy shoots. The samples were split into two groups to be soaked in labelled water. The labelled water was named after the source where it was collected: Antarctic water had the oxygen isotope composition of -22.4‰, and rainwater collected from a tropical cyclone had the oxygen isotope composition of -0.8‰. There was a total of three replicates for each labelled water.

D. superba samples were collected from the Rangitoto Ranges, New Zealand (42.9985S, 170.7789E) during December 2021. *D. superba* samples were selected from large, healthy clumps. The moss, including the humus, was removed from the forest floor, taking care to minimise damage to the rhizoids. *D. superba* was kept in the shade house at the University of Waikato over the summer of 2021-2022, where it was misted twice a day with tap water. *D. superba* in this experiment showed no obvious signs of hydraulic failure, and appeared to be photosynthesising, as evidenced the samples responsiveness when misted and the photosynthetic tissues were still green.

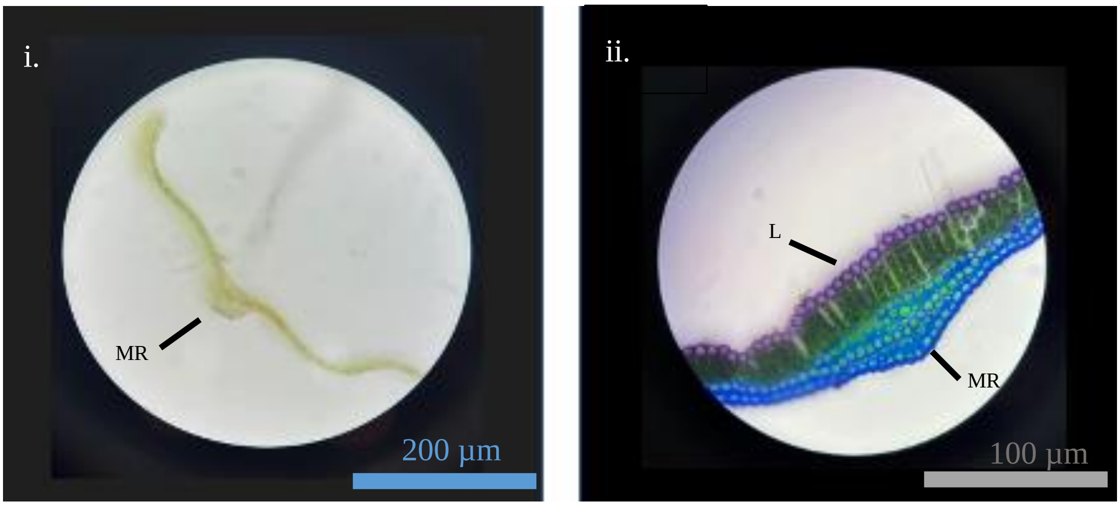

Figure 2.1. Comparative transverse cross-sectional photographs of the phyllids for: i) *Ptychomion aciculare* under 400x magnification. The blue solid line represents 200 µm. And ii) *D. superba* under 200x magnification. *D. superba* was dyed with toluidine blue to contrast the different organic compounds within the phyllid. The grey solid line represents 100 µm. MR = midrib, L = lamellae.

2.2.3 On-line gas exchange

2.2.3.1 Testing Rayleigh's theory in *P. aciculare*

To test whether the evaporative behaviour of *P. aciculare* leaf water is analogous to that of the hydrological cycle, the evaporative process of water was tested. 0.1 mL of labelled water was added to a 6 cm filter paper. The labelled water used in this experiment had $\delta^{18}O$ values of -22.4 and -0.7‰. The filter paper was placed into a 38 cm^2 custom-made leaf cuvette (Loucos *et al.*, 2015), attached to the LI-6400 portable photosynthesis system (Lir-Cor Inc., Lincoln, NE, USA). The CO_2 concentration was maintained at 400 µmol CO_2 mol^{-1}, PAR at 100 µmol m^{-2} s^{-1}, and temperature at 25°C. To only measure $\delta^{18}O$ of the water droplet vapour, dry air was sent to the cuvette and the flow rate was maintained at 500 µmol s^{-1} to minimize condensation in the tubing. The outlet flow from the cuvette was attached to an oxygen isotope vapour analyzer (IWA-35d-EP, Los Gatos Research, San Jose, CA, USA). The on-line gas exchange measurements were recorded at one-minute intervals. Each trial continued until relative humidity inside the cuvette was less than 10%. Three replicates for each of the two standards of labelled water were investigated.

For *P. aciculare,* drying measurements were performed using a LI-6400 portable photosynthesis system (Lir-Cor Inc., Lincoln, NE, USA), with a custom-made 38 cm^2

chamber as described above. The moss samples were spread over a metal mesh with no overlap inside the chamber. The on-line gas exchange measurements were recorded at 20-second intervals. The environmental conditions inside the chamber were set to match the filter paper measurements; concentration of CO_2 was maintained at 400 µmol CO_2 mol^{-1}, light intensity level at 100 µmol m^{-2} s^{-1}, and temperature was 25°C. The flow rate inside the cuvette was kept at 500 µmol s^{-1}. Each replicate continued until relative humidity inside the cuvette was less than 10%. Excess water was removed from *P. aciculare* samples prior to sealing in the leaf chamber using a paper towel so only the water inside the leaf was being measured. The initial weight and weight after the trial were measured as an estimation of leaf water content.

2.2.3.2 *D. superba* transpiration

For *D. superba,* measurements were performed using the LI-6400 fitted with a 3 x 2 cm^2 cuvette. The LI-6400 was attached to a bubbler system that increased the water vapour concentration inside the cuvette (see Appendix Fig.A.1). Relative humidity decreased every 40 minutes for a total of five steps. Relative humidity was manipulated by increasing the drierite scrub attached the LI-6400 water vapour inlet to reduce the volume of water vapour from the bubbler into the IRGA chamber. The CO_2 concentration inside the cuvette was maintained at 400 µmol CO_2 mol^{-1}, temperature at 25°C, PAR at 200 µmol m^{-2} s^{-1}, and flow rate was kept at 500 µmol m^{-2} s^{-1}. The flow rate was increased to 700 µmol s^{-1} at the last step to decrease the humidity in the chamber further. Relative humidity was maintained between 10 to 80% to ensure sufficient water vapour was going to the oxygen isotope analyser (IWA-35d-EP, Los Gatos Research, San Jose, CA, USA) for accurate measurements. The water in the bubbler system was replaced using the same water source at the beginning of each replicate. To detect changes in the $\delta^{18}O$ of the bubbler over time, measurements of an empty chamber at high humidity (i.e. full bypass through the drierite trap) were made at the start and end of each trial. Tests indicated that drierite had no significant effect on the stable isotope composition of vapour entering the leaf chamber. This experiment was replicated six times, but two replicates indicated a loss of hydraulic conductance within the moss so were excluded from further analyses.

2.2.4 Calculations for surface area of mosses

As the calculations for transpiration rate are area-based, the surface area of mosses inside the chamber was estimated. The image processing and analysis program ImageJ (Schneider *et al.*, 2012) was used to determine the surface area of both *P. aciculare* and *D. superba*. The mosses used in this study were photographed and imported to the ImageJ software. By using the threshold setting on ImageJ, an estimate of the surface area was determined.

2.2.5 Data analysis

All data were processed and analyzed through Microsoft Excel (Microsoft Corporation, 2017). The relationship between relative humidity with transpiration rates and $\delta^{18}O_E$ were graphed on RStudio (RStudio, 2020), using the ggplot2 package (Wickham, 2016).

2.2.5.1 Comparing Rayleigh's theory to *P. aciculare* phyllid water vapour

To fit the measured water oxygen isotope vapour to the Rayleigh equation, data from the LI-6400 and LGR were matched, with an approximately 20 second delay between the two datasets to account for the time it takes water vapour to move from the LI-6400 to the oxygen isotope analyser. The oxygen isotope ratio of the sample water was measured and used as the initial oxygen isotope ratio of source water. The water content of mosses was determined to be the difference in the moss wet and dry weight. The initial water content was used to calculate the proportion of water remaining over the period of each trial. The mol lost during the experiment was calculated as the transpiration *rate x area x time*. Equation 2.1 was used to determine the change in $\delta^{18}O$ of the water vapour as the moss dried, if assuming Rayleigh's distillation. The measured $\delta^{18}O$ of the water vapour from the mosses were compared to the calculated change in $\delta^{18}O$ of water vapour.

2.2.5.2 Oxygen isotope composition of transpired water vapour from *D. superba*

The measurements of $\delta^{18}O_v$ from the empty chamber revealed changes in the oxygen isotope composition of the bubbler vapour over time. The change in the oxygen isotope of the bubbler water was extrapolated by creating a linear regression model for each trial using the measurements taken of the empty chamber at the start and end of each trial (Table. 2.1).

Table 2.1. Simple linear regression models for the change in $\delta^{18}O$ and δD of bubbler water over time (seconds). Simple linear regression models were extrapolated from the measurements of an empty IRGA chamber at the start and end of each trial.

Sample	Bubbler $\delta^{18}O$	bubbler δD
Sample 2	$\delta^{18}O$ = 0.429 * time -13.089	$\delta^{1}H$ = -10.299 * time -103.17
Sample 3	$\delta^{18}O$ = 12.471 * time -5.836	$\delta^{1}H$ = -42. 263 * time -86.844
Sample 5	$\delta^{18}O$ = 18.897 * time -0.763	$\delta^{1}H$ = -21.703* time -88.475
Sample 6	$\delta^{18}O$ = 17.359*time -5.167	$\delta^{1}H$ = -97.502*time -67.391

The calculation of $\delta^{18}O_E$ was based on the mass balance of the $\delta^{18}O$ and concentration of water vapour entering and leaving the chamber (Wang *et al.*, 2012), where the inlet was receiving water vapour from the bubbler (ambient), and the vapour leaving the chamber was a mixture of transpired moss water vapour and bubbler vapour. Since the change in ambient water vapour was known, the change in bulk water vapour inside the leaf chamber (V_C [m^3]) is described as (Wang *et al.*, 2012):

$$V_c \frac{d(C_c R_c)}{dt} = q_A C_A R_A + A_L E R_L - q_M C_M R_M, \qquad [2.7]$$

where q_A is the is the flow rate of ambient air going into the chamber and q_{Mi} is the flow rate of mixed air entering into the oxygen isotope analyser (m^{-3} s^{-1}), C_A, C_C, and C_M is the water concentration in ambient air of the leaf chamber, bulk water vapour inside the leaf chamber, and mixed air of oxygen analyser (mol m^{-3}), respectively, E is the transpiration rate of *D. superba* in the leaf chamber (mol m^{-1} s^{-1}), R_A is the isotopic ratio of ambient air, R_L is the isotopic ratio of transpired leaf water, R_C is the isotopic composition of the water vapour inside the chamber, R_M is the isotopic composition of the well mixed water vapour, and A_L is the transpiring leaf surface.

It is assumed that the volume inside the leaf chamber and the oxygen isotope analyser was well-mixed, so that $C_C = C_M$ and $R_C = R_M$ within the volume V_C. Under steady state conditions, $\delta^{18}O$ of the transpired leaf water can be expressed as (Wang *et al.*, 2012):

$$\delta^{18}O_E = \frac{C_M \delta_M q_M - C_A \delta_A q_A}{C_M q_M - C_A q_A}, \quad [2.8]$$

where δ_M and δ_A are the oxygen isotopic composition of mixed air and ambient air respectively.

2.3 Results

2.3.1 Rayleigh's theory and the evaporation of *P. aciculare* leaf water

The oxygen isotope composition of the water vapour became more enriched as the droplet from the filter paper dried (Fig. 2.2). The measured $\delta^{18}O$ of water vapour from Antarctic and tropical water fell on the $\delta^{18}O_V$ line, as predicted by Rayleigh's theory.

The oxygen isotope composition of *P. aciculare* phyllid water vapour varied from the theoretical composition but generally became more enriched as the moss dried (Fig. 2.3). The replicates for the moss soaked in -0.7‰ $\delta^{18}O$ labelled water varied from the theory more than the other labelled water trials (Fig. 2.3.i). Only one replicate from the -0.7‰ $\delta^{18}O$ labelled water was similar to the theory. One replicate measured 6‰ above that expected from Rayleigh's theory (Fig. 2.3.i). The measured $\delta^{18}O$ *P.aciculare* phyllid vapour treated with -22.4‰ labelled water was 3 to 5‰ higher than expected when the moss was fully saturated and two replicates measured 9 to 10‰ higher than expected when the moss was dried (Fig. 2.3.ii). One replicate was only 1‰ lower than expected as the moss dried.

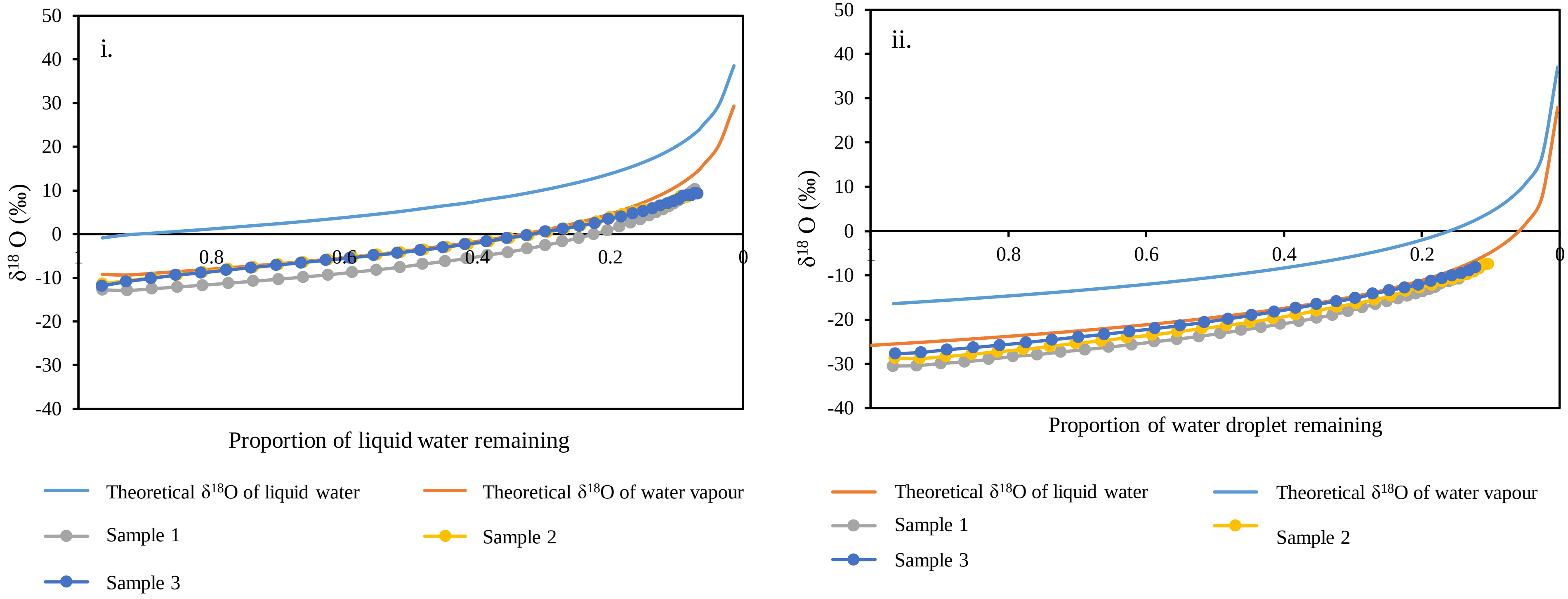

Figure 2.2. Scatterplots of measured δ^{18}O water vapour compared to Rayleigh's theory, as the water droplet on the filter paper dried. i) change in δ^{18}O for -0.7‰ water, and ii) change in δ^{18}O for -22.4‰ labelled water. The blue solid line and the orange solid line represent the δ^{18}O of liquid water and water vapour, respectively, as modeled by Rayleigh's distillation theory. The grey, yellow, and green points represent replicates of the measured δ^{18}O water vapour from the drying filter paper.

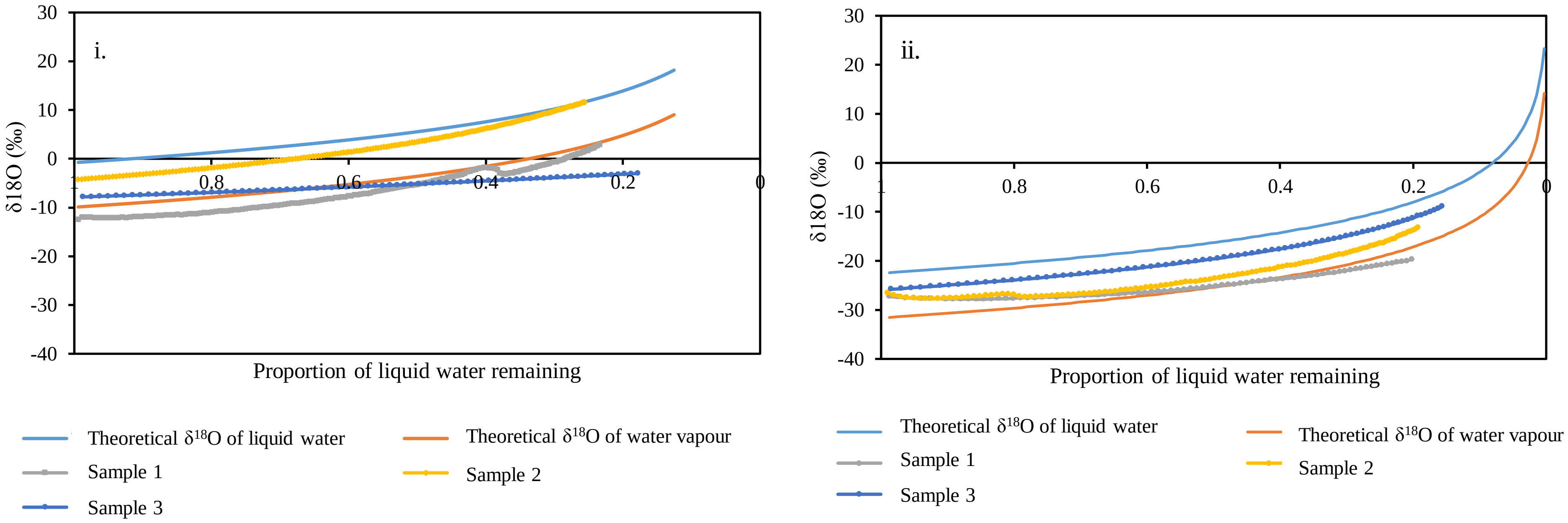

Figure 2.3. Scatterplots of measured $\delta^{18}O$ *P. aciculare* water vapour compared to Rayleigh's theory, as the moss dried. i) change in oxygen isotope composition of -0.7‰ labelled water, ii) change in oxygen isotope composition of-22.4‰ labelled water. The blue solid line and the orange solid line represents the $\delta^{18}O$ of liquid water and water vapour, respectively, as modeled by Rayleigh's distillation theory. The grey, yellow, and dark blue dotted line represent replicates of the measured $\delta^{18}O$ moss phyllid transpired water vapour.

2.3.2 Changes in $\delta^{18}O_E$ and transpiration rate with relative humidity in *D. superba*

There was a negative relationship between the oxygen isotopic composition of transpired water vapour from *D. superba* phyllids and relative humidity (Fig. 2.6.A). $\delta^{18}O_E$ of *D. superba* was more variable at low relative humidity than at high relative humidity. The range of $\delta^{18}O_E$ measured between 25% to 30% relative humidity was between -0.1‰ and -8.4‰. Between 70% to 80% relative humidity, $\delta^{18}O_E$ was between -11‰ to -15‰.

D, superba transpiration rates varied among the replicates (Fig. 2.4.B). The transpiration rate for replicate three and five decreased with increasing relative humidity. In contrast the transpiration rate of replicate six increased as relative humidity increased. Overall, stayed within the average rate of 3 mmol m^{-2} s^{-1} to 4 mmol m^{-2} s^{-1}.

Note that, unlike evaporation from filter paper, transpiration rate was not linearly and negatively related to relative humidity, but was relatively constant with RH. This suggests a degree of regulation of water loss in *D. superba*.

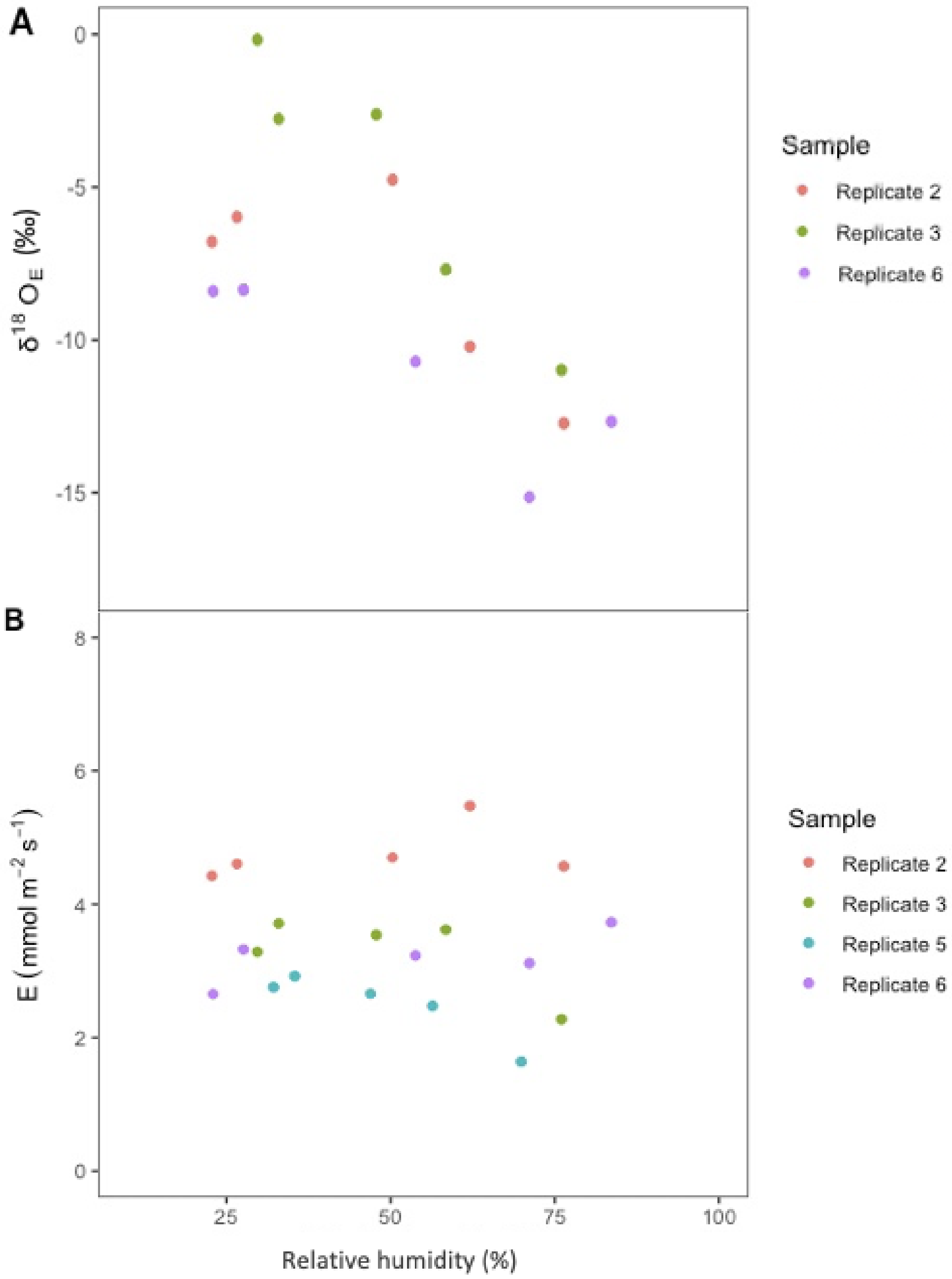

Figure 2.4. Relationship between relative humidity (%) and A) oxygen isotope composition of transpired vapour ($\delta^{18}O_E$ (‰)), as well as B) transpiration rate (E (mmol m^{-2} s^{-1})) in *D. superba*. Coloured points represent average data values at each step change of relative humidity and are coloured according to replicate number. Replicate 5 was excluded from the $\delta^{18}O_E$ and relative humidity simple linear regression due to errors in $\delta^{18}O_E$ calculations.

2.3.3 ^{18}O enrichment at the evaporative site and transpiration rate in *D. superba*

The oxygen isotopic composition at the evaporative site of *D. superba* increased as the transpiration rate (mmol m^{-2} s^{-1}) increased (Fig. 2.6). The relationship between $\delta^{18}O_e$ and transpiration varied greatly within each replicate. Overall, $\delta^{18}O_e$ increased by 16.4 with every one unit increase of transpiration. However, only 14% of the variation observed in $\delta^{18}O_e$ was explained by transpiration rates.

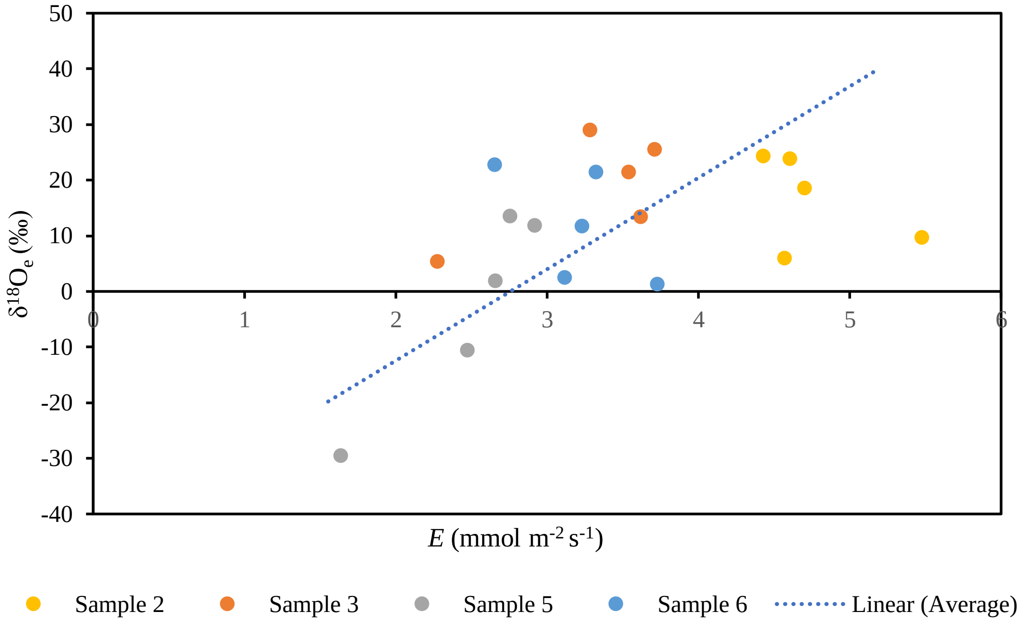

Figure 2.5. Relationship between $\delta^{18}O$ (‰) and transpiration rate (E mmol m^{-2} s^{-1}) in *D. superba*. Transpiration rates were manipulated by altering the relative humidity inside the gas exchange chamber. The different colours represent four replicates. Each value is the mean $\delta^{18}O_e$ at different relative humidity. (y=16.429 x–45.296; R^2=0.14; P=0.52; n=4).

2.4 Discussion

The results from this study demonstrate that the $\delta^{18}O$ of evaporated water from *P. aciculare* and *D. superba* phyllids were influenced by differences in their anatomical structure. The evaporation of water from moss phyllids that are one cell layer thick is similar to that of free water on filter paper. In contrast, the evaporation of water from mosses with specialized leaf cells suggests mechanisms to regulate water loss as indicated by the transpiration rate and oxygen isotope composition of transpired water.

Although the measured $\delta^{18}O$ of evaporated *P. aciculare* water varied more from Rayleigh's theory than the water droplet on a sheet of filter paper, the change in $\delta^{18}O$ from *P. aciculare* did increase as the moss dried. The structural features of the moss are related to the availability and uptake of water (Schofield, 1981). Additionally, the growth forms reflect the adaptive characteristics associated with desiccation and water loss (Scheirer, 1980). The leaf arrangement of *P. aciculare* overlaps and forms pockets that can retain water (Scheirer, 1980). The discrepancies between the measured $\delta^{18}O$ and Rayleigh's theory could be due to some retention of environmental water.

Despite the variation observed from the Rayleigh's theory test, this experiment highlighted the use of Rayleigh's theory of moss leaf water to predict the isotopic composition of evaporated water in field conditions, with some considerations. The water content of mosses are divided into three components: the external capillary water, symplast water, and apoplast water (Dilks & Proctor, 1978). The experiment presented in this study ignored the influences that the external capillary water movement might have on moss leaf water. Price et al (2009) observed variations in $\delta^{18}O$ of *Sphagnum* sp. hyaline cell water in response to surface evaporation over a course of seven days. The results showed an increase in $\delta^{18}O$ in response to higher relative humidity, but that $\delta^{18}O$ decreased as the days passed. Price et al (2009) concluded the variation observed was likely to due to both the downward diffusion of heavy isotopes when evaporation was low, and the upward rise in isotopically depleted hyaline water from depth when the surface of the moss was dried.

The complexity of water movement in mosses should be considered when interpreting $\delta^{18}O$ of moss cellulose ($\delta^{18}O_C$) within paleoclimate studies. Royles et al (2013b) highlighted the absence of seasonal variation in $\delta^{18}O$ of moss cellulose ($\delta^{18}O_C$), regardless of the clear trend in $\delta^{18}O$ of precipitation ($\delta^{18}O_P$) at their site. A fractionation of up to 5‰ was observed between $\delta^{18}O_C$ and $\delta^{18}O_P$, after accounting for the constant biochemical fractionation of 27±3‰ during cellulose synthesis. The difference in $\delta^{18}O$ reflect periods of strong evaporative enrichment of leaf water (Royles *et al.*, 2013b). Failure to consider the effects of different water sources on $\delta^{18}O_L$ may lead to a misrepresented timeline of the change in the local hydrological cycle.

The results presented in this study offer the first measurements of the changes in *D. superba* transpiration rates and $\delta^{18}O_e$ in response to changes in relative humidity. The calculations for transpiration were based on the mathematical equations for the transpiration rate of vascular plants. Transpiration rates in vascular plants are influenced by the evaporative demand of the environment and stomatal conductance (Farquhar & Gan, 2003). In respect to this study, the lamellae were viewed as synonymous to stomata in vascular plants. Currently, studies on the function of lamellae are focused on their influences on photosynthesis (Brodribb *et al.*, 2007; Proctor, 2013). To date, this is the first study that explored the direct effects of the lamellae on transpiration. The previous studies concluded that the main function of the lamellae are to increase the area required for CO_2 uptake (Brodribb *et al.*, 2020), rather than a response to water loss (Proctor, 2013).

$\delta^{18}O$ values of transpired plant water are also influenced by changes in relative humidity and regulation of water loss (Farquhar *et al.*, 2007). If the relative humidity of ambient air is reduced, the evaporative demand therefore increases and there are observable patterns in the enrichment of leaf water (Helliker & Ehleringer, 2002). On the other hand, the variation in leaf water caused by stomatal conductance is not as simple as a direct transfer (Farquhar & Gan, 2003). Increased stomatal conductance may lead to a negative relationship between transpiration and leaf isotopic enrichment by two factors: 1) the fractionation associated with stomatal resistance (Eqn. 2.6) tends to dominate when the resistance increases, leading to an increase in ε_k, and 2) stomatal closure can increase leaf temperature, which increases the temperature dependent fractionation, ε^+ (Farquhar *et al.*, 2007). As the measured $\delta^{18}O_E$ in this study increased with increasing transpiration, it is likely that relative humidity was the main driving force of variations in $\delta^{18}O_E$ until the influence of lamellae regulation of water loss dominated at low relative humidity.

This study has applied leaf water enrichment models used in vascular plants to specialized nonvascular plants. One could argue that the calculation for ε_k (Eqn. 2.6) is inappropriately applied to this analysis as *D. superba* lack stomata. Further investigation into the influence that the lamellae have on gas exchange is required to develop a model for the leaf water enrichment of Polytrichaceae. The lamellae on the upper surface have been observed to shrink in response to evaporation (Proctor, 2013), causing the leaf margins to curl inwards and reducing the surface area exposed to the atmosphere. This leads to a decrease in the gas exchange between leaf and atmosphere. Future work should investigate the area-based changes in transpiration and the boundary layer to accurately model the kinetic fractionation that occurs as the lamellae curls inwards.

The study presented here provides strong evidence for the leaf water enrichment in *D. superba*. The results show the change in $\delta^{18}O$ in response to water loss is more similar to vascular plants than simple mosses. Future studies could investigate evidence of a Péclet effect, which is primarily used in conjunction with the Craig–Gordon model to accurately describe vascular plant leaf water (Farquhar & Gan, 2003). The Péclet effect describes the mass flow of unenriched xylem water to the sites of evaporation opposed by the backward diffusion of $H_2{}^{18}O$ from these sites into the leaf. It also accounts for the progressive variation of leaf water enrichment along the leaf mesophyll tissue due to convection and diffusive mixing of the two water sources. Previous studies have found the observed leaf oxygen enrichment to be less than that predicted by the Craig–Gordon model (Ripullone *et al.*, 2008). By accounting for the Péclet effect, Ripullone (2008) could more accurately explain the variation in the evaporative enrichment in *Gossypium hirsutum* (cotton) than with the Craig–Gordon model alone. Describing the evaporative enrichment in leaves accurately is important for selective crop breeding as it provides information on the water use efficiency of a plant (Barbour *et al.*, 2000). However, the Péclet effect may be more difficult to measure in *D. superba*, due to the small size of the phyllids and as there is only one vein, as opposed to vascular plants, where the internal vein architecture can be quite complex.

Chapter 3

The δ^{18}O and δ^{13}C compositions recorded along *Dawsonia superba* (Polytrichaceae) (Grev.,) stems

3.1 Introduction

Stable isotope techniques are often used in plant science to understand how the environmental conditions affect metabolic reactions (Dawson *et al.*, 2002). Analyses of stable isotopic composition in tree rings or peat cores are widely used for past climatic reconstruction where temperature or precipitation are the limiting factors (Rebetez *et al.*, 2003). The oxygen isotopic composition of plant material is determined by the isotope composition of leaf water, and the fractionation process that occurs during cellulose synthesis (Barbour, 2007). As mosses rely on diffusion of water to the site of photosynthesis, moss organic tissues reflect the oxygen isotopic composition of the water source, expressed as (Zanazzi & Mora, 2005; Xia *et al.*, 2020):

$$\delta^{18}O_p = \delta^{18}O_{SW} + \varepsilon_b + (\varepsilon_e + \varepsilon_k(1-h)), \qquad [3.1]$$

where $\delta^{18}O_p$ and $\delta^{18}O_{SW}$ represents the oxygen isotope composition of plant organic material and source water respectively, ε_b is the biochemical enrichment factor during cellulose synthesis, ε_e and ε_k is the liquid-vapour equilibrium and kinetic enrichment factor respectively, and *h* is humidity at the leaf temperature. Note that Equation 3.1 is equivalent to Equation. 2.3, but expressed relative to the VSMOW standard rather than as an enrichment above source water. The relationship between the oxygen isotopic composition of plant materials and the water source is relatively constant (De Niro & Epstein, 1979) as previous studies observed that organic plant material is generally 27 ± 3‰ more enriched in δ^{18}O than the water source (Sternberg *et al.*, 1986; Sternberg, 2009). This constant enrichment is associated with the reversible hydration of carbonyl intermediates from the equilibrated water at the site of cellulose synthesis (Sternberg, 1989).

Furthermore, δ^{18}O of organic material can reflect seasonal variation in environmental conditions such as temperature, and therefore can be used to investigate the growth rate of plants (Poussart *et al.*, 2004). Dendrochronology involves analyzing and comparing the year-to-year changes in tree annual growth rings to understand the age structure and growing conditions at the time the cells were formed (Wigley *et al.*, 1987). However, this method is generally applied to temperate trees, where there are distinct growing seasons resulting in the formation of distinct early and late wood. As tropical trees grow all year round, there is a general absence of distinct annual growth rings (Stahle, 1999). Since $\delta^{18}O$ composition of precipitation ($\delta^{18}O_{PRECIP}$) is influenced by the fractionation processes associated with evaporation and condensation phase changes, driven by temperature and humidity (Dansgaard, 1964; Gat, 2000), $\delta^{18}O_{BULK}$ could therefore reflect seasonal variations in $\delta^{18}O_{PRECIP}$. This concept has previously been applied to tropical tree rings where distinct annual rings are absent (Poussart *et al.*, 2004). The moss family Polytrichaceae have apically dominant growth and vertical stems. Transverse $\delta^{18}O_{BULK}$ analysis may shed light on $\delta^{18}O_{PRECIP}$ in a similar manner as tropical tree rings.

On the other hand, stable carbon isotopes ($\delta^{13}C$) provide markers for photosynthetic gas exchange processes and climatic changes (Farquhar *et al.*, 1993), where $\delta^{13}C$ of plant tissues reflect the photosynthetic capacity over a growing season (Proctor *et al.*, 1992). The $^{13}C/^{12}C$ ratio of atmospheric CO_2 is understood to be 1.1% of the heavier carbon (^{13}C) and 98.9% of the lighter carbon isotope (^{12}C) (O'Leary, 1988; Farquhar *et al.*, 1989a). However, the ratios of $^{13}C/^{12}C$ observed in plant organic material contain less ^{13}C than atmospheric CO_2 due to the chemical and physical discrimination against the heavier isotope during CO_2 diffusion and carbon fixation by RuBisCO (O'Leary, 1988). Because of the simple physiology of mosses, the carbon isotope composition of moss organic material primarily reflects the balance between carboxylation and the diffusional limitations, expressed as the modified Farquhar et al. (1989) $\Delta^{13}C$ model (Meyer *et al.*, 2008):

$$\Delta = a_b \frac{C_a - C_w}{C_a} + (a_w + e_s)\frac{C_w - C_c}{C_a} + b\frac{C_c}{C_a} - f\frac{\Gamma^*}{C_\alpha} - e\frac{R_d}{kC_a}\ , \qquad [3.2]$$

where C_a, C_w, and C_c represent the CO_2 mole fractions in ambient air, at the surface of the external liquid layer and at the sites of carboxylation, respectively, a_b is the isotopic fractionation factor of CO_2 during diffusion through the leaf boundary layer (2.9‰), a_w is the fractionation of CO_2 during diffusion in the liquid phase (0.7‰), e_s is the fractionation during CO_2 dissolution (1.1‰ at 25°C), b is the fractionation during carboxylation (29‰), *f* is the fractionation of photorespiration (approx. 8‰), *e* represents the day respiration fractionation, Γ^* is the CO_2 compensation point in absence of dark respiration, R_d is the day respiration rate, and *k* is the carboxylation efficiency (Meyer *et al.*, 2008; Royles *et al.*, 2012b). Since mosses require an external film of water over the plant surface for photosynthesis, the expression C_w can be replaced with C_x which accounts for CO_2 diffusion from the air, across the water film, and to the plant tissue surface (Meyer *et al.*, 2008). The thickness of this water film increases rapidly in rain or snow melt events and decreases when the water flow ceases, leading to moss desiccation (Royles *et al.*, 2012b). When the surface of the moss is dry, and the diffusion of CO_2 and carbon assimilation rates are maximized, the uptake of lighter $^{12}CO_2$ is favoured (O'Leary *et al.*, 1992). In contrast, when the surface of the moss is covered by the water film, CO_2 diffusional resistance increases, which limits photosynthetic rates and results in increased assimilation of heavier $^{13}CO_2$ (Farquhar *et al.*, 1989a). The $^{3}C/^{12}C$ ratios of bulk organic tissue reflects the $^{13}C/^{12}C$ ratios at the chloroplast where carboxylation takes place (O'Leary, 1988). Carboxylation is considered the irreversible step of photosynthesis (Park & Epstein, 1960; O'Leary, 1981), so the ratio of $^{13}C/^{12}C$ at the site of carboxylation reflects how $^{13}C/^{12}C$ diffused to the chloroplast, which is influenced by the water film. Thus, $\delta^{13}C_{BULK}$ reflects a shift in water availability and productivity. By understanding the relationship between carbon assimilation and water availability, mosses have the potential to be long term environmental proxies in environments where water availability is dependent on temperature.

Moreover, the correlation between $\delta^{13}C_{BULK}$ and $\delta^{18}O_{BULK}$ in vascular plants often reflects the stomatal conductance in an evaporative environment (Barbour *et al.*, 2002) and the photosynthetic assimilation rate, which is driven by temperature, irradiance, and nutrient availability (Scheidegger *et al.*, 2000). The relationship between $\delta^{13}C_{BULK}$ and $\delta^{18}O_{BULK}$ in non-vascular plants reflects the diffusional limitation of CO_2, caused by a water film, which reflects the carbon isotope ratio available to RuBisCO (Xia *et al.*, 2020), and the evaporative enrichment of ^{18}O in metabolic leaf water (Sternberg & Ellsworth, 2011). Therefore, the relationship between $\delta^{13}C_{BULK}$ and $\delta^{18}O_{BULK}$ in mosses could be used to understand whether photosynthetic rates are more limited by water availability or biochemical constraints (Scheidegger *et al.*, 2000). By having a multi-proxy approach while investigating $\delta^{13}C_{BULK}$ and $\delta^{18}O_{BULK}$, a detailed understanding of the environmental conditions may be resolved.

Mosses are assumed to be slow-growing due to their simple and constrained physiology. Despite the abundance of mosses in a wide range of environments, there are limited studies on their growth rates (Watson, 1975; Rincon & Grime, 1989). Most studies on the growth and productivity of mosses have been restricted to unbranched moss species and to specific environments (Rincon & Grimes, 1989), where species of the Polytrichaceae family are commonly used to investigate the growth rates of mosses (Longton, 1970; Watson, 1975; Green & Clayton-Greene, 1981). Members of the Polytrichaceae are easy to differentiate from other moss families due to their distinct features, including their relatively large size and specialized laminas covered with photosynthetic lamellae (Bell *et al.*, 2021). Polytrichaceae are typically found in isolated, homogeneous colonies, making them ideal candidates for labelling and measuring the growth of individual shoots (Rincon & Grime, 1989). Watson (1975) and Longton (1970) both observed a seasonal growth pattern in leaf morphology for *Polytrichum commune* in temperate (Watson, 1975) and Antarctic regions (Longton, 1970). The annual growth rate for *P. commune* observed in temperate forests was 4.55 ± 2.94 mm (Watson, 1975), compared to the annual growth rate of 3.6 mm in Antarctic regions (Longton, 1970). Additionally, Green and Clayton-Green (1981) recorded the annual growth rate of *D. superba*, which varied with microclimatic conditions. The fastest growth rate found in this investigation was 48 mm annually – one of the highest growth rates recorded for an unbranched terrestrial moss (Green & Clayton-Greene, 1981). Since *D. superba* have been observed to reach lengths of > 50 cm, the $\delta^{18}O$ and $\delta^{13}C$ have great potential to record seasonal variations in temperature and precipitation for the past decades.

As $\delta^{18}O$ and $\delta^{13}C$ have the potential to record seasonal variations in tropical regions, the same principles can be applied to *D. superba* stems to track seasonal variations in $\delta^{18}O_{PRECIP}$. Additionally, *D. superba* typically grows near upturned tree roots (Green & Clayton-Greene, 1981). If *D. superba* stems reflect seasonal changes, the age of the clump can be calculated based on seasons, which could be applied to understand regeneration of temperate forest in tree fall gaps.

3.1.1 Aims and objectives

The aim of this research was to measure and interpret the carbon and oxygen stable isotope composition in *D. superba*. Additionally, we propose the use of stable isotopes as a novel method to estimate growth rates and age of *D. superba,* based on seasonal changes that are observed in $\delta^{18}O_{BULK}$. This was achieved by taking small transverse sections at 10 mm intervals to analyze the carbon and oxygen composition.

3.2 Materials and methods

3.2.1 Sample site

D. superba samples were collected from a temperate forest in the Rangitoto Ranges, New Zealand (lat. 38.33°S, 175.47°E) during December 2021. The surrounding forest is a protected, mature Podocarp Forest, comprised predominantly of *Podocarpus totara, Beilschmiedia tawa*, and tree ferns in the lower elevation. The mean annual temperature is 10.3°C and the mean annual rainfall is 1830 mm (King, 2015).

Whole *D. superba* plants were collected from large, healthy clumps found in the understory. An individual shoot was carefully removed from each clump, taking care to minimize damage to the plant and transferred into a ziplock bag. A total of four stems were taken. One stem (stem four) was taken from a previously sampled site, therefore, the relative time of emergence of stem four was known. Unlike the other three stems that were growing on the forest floor, stem four was growing on a fallen tree fern. Moss samples were kept in large ziplock bags and stored in a fridge at the University of Waikato to be sectioned.

3.2.2 Sample preparation

D. superba were stripped of all lamina, scales, and rhizoids so only the stem was sampled. The stems were hand sliced into 10 mm transverse sections using a double-edged blade and the organic matter was dried to a constant mass at 60 °C. 0.4 mg of stem was hand sliced from the bottom of each sample for $\delta^{18}O$ analyses and 2 to 4 mg of dried stem material were taken from the top of each section for $\delta^{13}C$ analyses. For $\delta^{18}O$, the organic material was transferred into individual 5 x 3 mm silver capsules (Sercon., Cheshire, UK), and the organic material for $\delta^{13}C$ analysis were transferred into 5 x 3 mm tin capsules (UFS, Tauranga, NZ). The carbon and oxygen isotope analyses were taken at the Center of Stable Isotopes in Geochemistry (CSIB) (Berkley University, California, USA). $\delta^{18}O$ values were determined in a continuous flow using an Elementar Pyro Cube (Elementar, Elementar Americas, Inc., Mt. Laurel, NJ) interfaced to a GVI IsoPrime mass spectrometer (Elementar, Elementar Americas, Inc., Mt. Laurel, NJ). The precision for the analysis for replicated samples was ± 0.20 ‰. $\delta^{13}C$ values were determined by a continuous flow dual isotope analysis using a CHNOS Elemental Analyser (Elementar, Elementar Americas, Inc., Mt. Laurel, NJ) interfaced to an IsoPrime 100 mass spectrometer (Elementar, Elementar Americas, Inc., Mt. Laurel, NJ). The precision of the analysis was ± 0.10 ‰.

3.2.3 Environmental data and modelling $\delta^{18}O_{PRECIPITATION}$

Measured $\delta^{18}O_{PRECIP}$ from more than 55 sites around New Zealand between 2007 and 2010 (Frew *et al.*, 2011) was used to predict the oxygen isotopic composition of precipitation at Rangitoto Ranges. To model the $\delta^{18}O_{PRECIP}$, all available environmental data from weather stations around New Zealand between 2007 to 2010 was obtained from CliFlo (https://cliflo.niwa.co.nz, NIWA). These environmental parameters included relative humidity (%), rainfall (mm), minimum temperature (°C), maximum temperature (°C), site elevation, latitude, and longitude. Simple linear regression models between the measured $\delta^{18}O_{PRECIP}$ and the environmental data were conducted to find which environmental parameter best correlated with the measured $\delta^{18}O_{PRECIP}$. The results from this analysis indicated only minimum temperature (°C) had a consistent statistically significant correlation with measured $\delta^{18}O_{PRECIP}$.

To test the accuracy of the predictive model, monthly equations formulated from the simple linear models were used to predict $\delta^{18}O_{PRECIP}$ at five sites closest to Rangitoto Ranges: Rotorua, Hamilton, Waikato, Tauranga, and Taupo (Table. 3.1). Predicted $\delta^{18}O_{PRECIP}$ corresponded well with the measured values at these sites, except when the measured values were either very enriched or very depleted in $\delta^{18}O$ (see Appendix Fig. A.2).

As there were no weather stations at the Rangitoto Ranges, environmental records were taken from Pureora Forest as it is the closest site to Rangitoto Ranges. The monthly linear regression models were applied to Pureora's monthly mean minimum temperature to predict $\delta^{18}O_{PRECIP}$ from January 2017 to June 2022.

Table 3.1. Summary of the simple linear regression outputs for monthly minimum temperature (°C) and $\delta^{18}O_{PRECIP}$ for all weather stations in New Zealand between 2007 to 2010. The simple linear regression models were significant for all months except February (p = 0.3). The summary output was used to model the oxygen isotope composition of precipitation at Pureora Forest, New Zealand.

Month	R^2	P value	Slope	intercept
January	0.2060	1.7×10^{-7}	0.3802	-9.2086
February	0.0079	0.3471	0.0662	-7.2414
March	0.1129	4.0×10^{-4}	0.3126	-8.8689
April	0.0983	1.2×10^{-3}	0.1932	-8.0021
May	0.2074	9.3×10^{-7}	0.3656	-9.7372
June	0.2889	5.7×10^{-9}	0.3281	-8.9279
July	0.1219	5.6×10^{-4}	0.2229	-9.0303
August	0.5416	1.7×10^{-26}	0.5383	-10.2882
September	0.3494	9.5×10^{-15}	0.5396	-9.6274
October	0.5325	7.0×10^{-25}	0.5509	-9.4885
November	0.2078	1.9×10^{-8}	0.4385	-8.2584
December	0.2471	4.1×10^{10}	0.4694	-10.5723

3.2.4 Data analysis

The values of $\delta^{18}O_{PRECIP}$, $\delta^{18}O_{BULK}$, and $\delta^{13}C_{BULK}$ were graphed using Excel (Corporation, 2018). The relationship between $\delta^{18}O_{BULK}$ and $\delta^{13}C_{BULK}$ of the moss samples were statistically analysed with simple linear regression models in R Studio (RStudio, 2020) and graphed using the ggplot2 package (Wickham, 2016). The correlation between $\delta^{18}O_{BULK}$ and $\delta^{13}C_{BULK}$ was analysed with Pearson's correlation tests. The correlation test between $\delta^{18}O_{BULK}$ and $\delta^{13}C_{BULK}$ of stem four was excluded from this analysis due to only having three data points.

3.3 Results

3.3.1 $\delta^{18}O_{PRECIP}$ and seasonal variation

$\delta^{18}O_{PRECIP}$ was predicted to peak in enrichment one to three months before mean daily minimum temperature were at a peak (Fig.3.1). Estimated $\delta^{18}O_{PRECIP}$ was the most enriched during November to January months and became more depleted towards June, with minimum values between June and August (Fig.3.1.i). The seasonal amplitude of $\delta^{18}O_{PRECIP}$ during 2020 to 2022 was consistently 4.2 ‰.

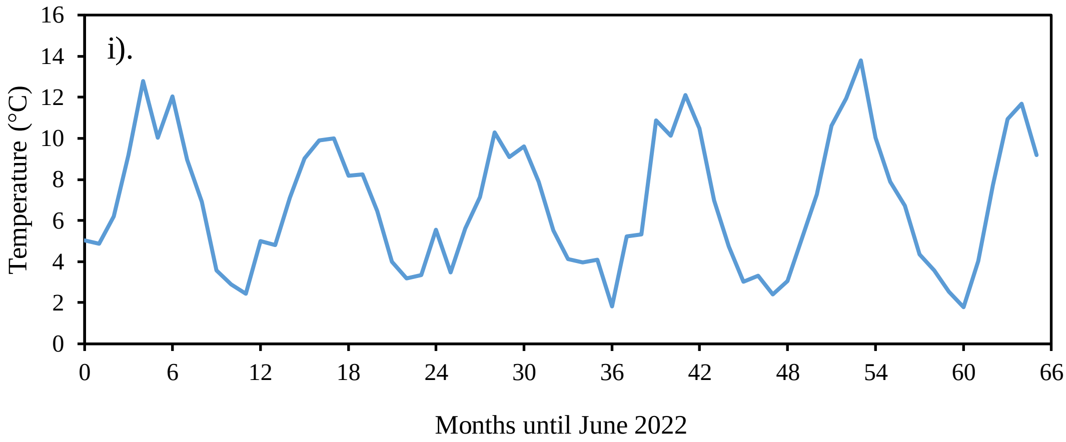

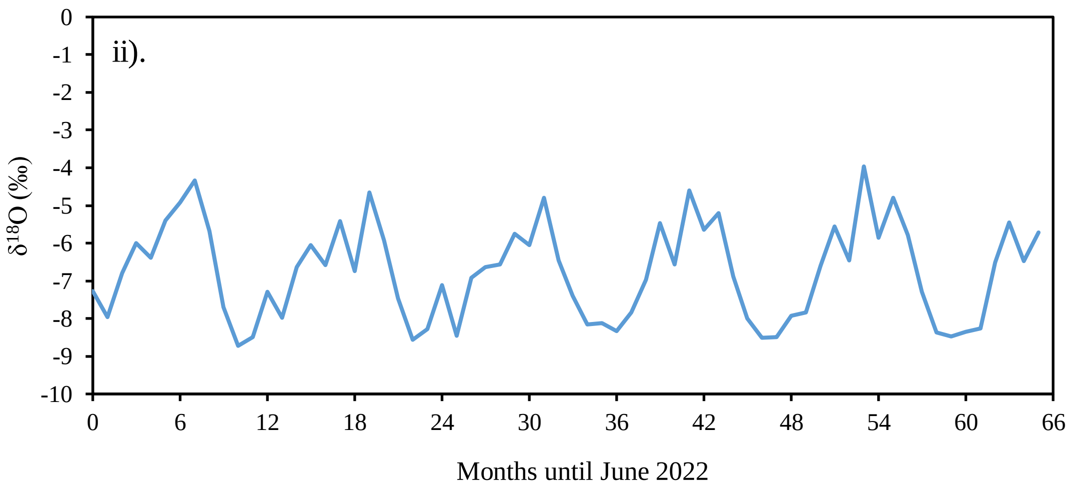

Figure 3.1. i) Mean monthly minimum temperature (°C) recorded at the Pureora Forest weather station from January 2017 to June 2022. ii) Modelled $\delta^{18}O_{PRECIP}$ based on the mean minimum monthly temperature recorded at the Pureora Forest weather station from January 2017 to June 2022. The y axis begins at June 2022 and descends back in time.

3.3.2 δ^{18}O values of *D. superba* stems

$\delta^{18}O_{BULK}$ values of the *D. superba* stems varied from 29 to 24‰ (Fig. 3.2). The tip of stem four was more depleted in δ^{18}O than the other tips. The tip of stem four had an oxygen isotope value of 24.7‰, while the other growing tips had oxygen isotope values of 26.5‰ to 27.3‰. The oxygen isotope values became more depleted from the growing tips of stem one, two, and three, to approximately 20 cm (~ -2‰). After this point, δ^{18}O increased again until approximately 40 cm from the growing tip (+2‰). $\delta^{18}O_{BULK}$ was variable between 40- 60 cm from growing tip. The average amplitude of all stems was less than 2‰.

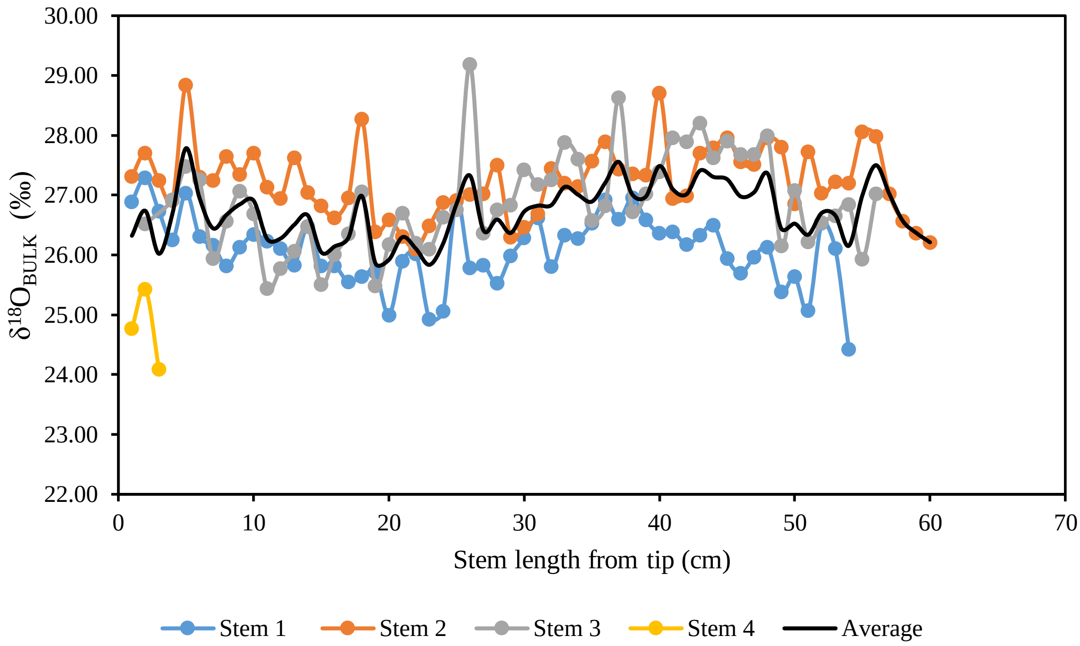

Figure 3.2. Oxygen isotope composition of cellulose ($\delta^{18}O_{BULK}$) of *D. superba* along the length of individual stems. The yellow line represents the δ^{18}O captured in a *D. superba* stem from December 2021 to March 2022.

3.3.3 $\delta^{13}C_{BULK}$ values of *D. superba* stems

$\delta^{13}C_{BULK}$ values ranged from -28.5‰ to -34.8‰ (Fig. 3.3). The general trend was that $\delta^{13}C_{BULK}$ became more depleted with distance from the moss tip. The slope of the trend indicated that $\delta^{13}C_{BULK}$ decreased by 0.07‰ with every 1 cm increase in distance from the stem tip ($\delta^{13}C_{BULK}$ = 0.0713 x length (cm) – 29.534).

The tip of the stems had $\delta^{13}C_{BULK}$ values that ranged from -28.5 to -31 ‰. Stems one, three, and four had similar $\delta^{13}C_{BULK}$ values down the stem but stem two deviated from the trend at approximately 42 cm from the growing tip. At this point, stem two rapidly became depleted in $\delta^{13}C$ as the value went from -32‰ to -34‰. Stem two remained more depleted than the other stems.

The base of stem four was more enriched than the other growing tips sampled. The carbon isotope value at the base of stem four was -28‰ while the growing tip had a carbon isotope value of -31‰. The trend observed in stem four is the opposite of what was observed in the other stems. However, the carbon isotope values of stem four still fit with the carbon isotope values of the other stem growing tips.

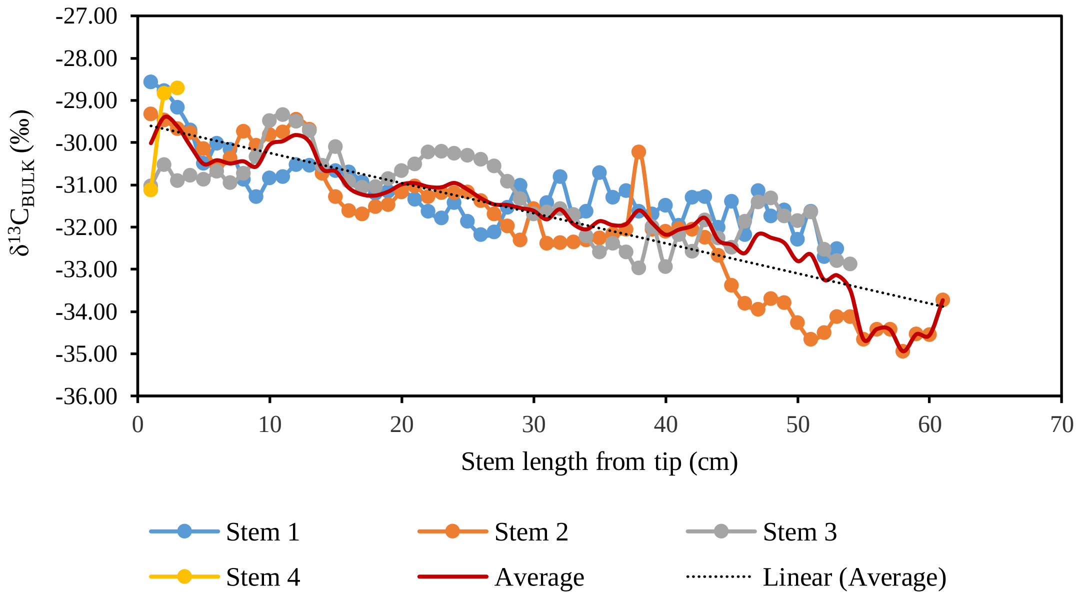

Figure 3.3. $\delta^{13}C_{BULK}$ of *D. superba* from tip to base. Each line represents a different stem collected from isolated patches. The yellow line represents the $\delta^{13}C$ captured in a *D. superba* stem from December 2021 to March 2022. The red line represents the average $\delta^{13}C_{BULK}$ values of the stems and the black dotted line represents the line of best fit ($\delta^{13}C_{BULK}$ values = 0.0713 x length (cm) – 29.534).

3.3.4 Correlations between $\delta^{18}O$ vs $\delta^{13}C$ bulk tissue

The slope between $\delta^{18}O_{BULK}$ and $\delta^{13}C_{BULK}$ varied greatly between the individual stems (Fig. 3.4). Stem one had a negative slope, with a decrease of 0.4‰ in $\delta^{18}O_{BULK}$ per 1‰ increase in $\delta^{13}C_{BULK}$. The relationship between $\delta^{18}O_{BULK}$ and $\delta^{13}C_{BULK}$ for stem one was statistically significant ($p = 0.0487$), and Pearson's correlation was -0.27. The majority of the data points clumped within the range of -30 to -32‰ $\delta^{13}C_{BULK}$ and 25.6 to 27‰ $\delta^{18}O_{BULK}$ (Fig. 3.4a).

There was no significant relationship in stem two ($p = 0.7722$; Fig. 3.4b). There was a slight negative slope in the relationship, as for every 1‰ increase in $\delta^{13}C_{BULK}$, $\delta^{18}O_{BULK}$ decreased by -0.12‰. The correlation between $\delta^{18}O_{BULK}$ and $\delta^{13}C_{BULK}$ of stem two was Pearson's $r = -0.03$. Most of the scatter was outside of the 95% confidence interval.

Stem three had a significant positive slope ($p < 0.001$), as $\delta^{18}O_{BULK}$ increased by 0.46‰ for every 1‰ increase in $\delta^{13}C_{BULK}$. $\delta^{18}O_{BULK}$ and $\delta^{13}C_{BULK}$ of stem three was somewhat correlated as Pearson's coefficient was 0.56 (Fig. 3.4c). Most of the scatter was outside the 95% confidence interval but the scatter increased positively.

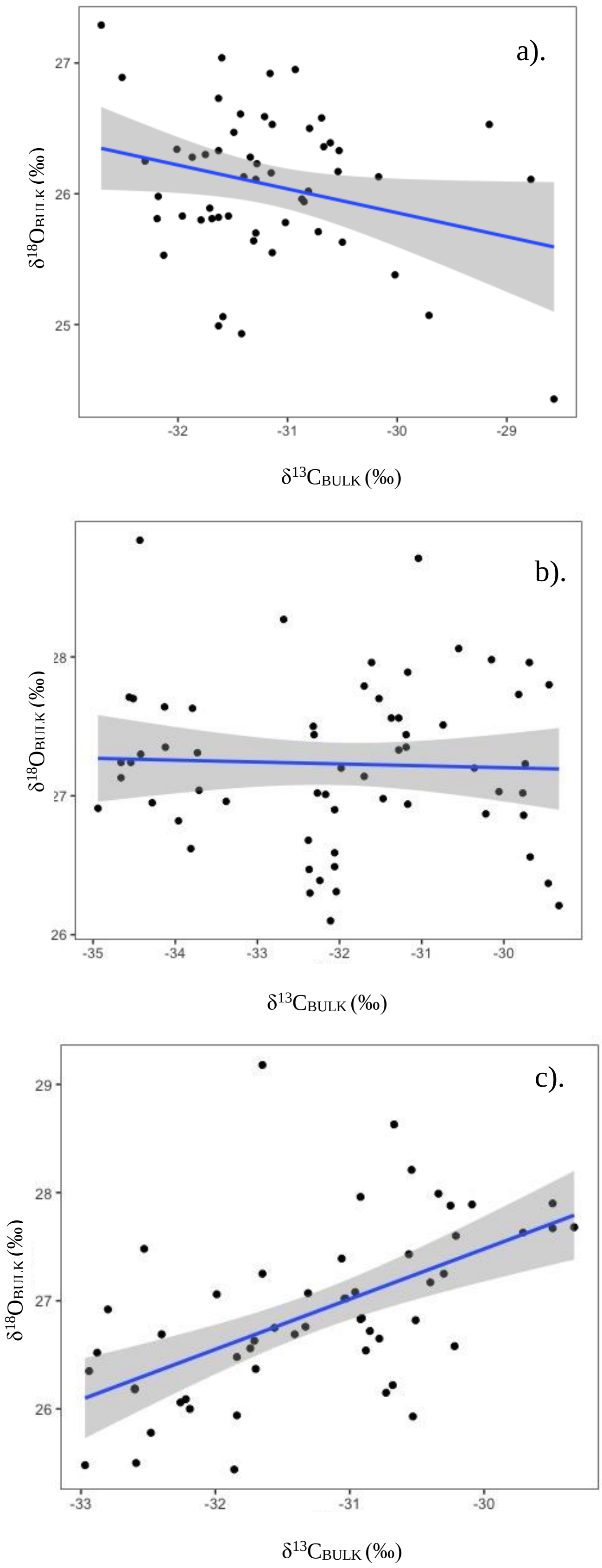

Figure 3.4. Simple linear regression models for the relationship between $\delta^{18}O$ and $\delta^{13}C$ of bulk tissue for a) stem 1, b) stem 2, and c) stem 3. For all graphs, the blue line represents the line of best fit and the grey space represents the 95% confidence interval. The simple linear regression models were: a) $\delta^{18}O_{BULK}$ = -0.41*$\delta^{13}C_{BULK}$ – 20.6, b) $\delta^{18}O_{BULK}$ = -0.11*$\delta^{13}C_{BULK}$ – 20.1 c) $\delta^{18}O_{BULK}$ = 0.45*$\delta^{13}C_{BULK}$ +41.4.

3.4 Discussion

The observations from this study demonstrated that stable isotopes can be used as a proxy for environmental seasonal variation and growth rates for unbranched mosses. The results indicated that $\delta^{18}O_{BULK}$ reflected the seasonal variation in $\delta^{18}O_{PRECIP}$, driven by temperature, but $\delta^{13}C_{BULK}$ did not. Surprisingly, the relationship between $\delta^{13}C_{BULK}$ and $\delta^{18}O_{BULK}$ was not consistent between the three stems analysed.

The seasonal amplitude of $\delta^{18}O_{BULK}$ compared to $\delta^{18}O_{PRECIP}$ was slightly lower than expected (2‰, and 4‰, respectively). The difference between $\delta^{18}O_{BULK}$ and predicted $\delta^{18}O_{PRECIP}$ was approximately +33‰, a value that compares well with the observed ^{18}O biochemical fractionation during cellulose synthesis of +27 ± 3 ‰ (De Niro & Epstein, 1979). This fractionation process is temperature dependent, with a particular sensitivity to low temperatures (5 to 10 °C) (Sternberg & Ellsworth, 2011). At low temperatures, the biochemical fractionation factor could be as large as +31‰ (Sternberg & Ellsworth, 2011). A similar pattern of seasonality of $\delta^{18}O_{BULK}$ with a similar seasonal amplitude difference with $\delta^{18}O_{PRECIP}$ was observed in *Sphagnum*-dominated peat bogs in Patagonia (Xia *et al.*, 2020). The results from this analysis suggest the understorey of Rangitoto Ranges had relatively low temperatures, as indicated by the difference in the oxygen isotopic composition of *D. superba* bulk tissue and precipitation.

Another possibility in the trends observed in $\delta^{18}O_{BULK}$ is the effect of *D. superba*'s lamellae. The lamellae are hypothesized to help regulate water loss in a manner similar to the stomata of vascular plants (Marschall & Proctor, 2004). As there is an inverse relationship between temperature and relative humidity (Sakurai *et al.*, 2021), the difference between expected and observed $\delta^{18}O$ could be caused by evapotranspiration. As the temperature increases, the air becomes drier and relative humidity decreases, which subsequently increases the rate of evapotranspiration (Rebetez *et al.*, 2003). When hydrated, the lamellae act as a ventilated system to allow rapid exchange of water and CO_2 between the leaf and atmosphere (Brodribb *et al.*, 2020). But as the plant begins to experience water stress, the leaf margins curl inwards causing the lamellae to restrict gas exchange (Carriqui *et al.*, 2019). The non-stomatal diffusive conductance may cause some leaf water enrichment like that observed in vascular plants. However, until there are sufficient data on the oxygen isotope composition of evaporated water from *D. superba*, it is difficult to say with certainty whether the lamellae influenced leaf water oxygen isotope composition, and in turn, affected $\delta^{18}O_C$.

As *D. superba* grew higher above the forest floor, $\delta^{13}C_{BULK}$ increased. The two major sources of CO_2 in a forest environment are from the atmosphere and ecosystem respiration (Schleser & Jayasekera, 1985), with ecosystem-respired CO_2 being relatively depleted in ^{13}C compared to atmospheric CO_2. Previous studies of the vertical $^{13}CO_2$ profile suggest turbulent mixing of the two sources within the canopy so that carbon fixed during photosynthesis is more depleted near the soil surface than at the top of the canopy (Broadmeadow *et al.*, 1992; Kao *et al.*, 2000). The vertical $\delta^{13}C$ profile of a temperate rainforest becomes exponentially less depleted from the forest floor but is constant from approximately 3 m above forest floor to the upper canopy (Tissue *et al.*, 2006), indicating turbulent mixing of air within the canopy. $\delta^{13}C_{BULK}$ in the moss became less negative as the plant grew above the forest floor, perhaps indicating the moss was fixing CO_2 increasingly less influenced by soil respiration. The $\delta^{13}C_{BULK}$ of stem four was relatively less depleted than the other stems, possibly reflecting the $^{13}CO_2$ concentration at height above the forest floor, as it was collected from a fallen tree fern.

Similarly, $\delta^{13}C_{BULK}$ in the stems of *D. superba* were stable between the base to 20 cm from the base, likely reflecting the $\delta^{13}C$ of CO_2 within the soil pore space. Bowling et al. (2015) found the $\delta^{13}C$ in the soil pore space was most enriched at the surface, with $\delta^{13}C$ values of -17‰ at the forest floor which rapidly depleted by 5‰ at 10 cm depth. The $\delta^{13}C$ values of the soil pore space remained constant with depth with the value of -19‰. We found that the lower 30 cm of stem one and three in this study were quite isotopically constant, with values ranging between -31.3 to -32.2‰ for stem one and -31.8 to -32.6‰ for stem three. It is likely that only 30 cm of the plant was above ground and $\delta^{13}C_{BULK}$ of *D. superba* stems from 30 cm to the base reflects the soil CO_2 $\delta^{13}C$ composition at depth.

Interestingly, the relationship between $\delta^{13}C_{BULK}$ and $\delta^{18}O_{BULK}$ varied greatly between the three stems sampled in this study. The relationship of $\delta^{13}C_{BULK}$ and $\delta^{18}O_{BULK}$ for vascular plants often depends on environmental VPD and water availability (Barbour *et al.*, 2002). Barbour et al (2002) predicted that a change in VPD alone would have a greater influence on $\delta^{18}O$ than $\delta^{13}C$, and stomatal conductance (which is influenced by water availability) would influence both $\delta^{18}O$ and $\delta^{13}C$. The relationship between $\delta^{18}O$ and $\delta^{13}C$ in *D. superba* stems from this study suggests differences in the microclimate, despite only being a few 100 m apart. To understand the water relations of *D. superba* and their environment, future studies should monitor microclimatic variables over many seasons to track the seasonal variations in VPD and soil moisture content.

The results from this study suggest a faster growth rate than that observed by Green and Clayton-Green (1981). Based on their recorded growth rate, the samples used in this study would have an estimated age of 16 years. However, the shoots in this study are likely to be approximately 1.5 years old, based on the seasonal variations in the isotopic composition of oxygen recorded in the moss cellulose. Like other members of the Polytrichaceae, *D. superba* has unique morphological features that are distinctive of this family (Atala & Alfaro, 2013; Bell *et al.*, 2021). These features include a conductive system, below ground rhizoids, and specialized structures, known as lamellae, on the upper surface of the leaves (Marschall & Proctor, 2004; Proctor, 2013; Brodribb *et al.*, 2020). A comprehensive study by Marschall and Proctor (2004) found a relatively high chlorophyll content and a high rate of relative electron transfer rate comparable to vascular plants. Furthermore, the rhizoids can uptake and transport water from the soil to the leaves and sustain high rates of photosynthesis (Brodribb *et al.*, 2020). These features may allow *D. superba* to withstand life above the forest floor boundary layer and maintain hydrated for photosynthesis.

Moreover, the lack of seasonality of $\delta^{13}C_{BULK}$ values suggests *D. superba* at this site was growing continuously. This supports the growth observed in the study by Watson (1975), but contrasts with the situation found in the Antarctic population (Longton, 1970). This study and Watson (1975) were conducted in temperate regions, where water availability is controlled by precipitation, whereas the water availability in Longton's (1970) study is largely influenced by the freeze-thaw pattern characteristic of polar regions (Jouzel & Merlivat, 1984). The results from this analysis were more similar to the trends observed in $\delta^{13}C_{BULK}$ by Watson (1975) than Longton (1970).

Chapter 4
Relationship between the stable carbon and oxygen isotopic composition of *Sphagnum cuspidatum* bulk tissue and source water

1.1 Introduction

Mosses are part of the phylogenetic group known as Bryophytes, which are hypothesized to reflect 'primitive' land plants (Royles *et al.*, 2014). Like all bryophytes, mosses are dominated by the haploid gametophyte stage, which lacks stomata, and often lacks a differentiated vascular system. The relationship mosses have with water is particularly important as they require water to facilitate sexual reproduction (Clymo & Hayward, 1982), and the lack of stomata means absorption of water is necessary to maintain a positive water balance (Royles *et al.*, 2014). Mosses are typically found in higher latitudes, where vascular plants are often constrained (Porada *et al.*, 2013). *Sphagnum* moss makes up 80-100% of the vegetation composition of peat banks (Porada *et al.*, 2013). *Sphagnum* have the unique ability to modify their environment by forming peat when they die (Clymo & Hayward, 1982; Hajek & Beckett, 2008). Peat forming environments tend to be anoxic, acidic, and depleted in nutrients (Bengtsson *et al.*, 2016). These conditions created by deposited *Sphagnum* mean that the annual net primary productivity exceeds the annual decomposition rate, and the carbon fixed in plant tissue is stored within the system (Frolking *et al.*, 2001).

Not only are peat environments and peat mosses extremely important as a global carbon storage pool, they are also are the dominant vegetation type where vascular plants are constrained – such as in Antarctica (Robinson *et al.*, 2018). What was once a stable and predictable environment, Antarctica is now experiencing rapid changes (Royles & Griffiths, 2015), and is likely to be among the first environment to be affected by the onset of climate change (Wasley *et al.*, 2006). Climate change is predicted to elevate surface temperatures, and increase precipitation (Ye & Mather, 1997). Presently, climatic variations in Antarctica are measured primarily with meteorological instruments and ice cores (Royles *et al.*, 2012b). However, meteorological measurements began in the 1950s

(Royles *et al.*, 2012b), and ice cores only produce centennial to millennial-scale variations that primarily reflect winter conditions and snow formation (Schneider *et al.*, 2006). Consequently, there is a need for a sensitive proxy to monitor microclimatic changes in Antarctica (Royles *et al.*, 2012b). Peat banks in Antarctic regions vary in their age, accumulation rate, and continuity, with the oldest dating back 5500 years (Björck *et al.*, 1991). As peat accumulation rates depend on enzymatic processes involved during photosynthesis, influenced by water availability, peat cores provide invaluable evidence of periods where climatic conditions supported photosynthesis (Royles & Griffiths, 2015). Therefore, the stable isotope composition of mosses in Antarctic peat banks are suggested to contain a valuable environmental record. However, interpretations of the stable isotope values fixed in cellulose is often complex due to multiple factors influencing the ratios at which isotopes are fixed, and species specificity to environmental changes.

In general, the oxygen isotope composition in plant tissue depends on the isotopic composition of the water sources, isotope enrichment associated with evaporation from the plant surfaces, and biochemical fractionation (Dawson *et al.*, 2002; Barbour, 2007). This process can be expressed as a modified Craig–Gordon model (Sauer *et al.*, 2001):

$$\delta^{18}O_{\ cell} = \delta^{18}O_{\ SW} + \delta_b + (\varepsilon_e + \varepsilon_k)(1 - h), \qquad [4.1]$$

where $\delta^{18}O_{SW}$ is the isotopic composition of source water, δ_b is the biochemical fractionation, ε_e is the liquid-vapour equilibrium fractionation effects associated with leaf water enrichment, ε_k is the liquid-vapour kinetic fractionation effects associated with evaporation, and h is relative humidity. Equation 4.1 can be altered to account for differences in the biophysics and biochemistry of different plant functional groups and species. As mosses are unable to regulate their water content due to the lack of stomata, they are frequently in equilibrium with the relative humidity of their environment (Proctor, 1993). Therefore, for mosses, Equation 4.1 can be simplified to account for their simple physiology (Zanazzi & Mora, 2005):

$$\delta^{18}O_{\ cell} = \delta^{18}O_{\ SW} + \varepsilon_b, \qquad [4.2]$$

Experimental and observational measurements indicate the biochemical fractionation factor is 27 ± 3‰ (De Niro & Epstein, 1979; Sternberg *et al.*, 1986). This constant factor is caused by the hydration of carbonyl intermediates during cellulose synthesis (De Niro & Epstein, 1979). The biochemical fractionation is sensitive to low temperatures, and increases to 31‰ at temperatures around 5°C (Sternberg & Ellsworth, 2011). The biochemical fractionation at different temperatures can be expressed by (Sternberg & Ellsworth, 2011):

$$e_{bio}(i,j) = \left[\frac{\delta_{cell}(i,j) - (0.58\ x\ \delta_{NE})}{0.42}\right] - \delta_{SW}(i,j), \qquad [4.3]$$

where $\delta_{cell}(i,j)$ and $\delta_{SW}(i,j)$are the oxygen isotope ratios of cellulose and water, with water enrichment *I* and temperature *j*, and δ_{NE} is the non-exchangeable oxygen during fixed in carbohydrate intermediates at enrichment *i* and temperature *j* (Sternberg *et al.*, 2006).

Since the biochemical fractionation is generally considered constant under temperatures relevant to biophysiological processes, changes in $\delta^{18}O$ of plant tissue are hypothesized to only reflect changes in $\delta^{18}O_{SW}$ at the time of cellulose synthesis.

As mosses require the presence of bioavailable water, $\delta^{13}C_{BULK}$ could reflect their photosynthetic activity. Differences in stable carbon isotope values reflect degrees of limitation of photosynthesis by diffusion resistance during CO_2 uptake, and differences in the isotope ratios of source CO_2 (Proctor *et al.*, 1992). In mosses, the total resistance to CO_2 diffusion is the sum of atmospheric boundary layer resistance (r_a) and the internal resistance (r_L) (Proctor, 1982). The fractionation of $^{13}CO_2$ during dissolution and diffusion within water is approximately 1.8‰ (O'Leary, 1988; Farquhar *et al.*, 1989a). Additionally, $^{13}CO_2$ is slower to react biochemically than $^{12}CO_2$, and RuBisCO can express a maximum biochemical discrimination against $^{13}CO_2$ of up to 29‰ (O'Leary, 1988).

The presence and thickness of a surface water film and the density of plant tissue determines the relative dominance and magnitude of diffusion over metabolic fractionation (Royles *et al.*, 2014). At low temperatures, water freezes and becomes biologically unavailable for plant use (Wasley *et al.*, 2006). Therefore, the growth of mosses reflect the freeze-thaw patterns, which is influenced by temperature. When the moss is not submerged, the stable carbon isotope signature depends mostly on the concentration and isotopic composition of CO_2 in the chloroplast, which alters isotope discrimination during biochemical fixation of CO_2 (Farquhar *et al.*, 1989a). The concentration of CO_2 in moss chloroplasts is determined by temperature, light availability, partial pressure, and the plant water status (Royles *et al.*, 2014). Therefore, stable carbon isotopes fixed within mosses maybe an integrated measure of the bioavailability of water as a result of the preferential fixation of the lighter carbon by RuBisCO (Farquhar *et al.*, 1989a; Rice & Giles, 1996).

Together, tissue carbon and oxygen isotope composition of moss and peat are controlled by both environmental factors at the micro– and macro– scale, and by the species-specific differences that relate to water balance and carbon dynamics (Granath *et al.*, 2018). Despite its potential as a climatic archive, the application of peat cellulose as a paleoclimate proxy is still uncertain (Zanazzi & Mora, 2005). There are limited studies that have systematically investigated the variation in cellulose oxygen isotope ratios. Our understanding of the isotopic variations in *Sphagnum* has greatly improved in recent years (Xia *et al.*, 2020). However, most of the studies are field-based observations, with limited control of environmental conditions. This study aims to investigate the relationship between $\delta^{18}O_{SW}$ and $\delta^{18}O_{BULK}$ of *Sphagnum* in a laboratory environment.

1.1.1 Aim and objective

The aim of this research was to understand the relationship between moss tissue $\delta^{18}O$ and their water environment for future climate reconstruction. To do so, mosses were grown under laboratory conditions and treated with different isotopically labelled water. New moss tissue was harvested and analysed for $\delta^{18}O_{BULK}$ composition.

1.2 Materials and methods

1.2.1 Plant materials

S. cuspidatum was purchased from an online website during January 2021 and again during November 2021 (https://www.magicmoss.co.nz). The moss originated from the Maruia Basin, on the western side of the alpine fault of the South Island, New Zealand. A preliminary trial was undertaken to understand the conditions required to maximize growth rate. The first set of moss was grown in two 322 mm x 138 mm transparent containers. Each container was lined with approximately 3 cm of coarse pebbles for drainage with a sheet of shade cloth on top. A thin layer of activated charcoal was spread on top of the shade cloth to deter algal growth (see Appendix Fig. A.3). Generic potting mix was used as a growing medium for the *Sphagnum* and the mosses were misted with tap water from the University of Waikato, New Zealand. After a few weeks of growing, the mosses started to brown. It was concluded that possibly the chlorine in the tap water was causing this effect. Therefore, rainwater was collected during December 2021 and used to water the moss. The moss showed no reaction to rainwater, so the water collected was used throughout the experiment for watering. The rainwater collected during this period had an isotopic composition of -7.76‰ $\delta^{18}O$. The oxygen isotope ratio of rainwater and labelled waters were measured with an oxygen isotope vapour analyzer (IWA-35d-EP, Los Gatos Research, CA, US; see Chapter 2 for details).

1.2.2 Growing experiments

The *Sphagnum* mats were separated and placed in one of four 322 x 138 mm transparent containers under natural light in the Plant Physiology Laboratory at the University of Waikato, New Zealand. Each container was treated with a different labelled $\delta^{18}O$ water of 3.4, 21.7, 33.1, and 48.9‰. The mosses were rinsed with rainwater and all terrestrial debris were removed from the moss mats to ensure a pure culture of *S. cuspidatum* was used in this experiment.

Mosses were grown on a layer of potting mix with a thin layer of activated charcoal to deter algal growth. At the bottom of the container, a layer of coarse pebbles were used as a drainage system. The capitulum was gently pulled through the 2 cm holes in the bird cloth with another layer of stretched bird cloth on top. The capitulum were in line with the gaps of the top bird cloth layer to ensure that new growth grew between the gaps for accurate new growth harvest (see Appendix Fig. A.3 and Appendix Fig. A.4).

The mosses were misted with the labelled water twice a week to minimize dehydration. The edges of the container were sealed using reusable putty to restrict gas exchange with the room environment and to avoid excessive dehydration. Samples were cultivated for a period of six months from November 2021 to April 2022 and the new growth was harvested for stable isotope analysis at the end of the growing period. However, half of mosses treated with 21.7‰ $\delta^{18}O$ water possibly underwent photo-damage during January 2022 and became dormant throughout the remaining time of this experiment. The dormant mosses were not removed from the container and another growth chamber was set up in February 2022 with new moss and treated with 21.7‰ $\delta^{18}O$ water. The new sample of mosses were rinsed and cleaned of all terrestrial debris before the experiment started.

1.2.3 Sample preparation

After six months of growing, new growth of *S. cuspidatum* was harvested from three different locations in each container and placed in a paper drying bag. The organic material was dried at 60°C until the dry weight was stable. In preparation for $\delta^{13}C$ and $\delta^{18}O$ analyses, each sample was ground into a fine powder using a mortar and pestle. 0.4 mg of whole moss powder was weighed directly into silver capsules (Sercon., Cheshire, UK) and sealed for $\delta^{18}O_{BULK}$ analysis. Between 2 to 4 mg of whole moss powder was weighed directly into tin capsules (UFS, Tauranga, NZ) for $\delta^{13}C_{BULK}$ analysis. Stable isotope analyses were completed at the Center of Stable Isotopes in Biogeochemistry lab (Berkley University, USA). $\delta^{18}O$ values were determined in a continuous flow using an Elementar Pyro Cube (Elementar, Elementar Americas, Inc., Mt. Laurel, NJ) interfaced to a GVI IsoPrime mass spectrometer (Elementar, Elementar Americas, Inc., Mt. Laurel, NJ). The precision for the analysis for replicated samples was ± 0.20 ‰. $\delta^{13}C$ values were determined by a continuous flow dual isotope analysis using a CHNOS Elemental Analyser (Elementar, Elementar Americas, Inc., Mt. Laurel, NJ) interfaced to an IsoPrime

100 mass spectrometer (Elementar, Elementar Americas, Inc., Mt. Laurel, NJ). The precision of the analysis was ± 0.10 ‰.

1.2.4 $\delta^{13}C$ of CO_2 in growing containers and atmosphere

Measurements of the $\delta^{13}C$ of atmospheric CO_2 and $\delta^{13}C$ of atmospheric CO_2 growing containers were taken post-hoc. Containers were resealed after harvesting and left in the lab for a week. To measure the $\delta^{13}C$ of the containers, a 10 mm hole was drilled into the lid of each container. A plastic pipe was inserted into the hole and connected to a carbon dioxide isotope analyzer (Model 912-0003, Los Gatos Research, CA, US). The air was dried using drierite to reduce the H_2O concentration in the air stream entering the carbon isotope analyser (a water-concentration dependence of $\delta^{13}C$ was previously observed for this instrument). Three 5 L Tedlar bags (Supelco Inc, PA, US) were filled with air pumped from outside the building using an air compressor (Tooline AC2041, Tooline, CH, NZ) and also measured on the carbon dioxide analyser. The analyser was not calibrated, therefore $\delta^{13}C$ values serve only for comparison with outside air $\delta^{13}C$.

1.2.5 Data analysis

All data was analyzed using Excel (Microsoft Corporation, 2018). One data point from the +20‰ $\delta^{18}O_{SW}$ treatment was excluded from our analysis as the values for $\delta^{18}O_{BULK}$ and $\delta^{13}C_{BULK}$ were different from the other samples from the same container (Appendix Fig. A.5). Removing these data points did not significantly alter the results presented in this study (Fig. 4.2; Fig 4.3; Appendix Fig. A.5 and Appendix Fig. A. 6).

1.3 Results

Table 4.1. Summary of measured $\delta^{13}C$ of CO_2 in the atmosphere and in three growing containers. $\delta^{13}C$ values for atmospheric air is an average of two measurements.

Sample	$\delta^{13}C$ (‰)
Outside air	-9.3
21.7‰ container	-23.1
33.1‰ container	-22.0
48.9‰ container	-21.0

The growing containers were over twice as depleted in ^{13}C as atmospheric air (Table. 4.1). The average $\delta^{13}C$ of atmospheric air was -9.3‰. $\delta^{13}C$ values in the 33.1‰ and 48.9‰ were similar with 22.0‰ and 21.0‰ respectively. The 21.7‰ growing chamber was slightly more depleted as $\delta^{13}C$ was -23.1‰.

1.3.1 $\delta^{13}C$ of the new growth of *S. cuspidatum*

The $\delta^{13}C$ values of the growing tips were very depleted, with the majority of the samples ranging from -41 to -42‰ (Fig. 4.1). Sphagnum treated with 21.7‰ $\delta^{18}O$ water had $\delta^{13}C$ values that ranged from -44.5 to -45.5‰, which was 3‰ more depleted than the growing tips in the other growing chambers.

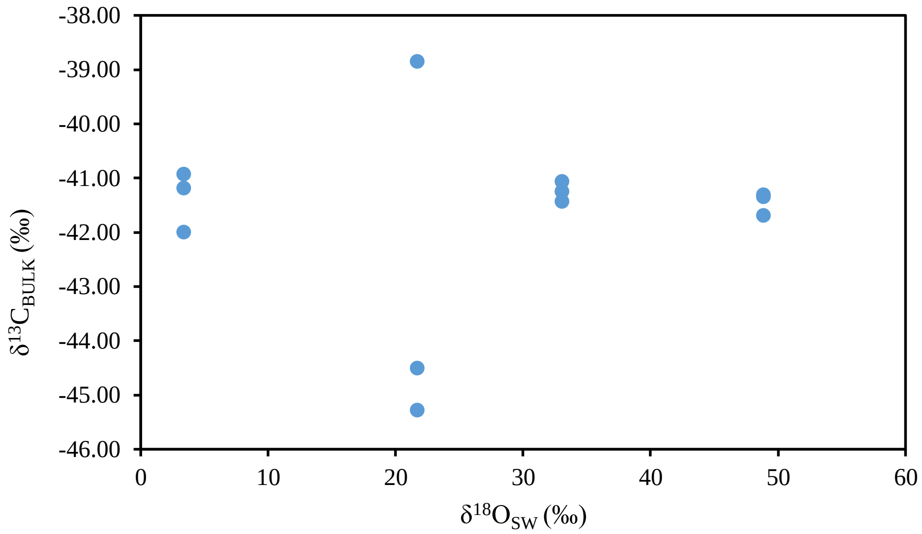

Figure 4.1. Carbon isotope values of the bulk tissue in the *S. cuspidatum* growing tips. Each blue dot represents a sample datapoint.

1.3.2 $\delta^{18}O$ values of growing tips bulk tissue

There was a strong positive relationship between the oxygen isotope composition of source water and moss bulk organic tissue (r^2 = 0.9707) (Fig. 4.2). The fit of this relationship indicated that the isotopic composition of source water explained 97% of the variation in cellulose oxygen isotope values.

The relationship between $\delta^{18}O_{SW}$ and $\delta^{18}O_{BULK}$ followed the equation:

$$\delta^{18}O_{BULK} = 0.17\ \delta^{18}O_{SW} + 25.93\ ‰, \qquad [4.4]$$

which indicated $\delta^{18}O_{BULK}$ increased by 0.17‰ with every 1‰ increase in $\delta^{18}O_{SW}$. The slope from our experiment was shallower compared to the theoretical slope of the relationship between $\delta^{18}O_{BULK}$ and $\delta^{18}O_{SW}$, with a slope of one (Eqn. 4.2).

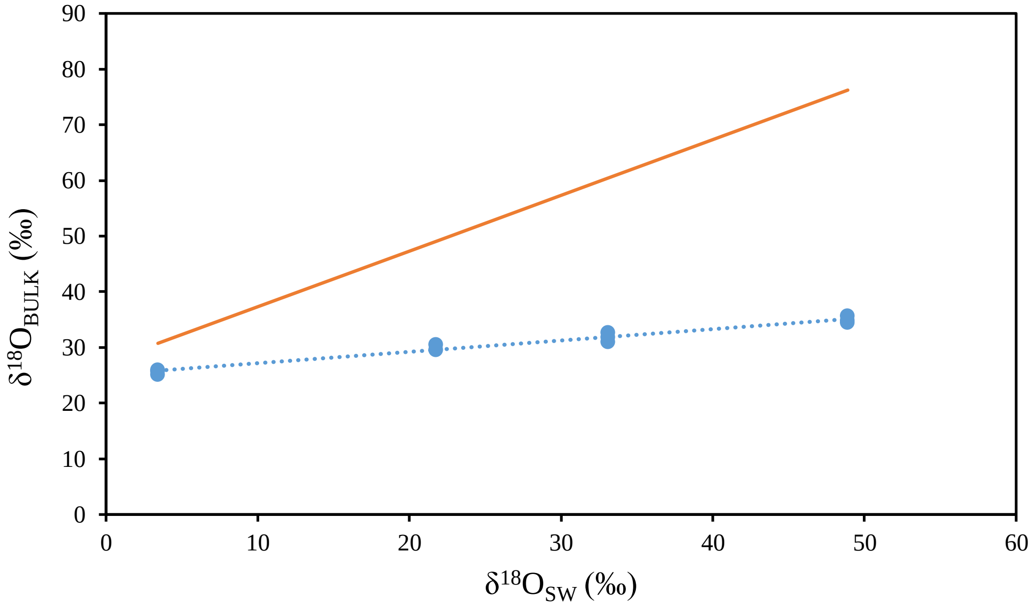

Figure 4.2. Relationship between $\delta^{18}O_{SW}$ and $\delta^{18}O_{BULK}$ of *S. cuspidatum*. The line of best fit is represented by the blue dotted line ($y = 0.1871\ x + 25.934$; $r^2 = 0.9707$). The orange line represents the theoretical relationship between $\delta^{18}O_{BULK}$ and $\delta^{18}O_{SW}$ if only $\delta^{18}O_{SW}$ determined $\delta^{18}O_{BULK}$ (Eqn. 3.2).

1.4 Discussion

The results from the $\delta^{18}O_{BULK}$ analyses presented in this study did not support the theoretical equation between $\delta^{18}O_{BULK}$ and $\delta^{18}O_{SW}$, indicating $\delta^{18}O_{SW}$ is not directly translated into $\delta^{18}O_{BULK}$ as previously assumed. Additionally, $\delta^{13}C_{BULK}$ presented in this study showed a surprisingly low value, much lower than that expected in natural systems.

It is well understood that *Sphagnum* cellulose $\delta^{18}O$ is controlled by source water, and offset by the biochemical fractionation constant (Xia *et al.*, 2020). However, the slope observed in this study was shallower than expected ($\delta^{18}O_{BULK} = 0.17\ \delta^{18}O_{SW} + 25.93$ ‰, Fig. 3.3), which does not support the theoretical relationship between the two variables (Sauer *et al.*, 2001; Zanazzi & Mora, 2005). The lower-than-expected slope and the little variation between $\delta^{18}O_{BULK}$ of the samples suggests other factors, such as evaporation and isotopic exchange, may influence $\delta^{18}O_{BULK}$ values. Field studies of $\delta^{18}O$ in *Sphagnum* tissues have often compared the $\delta^{18}O$ composition of hummock and hollow plants (Aravena & Warner, 1992; Ménot-Combes *et al.*, 2002; Xia *et al.*, 2020). The relationship between $\delta^{18}O$ plant tissue and $\delta^{18}O$ source water is almost one-to-one for hollow species, while the relationship for hummock species is slightly lower (Ménot-Combes *et al.*, 2002; Xia *et al.*, 2020). The experimental design of this study likely represented hummock species as the mosses were fed water from the surface and were not completely submerged. Ménot-Combes et al. (2002) observed higher evaporation rates in hummocks than hollows, which led to lower $\delta^{18}O$ values in the plant tissue. The evaporative rates depend on the vapour pressure of the water in air, the shape of the water-air boundary, and temperature of water (Horita *et al.*, 2008).

The evaporative effect partially explains the results observed in this experiment. As the slope of this relationship was much lower than expected, isotopic exchange between atmospheric air and evaporative water vapour may be influencing the actual isotopic ratio fixed in plant cellulose. The $\delta^{18}O_{BULK}$ of this experiment increased slightly with every 1‰ change in $\delta^{18}O_{SW}$ – so much so that $\delta^{18}O_{BULK}$ appeared almost constant regardless of $\delta^{18}O_{SW}$. During the initial evaporation of source water where environmental conditions (temperature, relative humidity, and turbulence) are stable, the vaporized H_2O molecules form a layer of saturated vapour above a water surface and become isotopically equilibrated with the liquid water phase (Gonfiantini *et al.*, 2018). Some of the vapour in this 'layer' escapes via molecular or turbulent diffusion and mixes with the atmosphere.

In a still environment, the vapour in the free atmosphere re-equilibrates with the liquid-vapour interface. Thus, even though initial $\delta^{18}O_{SW}$ was different, the growing chamber conditions may have ultimately approached similar $\delta^{18}O$ values (Gonfiantini *et al.*, 2018). The evaporated water was likely condensing on the surface of the moss when the temperature dropped at night, creating a thin water film with a different isotopic signature than the source water. It is therefore the isotopic composition of this water film that is likely influencing $\delta^{18}O_{BULK}$. The results highlight the complexity of $\delta^{18}O_{BULK}$ and $\delta^{18}O_{SW}$ as there is not a direct transfer of oxygen isotopes in a humid and still environment. Future studies should explore the isotopic composition of the water film on moss tissues.

Although temperature in the growing chambers was not measured in this experiment, temperature was assumed to be relatively constant as the growing chambers were set up inside an air-conditioned office. Because the oxygen isotope biochemical fractionation between water and organic molecules is not very sensitive to temperatures above 5°C, and temperatures within the office would have remained between 18 and 25°C, it is assumed there were no temperature effects on the isotopic composition of plant tissues. In natural systems, temperature and air flow are known to influence changes in relative humidity (Nichols & Brown, 1980). The growing chambers were sealed from the environment, with no turbulent air flow through the chambers. This would increase the relative humidity and reduce the boundary layer diffusivity.

$\delta^{13}C_{BULK}$ of the growing tips were very similar for 3.3, 31.1, and 48.9‰ $\delta^{18}O_{SW}$ treatment groups (-41 to -42‰). However, $\delta^{13}C_{BULK}$ of the growing tips in the container where half of the biomass was not photosynthesizing had particularly low $\delta^{13}C_{BULK}$ values (growing chamber treated with 21.7‰ $\delta^{18}O_{SW}$).

$\delta^{13}C_{BULK}$ of plant tissue varies depending on the degree of diffusional resistance during CO_2 uptake, and the $\delta^{13}C$ of the source CO_2 (Proctor *et al.*, 1992). The capitula of *S. cuspidatum* in this experiment were more depleted in ^{13}C than that expected in natural systems (Proctor *et al.*, 1992; Bramley-Alves *et al.*, 2016; Royles *et al.*, 2016; Turetsky & Wieder, 2016). As the mosses in this experiment were misted regularly, a thin film of water was always present on the moss surface. A field observation conducted by Bramley-Alves et al. (2016) observed non-significant differences in $\delta^{13}C_{BULK}$ between wet and dry environments in Antarctica. Although the results are more depleted in ^{13}C, it is unlikely the differences observed between natural and laboratory experiments are caused by diffusional resistance to CO_2 uptake, because the difference of 3‰ is too large.

The other factor that influences $\delta^{13}C_{BULK}$ is the carbon isotope ratio of source CO_2 (Proctor *et al.*, 1992). Natural $\delta^{13}C$ values of atmospheric CO_2 in New Zealand are approximately -8‰ (Longinelli *et al.*, 2012). The $\delta^{13}C$ of the air in each growing container was found to be more depleted than atmospheric CO_2 sampled outside the building, even after just one week of being sealed from the environment. The CO_2 released during respiration is typically slightly more enriched than $\delta^{13}C$ within the plant (Ghashghaie & Badeck, 2014), but significantly depleted compared to the atmosphere. Radioactively labelled CO_2 ($^{14}CO_2$) has been applied in previous *Sphagnum* growing experiments to understand refixation of respired CO_2 (Turetsky & Wieder, 2016). Turetsky and Wieder (2016) demonstrated that $^{14}CO_2$ was more prevalent in the growing tips than in sections 2+ cm from the surface. Therefore, it is likely that the depletion in $\delta^{13}C$ observed in this experiment was caused by the depleted source CO_2 from respiration, rather than CO_2 uptake diffusion resistance. In support of this idea, approximately 20% of CO_2 respired from deep peat is estimated to be refixed into living tissues (Tolonen *et al.*, 1992).

A field study by Proctor et al (1992) observed that the $\delta^{13}C_{BULK}$ of *S. cuspidatum* was more depleted than the other *Sphagnum* species in their study. The morphology of *S. cuspidatum* are characterized by having small capitula, sparse open branching and large low density leaves (Proctor *et al.*, 1992). These characteristics are likely to cause a low boundary layer resistance and lead to respired CO_2 being fixed.

Interestingly, the $\delta^{13}C_{BULK}$ values for the *Sphagnum* treated with 21.7‰ was more depleted than the other samples. Half of the *Sphagnum* in this growing container experienced more exposure to direct sunlight during summer 2022, as it was not kept shaded like the other growing containers. In general, mosses are saturated at relatively low light, often <500 μmol m^{-2} s^{-1} (Proctor & Smirnoff, 2011). When irradiance exceeds saturation, mosses deploy photoprotective mechanisms to prevent absorption and damage from excess radiation (Lovelock *et al.*, 1995; Robinson & Waterman, 2014). However, light levels were not measured in this experiment.

Although *Sphagnum* can recover within a few days of desiccation and photoinhibition, the moss in this container did not recover during this study. The respiration of growing and dead moss material in this growing chamber was likely to be higher than the others, therefore more respired CO_2 was refixed in new tissues (Tuittila *et al.*, 2004). Therefore, the difference in $\delta^{13}C_{BULK}$ in the capitula of *S. cuspidatum* treated with 21.7‰ $\delta^{18}O_{SW}$ compared to the others likely reflects proportionally higher carbon refixation from respiring dormant *Sphagnum*.

The results presented in this study were different to those observed in natural systems, highlighting the sensitivity of $\delta^{13}C$ and $\delta^{18}O$ in moss to environmental conditions. $\delta^{18}O_{BULK}$ values recorded in this experiment reflected the isotopic equilibrium exchange between the water vapour inside the growth chamber and atmospheric vapour, which is not expected in natural systems. These results suggest a consideration of boundary layer thickness and atmospheric mixing in field sites as isotopic effects during these processes may influence what is fixed in plant organic materials. The results also highlight the importance of considering CO_2 refixation when applying $\delta^{13}C$ as a tool in past climate reconstruction. Currently, $\delta^{13}C_{BULK}$ analysis focuses only on water availability and atmospheric CO_2 concentrations. Failure to acknowledge the effects of respired CO_2 refixation may lead to incorrect interpretations in long-term reconstructions, especially as the climatic temperatures and irradiance in polar regions are continually increasing. To understand the natural $\delta^{13}C$ and $\delta^{18}O$ compositions of moss tissues, future laboratory studies should include turbulent air flow through the growing chambers to imitate natural systems.

Chapter 5
Conclusion and future directions

The analyses of stable isotope composition in plant organic matter has emerged as a powerful tool in plant science and plant ecophysiological studies. The primary aim of this thesis was to investigate the use of stable oxygen isotopes as indicators of past abiotic conditions. This project included the first study in understanding the stable oxygen isoflux during transpiration from a poikilohydric and endohydric moss species, as a progress toward a mechanistic understanding of water isotope fractionation processes in mosses. These experiments highlighted the broad uses of stable isotopes and the possibilities left to explore.

The thesis here offered: a novel approach to model the past oxygen isotopic composition of precipitation ($\delta^{18}O_{PRECIP}$) , by analysing fluctuations in the oxygen isotope composition of *Dawsonia superba* (Polytrichaceae) stems (Chapter 3), a laboratory investigation of how the oxygen isotope composition of source water ($\delta^{18}O_{SW}$) is translated into the oxygen isotope composition of bulk *Sphagnum cuspidatum* (Sphagnaceae) tissue ($\delta^{18}O_{BULK}$) (Chapter 4), and to date, the first investigation into the isotopic composition of transpired water in *D. superba* (Chapter 2).

5.1 Moss $\delta^{18}O$ as a proxy for past water environments

The most studied stable isotopes in paleoclimate reconstruction from mosses are carbon isotopes (Price *et al.*, 1997; Royles *et al.*, 2012b; Royles *et al.*, 2014). The advantage of studying carbon isotopes is that they provide an indication of the balance between carbon supply and demand, or water-use efficiency over time (Dawson *et al.*, 2002). However, stable carbon isotopes alone do not tell us whether variation is due to changes in carbon supply (diffusional conductance) or demand (photosynthetic rates) when the plant was photosynthetically active. Oxygen isotopes may provide complementary information on environmental and physiological variation, but to take full advantage of a dual-isotope approach, it is necessary to understand the complex interactions among the factors that influence plant oxygen isotope composition.

Chapters 3 and 4 offers an investigation into $\delta^{18}O_{BULK}$ in relation to $\delta^{18}O_{SW}$, in both field (Chapter 3) and laboratory (Chapter 4) conditions. In chapter 3, there was a clear correlation between predicted $\delta^{18}O_{PRECIP}$ and measured $\delta^{18}O_{BULK}$ in *D. superba*, with an offset of about 33‰, close to that predicted by biochemical equilibrium fractionation (De Niro & Epstein, 1979; Sternberg *et al.*, 1986). The findings from Chapter 3 provide evidence for *D. superba* as a proxy for past climatic conditions, because the variations of $\delta^{18}O_{PRECIP}$ relates to temperature. However, the relationship between $\delta^{18}O_{SW}$ and *S. cuspidatum* $\delta^{18}O_{BULK}$ was not that obvious (Chapter 4). The result I was expecting from this experiment was a linear relationship with a slope of one between the oxygen isotope composition of plant tissue and source water, offset by the biochemical fractionation constant – the same relationship from Chapter 3. Instead, the relationship observed had a slope of 0.17, and the offset between $\delta^{18}O_{SW}$ and $\delta^{18}O_{BULK}$ varied from 25.1‰ (when grown at 3.4‰ $\delta^{18}O_{SW}$) to 34.4‰ (when grown at 48.9‰ $\delta^{18}O_{SW}$). This slope suggests a degree of equilibrium exchange between atmospheric and evaporated $\delta^{18}O$ within the closed and sealed growing containers, which was reflected in $\delta^{18}O$ of bulk tissue. Under field conditions, water vapour is usually close to equilibrium with the water film over the moss surface. Therefore, changes in the isotopic composition of the water source are also reflected in the vapour. The results from chapter 4 however, the water vapour would be a combination of equilibrium with source water, and vapour in the surrounding air. Consequently, the isotopic composition of *S. cuspidatum* tissue may reflect both source water and the equilibrated growth chamber-atmosphere water vapour. To date, there are no laboratory experiments investigating the relationship between $\delta^{18}O$ of source water and *Sphagnum* organic matter (Chapter 4). Although the results of this chapter are not in line with the field observations, it did shed light of the changes that could be made in the experimental design, that would allow for a better representation of the isotopic processes that occurs during water liquid-vapour exchange.

5.2 First look into leaf water enrichment in Polytrichaceae

Polytrichaceae is undoubtedly a unique family of mosses, that holds many evolutionary innovations. Their anatomical and morphological structure stands out from other moss families as they are free standing, and can grow to extraordinary heights, for a moss. Their anatomy and morphology have been considered analogous to vascular plants. Therefore, it asks the question of where they functionally stand on the scale of complexity – with mosses and vascular plants being at polar ends of the scale.

As the variations in $\delta^{18}O$ plant tissue are influenced by both $\delta^{18}O_{SW}$ and the evaporative environment, it is appropriate to have an integrated approach by understanding both the mechanistic regulation of water loss and the environmental drivers (Barbour *et al.*, 2004). Leaf water enrichment is a process that is not often associated with mosses, as mosses generally lack mechanism to control water fluxes in and out of cells. However, recent studies (e.g. Proctor 2013; Brodribb et al. 2020) and the observation seen in Chapter 2 of some regulation against water loss as relative humidity decreased, suggests that the water relations of Polytrichaceae mosses are significantly different to other bryophytes.

Chapter 2 applied two different models to explain the changes in $\delta^{18}O$ transpired moss water vapour. The fundamental differences between Rayleigh's distillation theory and the Craig–Gordon model (C–G model) is that the C–G model includes an unlimited supply of water to the evaporating surface (the Rayleigh model is for a finite body of water), and that it considers the kinetic fractionation processes that occur as water vapour diffuses through air and leaf structures. It was appropriate to apply the C–G model to *D. superba* $\delta^{18}O_e$, an endohydric moss, and the Rayleigh model to the poikilohydric *P. aciculare*.

5.3 Limitations and future directions

This thesis has advanced our knowledge of leaf water isotope enrichment in mosses and identified the need for further work to deepen our understanding of mosses as a paleoclimate proxy.

The biggest cofounding limitation I identified was in the experimental design and the lack of true replicates in Chapter 4. If I were to do this again, I would ensure the samples were true replicates. To do this, I would have separate growing chambers and take one sample from each chamber. This would allow me to average the values of each growing chamber and investigate how $\delta^{18}O$ of source water and is reflected in moss bulk tissue. Secondly, I would include a source of turbulent air flow in each growth chamber. This would ensure environment inside the chambers are well-mixed to minimize any artifacts that may influence the results. If these two changes were made, I would be able to closely examine if $\delta^{18}O_{BULK}$ is offset by the expected 27±3‰, or if there are other fractionation processes undocumented.

I was able to show a correlation between the predicted oxygen isotope composition of precipitation and *D. superba* bulk tissue (Chapter 3), but from a single site. Future work should sample from different sites around the country to determine if these results are applicable more broadly. If the results are replicable at other sites around New Zealand, a national trend in precipitation could be presented in *D. superba* stems. As $\delta^{18}O$ of precipitation are predicted to become progressively more isotopically depleted in higher latitudes (Dansgaard, 1964), future studies would offer a sensitive microclimatic marker of the subtle changes in $\delta^{18}O$ with respect to latitude and temperature.

And finally, Chapter 2 invites future research to investigate the Péclet effect in Polytrichaceae. As previous studies have shown that the C–G model often overestimates the enrichment of leaf water (Ripullone *et al.*, 2008), incorporating the Péclet effect would allow for an accurate representation of the observed leaf water oxygen isotope composition. The Péclet effect is well documented for vascular plants (Barbour & Farquhar, 2003; Farquhar & Gan, 2003; Barbour *et al.*, 2004), therefore, I would recommend future research to measure the Péclet effect of vascular plants for a comparative analysis of how relevant the Péclet effect is to Polytrichaceae.

References

Aravena, R., & Warner, B. G. (1992). Oxygen-18 composition of *Sphagnum*, and microenvironmenal water relations. *The Bryologist, 95*(4), 445-448.

Atala, C. (2011). Water transport and gas exchange in the non-vascular plant *Dendroligotrichum dendroides* (Brid. ex Hewd.) Broth. (Polytrichacaeae). *Gayana Botany, 61*(1), 89-92.

Barbour, M. M., Fischer, R. A., Sayre, K. D., & Farquhar, G. (2000). Oxygen isotope ratio of leaf and grain material correlates with stomatal conductance and grain yield in irrigated wheat. *Australian Journal of Plant Physiology, 27*, 625-637.

Barbour, M. M., Walcroft, A. S., & Farquhar, G. D. (2002). Seasonal variation in $\delta^{13}C$ and $\delta^{18}O$ of cellulose from growth rings in *Pinus radiata*. *Plant, Cell and Environment, 25*(1483-1499).

Barbour, M. M., & Farquhar, G. D. (2003). Do pathways of water movement and leaf anatomical dimensions allow development of gradients in HO between veins and the sites of evaporation within leaves? *Plant, Cell and Environment, 27*, 107-121.

Barbour, M. M., Roden, J. S., Farquhar, G. D., & Ehleringer, J. R. (2004). Expressing leaf water and cellulose oxygen isotope ratios as enrichment above source water reveals evidence of a Peclet effect. *Oecologia, 138*(3), 426-35.

Barbour, M. M. (2007). Stable oxygen isotope composition of plant tissue: a review. *Functional Plant Biology, 34*(2), 83-94.

Bell, N., Kariyawasam, I., Flores, J., & HyvÖNen, J. (2021). The diversity of the Polytrichopsida—a review. *Bryophyte Diversity and Evolution, 43*(1).

Belmecheri, S., & Lavergne, A. (2020). Compiled records of atmospheric CO_2 concentrations and stable carbon isotopes to reconstruct climate and derive plant ecophysiological indices from tree rings. *Dendrochronologia, 63*.

Bengtsson, F., Granath, G., & Rydin, H. (2016). Photosynthesis, growth, and decay traits in *Sphagnum* - a multispecies comparison. *Ecology and Evolution, 6*(10), 3325-41.

Björck, S., Malmer, N., Hjort, C., Sandgren, P., Ingólfsson, Ó., Wallén, B., Smith, R. I. L., & Jónsson, B. L. (1991). Stratigraphic and paleoclimatic studies of a 5500-year-old moss bank on Elephant Island, Antarctica. *Arctic and Alpine Reaarch, 23*(4), 361-374.

Bottinga, Y., & Craig, H. (1969). Oxygen isotope fractionation between CO_2 and water, and the isotopic composition of marine atmospheric CO_2. *Earth and Planetary Science Letters, 5*, 285-295.

Bramley-Alves, J., Wanek, W., French, K., & Robinson, S. A. (2015). Moss $\delta^{13}C$: an accurate proxy for past water environments in polar regions. *Global Change Biology, 21*(6), 2454-64.

Bramley-Alves, J., Wanek, W., & Robinson, S. A. (2016). Moss $\delta^{13}C$: Implications for subantarctic palaeohydrological reconstructions. *Palaeogeography, Palaeoclimatology, Palaeoecology, 453*, 20-29.

Broadmeadow, M. S. J., Griffiths, H., Maxwell, C., & Borland, A. M. (1992). The carbon isotope ratio of plant organic material reflects temporal and spatial variations in CO_2 within tropical forest formations in Trinidad. *Oecologia, 89*, 435-441.

Brodribb, T. J., Feild, T. S., & Jordan, G. J. (2007). Leaf maximum photosynthetic rate and venation are linked by hydraulics. *Plant Physiology, 144*(4), 1890-8.

Brodribb, T. J., Carriqui, M., Delzon, S., McAdam, S. A. M., & Holbrook, N. M. (2020). Advanced vascular function discovered in a widespread moss. *Nature Plants, 6*(3), 273-279.

Budke, J. M., Bernard, E. C., Gray, D. J., Huttunen, S., Piechulla, B., & Trigiano, R. N. (2018). Introduction to the Special Issue on Bryophytes. *Critical Reviews in Plant Sciences, 37*(2-3), 102-112.

Buryová, B., & Shaw, A. J. (2013). Phenotypic plasticity in *Philonotis fontana* (Bryopsida: Bartramiaceae). *Journal of Bryology, 27*(1), 13-22.

Carriqui, M., Roig-Oliver, M., Brodribb, T. J., Coopman, R., Gill, W., Mark, K., Niinemets, U., Perera-Castro, A. V., Ribas-Carbo, M., Sack, L., Tosens, T., Waite, M., & Flexas, J. (2019). Anatomical constraints to nonstomatal diffusion conductance and photosynthesis in lycophytes and bryophytes. *New Phytologist, 222*(3), 1256-1270.

Cernusak, L. A., Ubierna, N., Winter, K., Holtum, J. A., Marshall, J. D., & Farquhar, G. D. (2013). Environmental and physiological determinants of carbon isotope discrimination in terrestrial plants. *New Phytologist, 200*(4), 950-65.

Cernusak, L. A., Barbour, M. M., Arndt, S. K., Cheesman, A. W., English, N. B., Feild, T. S., Helliker, B. R., Holloway-Phillips, M. M., Holtum, J. A., Kahmen, A., McInerney, F. A., Munksgaard, N. C., Simonin, K. A., Song, X., Stuart-Williams, H., West, J. B., & Farquhar, G. D. (2016). Stable isotopes in leaf water of terrestrial plants. *Plant, Cell and Environment, 39*(5), 1087-102.

Clayton-Greene, K. A., Collins, N. J., Green, T. G. A., & Proctor, M. C. (1985). Surface wax, structure and function in leaves of Polytrichaceae. *Journal of Bryology, 13*(4), 549-562.

Clymo, R. S., & Hayward, P. M. (1982). The Ecology of Sphagnum. In *Bryophyte Ecology* (pp. 229-289). Springer Netherlands. 10.1007/978-94-009-5891-3_8.

Corporation, M. (2018). *Microsoft Excel*. https://office.microsoft.com/excel.

Craig, H. (1954). Carbon 13 in plants and the relationships between carbon 13 and carbon 14 variations in nature. *The Journal of Geology, 62*(2), 115-149.

Craig, H., & Gordon, L. I. (1965). Dueterium and oxygen-18 variations in the ocean and the marine atmosphere. In E. Tongiorgi (Ed.), *Proceedings of a conference on stable isotopes in oceanographic studies and paleotemperatures.* (pp. 9-130): Laboratory of Geology and Nuclear Science.

Dansgaard, W. (1964). Stable isotopes in precipitation. *Tellus, 16*(4), 436-468.

Dar, S. S., Ghosh, P., Swaraj, A., & Kumar, A. (2020). Craig–Gordon model validation using stable isotope ratios in water vapor over the Southern Ocean. *Atmospheric Chemistry and Physics, 20*(19), 11435-11449.

Dawson, T. E., & Brooks, P. D. (2001). Fundamentals of stable isotope chemistry and measurement. In M. Unkovich, J. Pate, A. McNeil & D. J. Gibbs (Eds.), *Stable*

Isotope Techniques in the Study of Biological Processes and Functioning of Ecosystems (Vol. 40, Chapter 1, pp. 1-18). Dordrecht: Springer.

Dawson, T. E., Mambelli, S., Plamboeck, A. H., Templer, P. H., & Tu, K. P. (2002). Stable Isotopes in Plant Ecology. *Annual Review of Ecology and Systematics, 33*(1), 507-559.

De Niro, M. J., & Epstein, S. (1979). Relationship between the oxygen isotope ratios of terrestrial plant cellulose, carbon dioxide, and water. *Science, 204*(4388), 51-53.

Dilks, T. J. K., & Proctor, M. C. (1978). Photosynthesis, respiration and water content in Bryophytes. *New Phytologist*, *82*, 97-114.

Dilks, T. J. K., & Proctor, M. C. F. (2013). The pattern of recovery of bryophytes after desiccation. *Journal of Bryology, 8*(1), 97-115.

Ellehoj, M. D., Steen-Larsen, H. C., Johnsen, S. J., & Maden, M. B. (2013). Ice-vapor equilibrium fractionational factor of hydrogen and oxygen isotopes: Experimental investigations and implications for stable water isotope studies. *Rapid Communications in Mass Spectrometry, 27*, 2149-2158.

Epstein, S., Thompson, P., & Yapp, C. J. (1977). Oxygen and hydrogen isotopic ratios in plant cellulose. *Science, 198*(4323), 1209-1215.

Farquhar, G., O'Leary, M. H., & Berry, J. A. (1982). On the relationship between carbon isotope discrimination and the intercellular carbon dioxide concentration in leaves. *Australian Journal of Plant Physiology, 9*(121-137).

Farquhar, G., & Lloyd, J. (1993). Carbon and oxygen isotope effects in the exchange of carbon dioxide between terrestrial plants and the atmosphere. In J. R. Ehleringer, J. Hall & G. Farquhar (Eds.), *Stable Isotopes and Plant Carbon-Water Relations* (pp. 47-70). New York, US: Academic Press.

Farquhar, G., Lloyd, J., Taylor, J. A., Flanagan, L. B., Syvertseni, J. P., Hubick, K. T., Wong, S. C., & Ehleringer, J. R. (1993). Vegetation effects on the isotope composition of oxygen in atmospheric CO_2. *Nature, 363*, 439-443.

Farquhar, G. D., Ehleringer, J. R., & Hubick, K. T. (1989a). Carbon isotope discrimination and photosynthesis. *40*, 503-537.

Farquhar, G. D., Hubick, K. T., Condon, A. G., & Richards, R. A. (1989b). Carbon isotope fractionation and plant water-use efficiency. In P. W. Rundel, J. R. Ehleringer & K. A. Nagy (Eds.), *Stable Isotopes in Ecological Research* (pp. 21-46). New York, USA: Springer-Verlag.

Farquhar, G. D., & Gan, K. S. (2003). On the progressive enrichment of the oxygen isotopic composition of water along a leaf. *Plant, Cell and Environment, 26*, 1579-1597.

Farquhar, G. D., & Cernusak, L. A. (2005). On the isotopic composition of leaf water in the non-steady state. *Functional Plant Biology, 32*(4), 293-303.

Farquhar, G. D., Cernusak, L. A., & Barnes, B. (2007). Heavy water fractionation during transpiration. *Plant Physiology, 143*(1), 11-8.

Flanagan, L. B., Comstock, J. P., & Ehleringer, J. R. (1991). Comparison of modeled and observed environmental influences on the stable oxygen and hydrogren isotope composition of leaf water in *Phaseolus vulgaris* L. *Plant Physiology, 96*(2), 588-596.

Flanagan, L. B., & Ehleringer, J. R. (1991). Stable isotope composition of stem and leaf water: Applications to the study of plant water use. *Functional Ecology, 5*(2), 270-277.

Flanagan, L. B. (1993). Environmental and biological influences on the stable oxygen and hydrogen isotopic composition of leaf water. In J. R. Ehleringer, A. E. Hall & G. D. Farquhar (Eds.), *Stable Isotopes and Plant Carbon-Water Relations* (Chapter 6, pp. 71-88). London, UK: Academic Press Inc.

Frew, R., Van Hale, R., & Moore, T. (2011). *A stable isotope rainfall map for the protection of NZ's biological and environmental resources.* University of Otago, Otago, New Zealand. 1-33p.

Friedman, I. (1962). Water-Vapor exchange between a water droplet and its environment. *Journal of Geophysical Research, 67*(7), 2761-2766.

Frolking, S., Roulet, N. T., Moore, T. R., Richard, P. J. H., Lavoie, M., & Muller, S. D. (2001). Modeling Northern Peatland Decomposition and Peat Accumulation. *Ecosystems, 4*(5), 479-498.

Gat, J. R. (1996). Oxygen and hydrogen isotopes in the hydrological cycle. *Annual Review of Earth and Planetary Sciences, 24*, 225-262.

Gat, J. R. (2000). Atmospheric water balance - the isotopic perspective. *Hydrological Processes, 14*, 1357-1369.

Gat, J. R. (2005). Some classical concepts of isotope hydrology. In P. K. Aggarwal, J. R. Gat & K. F. O. Froechlich (Eds.), *Isotopes in the Water Cycle* (Chapter 10, pp. 127-137). Dordrecht, Netherlands.: Springer.

Ghashghaie, J., & Badeck, F. W. (2014). Opposite carbon isotope discrimination during dark respiration in leaves versus roots - a review. *New Phytologist, 201*(3), 751-769.

Gonfiantini, R., Wassenaar, L. I., Araguas-Araguas, L., & Aggarwal, P. K. (2018). A unified Craig-Gordon isotope model of stable hydrogen and oxygen isotope fractionation during fresh or saltwater evaporation. *Geochimica et Cosmochimica Acta, 235*, 224-236.

Good, S. P., Noone, D., & bowen, G. J. (2015). Hydrologic connectivity constrains partioning of global terrestrial water fluxes. *Science, 349*(6244), 175-177.

Granath, G., Rydin, H., Baltzer, J. L., Bengtsson, F., Boncek, N., Bragazza, L., Bu, Z.-J., Caporn, S. J. M., Dorrepaal, E., Galanina, O., Gałka, M., Ganeva, A., Gillikin, D. P., Goia, I., Goncharova, N., Hájek, M., Haraguchi, A., Harris, L. I., Humphreys, E., Jiroušek, M., Kajukało, K., Karofeld, E., Koronatova, N. G., Kosykh, N. P., Lamentowicz, M., Lapshina, E., Limpens, J., Linkosalmi, M., Ma, J.-Z., Mauritz, M., Munir, T. M., Natali, S. M., Natcheva, R., Noskova, M., Payne, R. J., Pilkington, K., Robinson, S., Robroek, B. J. M., Rochefort, L., Singer, D., Stenøien, H. K., Tuittila, E.-S., Vellak, K., Verheyden, A., Waddington, J. M., & Rice, S. K. (2018). Environmental and taxonomic controls of carbon and oxygen stable isotope composition in *Sphagnum* across broad climatic and geographic ranges. *Biogeosciences, 15*(16), 5189-5202.

Green, T. G. A., & Clayton-Greene, K. A. (1981). Studies on *Dawsonia superba* Grev. II. Growth rate. *Journal of Bryology, 11*(4), 723-731.

Green, T. G. A., Sancho, L. G., & Pintado, A. (2011). Ecophysiology of Desiccation/Rehydration Cycles in Mosses and Lichens. In *Plant Desiccation Tolerance* (Chapter Chapter 6, pp. 89-120). 10.1007/978-3-642-19106-0_6.

Greenwood, J. L., Stark, L. R., & Chiquoine, L. P. (2019). Effects of rate of drying, life history phase, and ecotype on the ability of the moss *Bryum Argenteum* to survive desiccation events and the influence on conservation and selection of material for restoration. *Frontiers in Ecology and Evolution, 7*, 1-13.

Hajek, T., & Beckett, R. P. (2008). Effect of water content components on desiccation and recovery in *Sphagnum* mosses. *Annuals of Botany, 101*(1), 165-73.

Harrison, C. J., & Morris, J. L. (2018). The origin and early evolution of vascular plant shoots and leaves. *Philosphoical Transactions of the Royal Society B Biological Sciences, 373*(1739).

Hedderson, T. A., & Longton, R. E. (1996). Life history variation in mosses: Water relations, size and phylogeny. *Okios, 77*(1), 31-43.

Helliker, B. R., & Ehleringer, J. R. (2002). Differential ^{18}O enrichment of leaf cellulose in C_3 *versus* C4 grass. *Functional Plant Biology, 29*, 435-442.

Hobson, Keith A. (2007). Stable Isotope Ecology. . *The Quarterly Review of Biology, 82*(3), 298-299.

Horita, J., & Wesolowski, D. J. (1994). Liquid-vapor fractionation of oxygen and hydrogen isotopes of water from the freezing to the critical temperature. *Geochimica et Cosmochimica Acta, 58*(16), 3425-3437.

Horita, J., Rozanski, K., & Cohen, S. (2008). Isotope effects in the evaporation of water: a status report of the Craig-Gordon model. *Isotopes in Environmental and Health Sciences*, *44*(1), 23-49.

Huttunen, S., Bell, N., & Hedenäs, L. (2018). The evolutionary diversity of mosses – Taxonomic heterogeneity and its ecological drivers. *Critical Reviews in Plant Sciences, 37*(2-3), 128-174.

Jassey, V. E. J., & Signarbieux, C. (2019). Effects of climate warming on *Sphagnum* photosynthesis in peatlands depend on peat moisture and species-specific anatomical traits. *Global Change Biology, 25*(11), 3859-3870.

Jouzel, J., & Merlivat, L. (1984). Deuterium and Oxygen 18 in precipitation: Modeling of the isotopic effects during snow formation. *Journal of Geophysical Research, 89*(7), 11749-11757.

Kaislahti Tillman, P., Holzkämper, S., Kuhry, P., Sannel, A. B. K., Loader, N. J., & Robertson, I. (2010). Stable carbon and oxygen isotopes in *Sphagnum fuscum* peat from subarctic Canada: Implications for palaeoclimate studies. *Chemical Geology, 270*(1-4), 216-226.

Kao, W. Y., Chiu, Y. S., & Chen, W. H. (2000). Vertical profiles of CO_2 concentration and $\delta^{13}C$ values in a subalpine forest of Taiwan. *Botanical Bulletin of Academia Sinica, 41*, 213-218.

Kendall, C., & Caldwell, E. A. (1998). Fundamentals of sotope geochemistry. In C. Kendall & J. J. McDonnell (Eds.), *Isotope Tracers in Catchment Hydrology* (Chapter 2, pp. 51-86). Amsterdam: Elsevier.

King, C. M. (2015). *The drama of conservation: the history of Pureora Forest, New Zealand*. (Vol. 1). Springer Cham.

Krupa, J. (1976). The interdependence between transpiration intensity and the anatomical structure of moss leaves. *Acta Societatis, 46*(1), 57-68.

Krupa, J. (1984). Anatomical structure of moss leaves and their photosynthetic activity. *Acta Societatis Botanicorum Poloniae, 53*(1), 43-51.

Lewis, L. R., Rozzi, R., Goffinet, B., & Maggs, C. (2014). Direct long-distance dispersal shapes a New World amphitropical disjunction in the dispersal-limited dung moss *Tetraplodon* (Bryopsida: Splachnaceae). *Journal of Biogeography, 41*(12), 2385-2395.

Ligrone, R., Vaughn, K. C., Renzaglia, K. S., Knox, J. P., & Duckett, J. G. (2022). Diversity in the distribution of polysaccharide and glycoprotein epitopes in the cell walls of bryophtyes: new evidence for the multiple evolution of water-conducting cells. *New Phytologist, 156*, 491-508.

Lloyd, J., & Farquhar, G. D. (1994). ^{13}C discrimination during CO_2 assimilation by the terrestrial biosphere. *Oecologia, 99*, 201-215.

Longinelli, A., Giglio, F., Langone, L., Moggio, L., Ori, C., Selmo, E., & Sgavetti, M. (2012). Atmospheric CO_2 concentrations and $\delta^{13}C$ values between New Zealand and Antarctica, 1998 to 2010: some puzzling results. *Tellus B: Chemical and Physical Meteorology, 64*(1), 1-11.

Longton, R. E. (1970). Growth and productivity of the moss *Polytrichum alpestre* Hoppe in Antarctic regions. In M. W. Holdgate (Ed.), *Antarctic Ecology* (Vol. 2, Chapter XII). London, England: Academic Press.

Loucos, K. E., Simonin, K. A., Song, X., & Barbour, M. M. (2015). Observed relationships between leaf $H_2^{18}O$ Péclet effective length and leaf hydraulic conductance reflect assumptions in Craig–Gordon model calculations. *Tree Physiology, 00*, 1-11.

Lovelock, C. E., Jackson, A. E., Melick, D. R., & Seppelt, R. D. (1995). Reversible photoinhibition in Antarctic moss during freezing and thawing. *Plant Physiology, 109*, 955-961.

Marschall, M., & Proctor, M. C. (2004). Are bryophytes shade plants? Photosynthetic light responses and proportions of chlorophyll a, chlorophyll b and total carotenoids. *Annuals of Botany, 94*(4), 593-603.

McCarroll, D., & Loader, N. J. (2004). Stable isotopes in tree rings. *Quaternary Science Reviews, 23*(7-8), 771-801.

McCarter, C. P. R., & Price, J. S. (2014). Ecohydrology of *Sphagnum* moss hummocks: mechanisms of capitula water supply and simulated effects of evaporation. *Ecohydrology, 7*(1), 33-44.

Ménot-Combes, G., Burns, S. J., & Leuenberger, M. (2002). Variations of $^{18}O/^{16}O$ in plants from temperate peat bogs (Switzerland): implications for paleoclimatic studies. *Earth and Planetary Science Letters, 202*, 419-434.

Meyer, M., Seibt, U., & Griffiths, H. (2008). To concentrate or ventilate? Carbon acquisition, isotope discrimination and physiological ecology of early land plant life forms. *Philosphoical Transactions of The Royal Society B Biological Sciences, 363*(1504), 2767-78.

Mishler, B. D. (2001). The biology of bryophytes: Bryophytes arent just small tracheophytes. *Americal Journal of Botany, 88*(11), 2129-2131.

Nichols, D. S., & Brown, J. M. (1980). Evaporation from a *Sphagnum* moss surface. *Journal of Hydrology, 48*(3-4), 289-302.

Noone, D. (2008). The influence of midlatitude and tropical overturning circulation on the isotopic composition of atmospheric water vapor and Antarctic precipitation. *Journal of Geophysical Research, 113*(D4).

O'Leary, M. H. (1981). Carbon isotope fractionation in plants. *Phytochemistry, 4*, 552-567.

O'Leary, M. H. (1988). Carbon isotopes in photosynthesis. *BioScience, 38*(5), 328-336.

O'Leary, M. H., Madhavan, S., & Paneth, P. (1992). Physical and chemical basis of carbon isotope fractionation in plants. *Plant, Cell and Environment, 15*, 1099-1104.

O'Leary, M. H. (1993). Biochemical basis of carbon isotope fractionation. In J. R. Ehleringer, J. Hall & G. Farquhar (Eds.), *Stable Isotopes and Plant Carbon-Water Relations* (Chapter 3, pp. 19-28). Academic Press.

Oke, T. A., Turetsky, M. R., Weston, D. J., & Shaw, J. A. (2020). Tradeoffs between phenotypic plasticity and local adaptation influence the ecophysiology of the moss, *Sphagnum magellanicum*. *Oecologia, 193*(4), 867-877.

Oliver, M. J., Velten, J., & Mishler, B. D. (2005). Desiccation tolerance in Bryophytes: A reflection of the primitive strategy for plant survival in dehydrating habitats. *Integrative and Comparative Biology, 45*, 788-799.

Park, R., & Epstein, S. (1960). Carbon isotope fractionation during photosynthesis. *21*, 110-126.

Perera-Castro, A. V., Waterman, M. J., Robinson, S. A., & Flexas, J. (2022). Limitations to photosynthesis in bryophytes: certainties and uncertainties regarding methodology. *Journal of Experimental Botany*.

Peterson, B. J., & Fry, B. (1987). Stable isotopes in ecosystem studies. *Annual Review of Ecology and Systematics, 18*, 293-320.

Porada, P., Weber, B., Elbert, W., Pöschl, U., & Kleidon, A. (2013). Estimating global carbon uptake by lichens and bryophytes with a process-based model. *Biogeosciences, 10*(11), 6989-7033.

Poussart, P. F., Evans, M. N., & Schrag, D. P. (2004). Resolving seasonality in tropical trees: multi-decade, high-resolution oxygen and carbon isotope records from Indonesia and Thailand. *Earth and Planetary Science Letters, 218*(3-4), 301-316.

Price, G. D., McKenzie, J. E., Pilcher, J. R., & Hoper, S. T. (1997). Carbon-isotope variation in *Sphagnum* from hummock-hollow complexes: implications for Holocene climate reconstruction. *The Holocene, 7*(2), 229-233.

Price, J. S., Edwards, T. W. D., Yi, Y., & Whittington, P. N. (2009). Physical and isotopic characterization of evaporation from *Sphagnum* moss. *Journal of Hydrology, 369*(1-2), 175-182.

Proctor, M. C. (1982). Physiological Ecology: Water relations, light and temperature responses, carbon balance. In A. J. E. Smith (Ed.), *Bryophyte Ecology* (Chapter 10, pp. 333-381). Dordrecht: Springer.

Proctor, M. C., Raven, J. A., & Rice, S. K. (1992). Stable carbon isotope discrimination measurements in *Sphagnum* and other bryophytes: physiological and ecological implications. *Journal of Bryology, 17*(2), 193-202.

Proctor, M. C. (1993). Water-relations parameters of some bryophytes evaluated by thermocouple psychrometry. *Journal of Bryology*, *21*(4), 263-270.

Proctor, M. C., Nagy, Z., Csintalan, Z., & Takács, Z. (1998). Water-content components in bryophytes: analysis of pressure-volume relationships. *Journal of Experimental Botany, 49*(328), 1845-1854.

Proctor, M. C. (2000). The bryophyte paradox tolerance of desiccation, evasion of drought. *Plant Ecology*, *151*, 41-49.

Proctor, M. C., & Pence, V. C. (2002). Vegetative tissues: Bryophytes, vascular resurrection plants and vegetative propagules. In M. Black & H. W. Pritchard (Eds.), *Desiccation and Survival in Plants* (Chapter 7, pp. 204-237). Wallingford: CABI Publishing.

Proctor, M. C., & Tuba, Z. (2002). Pokilohydry and homoihydry: antithesis or spectrum of possibilities? *New Phytologist, 156*, 327-349.

Proctor, M. C., Ligrone, R., & Duckett, J. G. (2007). Desiccation tolerance in the moss *Polytrichum formosum*: physiological and fine-structural changes during desiccation and recovery. *Annuals of Botany*, *99*(1), 75-93.

Proctor, M. C. (2010). Trait correlations in Bryophytes: Exploring an alternative world. *New Phytologist*, *185*(1), 1-3.

Proctor, M. C., & Smirnoff, N. (2011). Ecophysiology of photosynthesis in bryophytes: major roles for oxygen photoreduction and non-photochemical quenching? *Physiologia Plantarum, 141*(2), 130-40.

Proctor, M. C. (2013). Why do Polytrichaceae have lamellae? *Journal of Bryology, 27*(3), 221-229.

Rayleigh, L. (1905). LIX. On the distillation of binary mixtures. *The London, Edinburgh, and Dublin Philosophical Magazine and Journal of Science, 4*(23), 521-537.

Rebetez, M., Saurer, M., & Cherubini, P. (2003). To what extent can oxygen isotopes in tree rings and precipitation be used to reconstruct past atmospheric temperature? A case study. *Climatic Change, 61*, 237-248.

Reski, R. (1997). Development, genetics and molecular biology of mosses. *Botanica Acta, 111*, 1-15.

Rice, S. K., & Giles, L. (1996). The influence of water content and leaf anatomy on carbon isotope discrimination and photosynthesis in *Sphagnum*. *Plant, Cell and Environment, 19*(1), 118-124.

Rincon, E., & Grime, J. P. (1989). An analysis of seasonal patterns of Bryophyte growth in a natural habitat. *Journal of Ecology, 77*(2), 447-455.

Ripullone, F., Matsuo, N., Stuart-Williams, H., Wong, S. C., Borghetti, M., Tani, M., & Farquhar, G. (2008). Environmental effects on oxygen isotope enrichment of leaf water in cotton leaves. *Plant Physiology, 146*(2), 729-36.

Robinson, S. A., & Waterman, M. J. (2014). Sunsafe Bryophytes: Photoprotection from Excess and Damaging Solar Radiation. In *Photosynthesis in Bryophytes and Early Land Plants* (Chapter Chapter 7, pp. 113-130). 10.1007/978-94-007-6988-5_7.

Robinson, S. A., King, D. H., Bramley-Alves, J., Waterman, M. J., Ashcroft, M. B., Wasley, J., Turnbull, J. D., Miller, R. E., Ryan-Colton, E., Benny, T., Mullany, K., Clarke, L. J., Barry, L. A., & Hua, Q. (2018). Rapid change in East Antarctic terrestrial vegetation in response to regional drying. *Nature Climate Change, 8*(10), 879-884.

Royles, J., Ogée, J., Wingate, L., Hodgson, D. A., Convey, P., & Griffiths, H. (2012a). Carbon isotope evidence for recent climate - related enhancement of CO_2 assimilation and peat accumulation rates in Antarctica. *Global Change Biology, 18*(10), 3112-3124.

Royles, J., Ogee, J., Wingate, L., Hodgson, D. A., Convey, P., & Griffiths, H. (2012b). Carbon isotope evidence for recent climate-related enhancement of CO_2 assimilation and peat accumulation rates in Antarctica. *Global Change Biology, 18*(10), 3112-3124.

Royles, J., Ogee, J., Wingate, L., Hodgson, D. A., Convey, P., & Griffiths, H. (2013a). Temporal separation between CO_2 assimilation and growth? Experimental and theoretical evidence from the desiccation-tolerant moss Syntrichia ruralis. *New Phytologist, 197*(4), 1152-1160.

Royles, J., Sime, L. C., Hodgson, D. A., Convey, P., & Griffiths, H. (2013b). Differing source water inputs, moderated by evaporative enrichment, determine the contrasting $\delta^{18}O_{CELLULOSE}$ signals in maritime Antarctic moss peat banks. *Journal of Geophysical Research: Biogeosciences, 118*(1), 184-194.

Royles, J., Horwath, A. B., & Griffiths, H. (2014). Interpreting bryophyte stable carbon isotope composition: Plants as temporal and spatial climate recorders. *Geochemistry, Geophysics, Geosystems, 15*(4), 1462-1475.

Royles, J., & Griffiths, H. (2015). Invited review: climate change impacts in polar regions: lessons from Antarctic moss bank archives. *Global Change Biology, 21*(3), 1041-57.

Royles, J., Amesbury, M. J., Roland, T. P., Jones, G. D., Convey, P., Griffiths, H., Hodgson, D. A., & Charman, D. J. (2016). Moss stable isotopes (carbon-13, oxygen-18) and testate amoebae reflect environmental inputs and microclimate along a latitudinal gradient on the Antarctic Peninsula. *Oecologia, 181*(3), 931-45.

RStudio. (2020). *RStudio: Integrated Development for R*. http://www.rstudio.com/.

Sakurai, H., Yamamoto, M., Seki, O., Omori, T., & Sato, T. (2021). Cellulose oxygen isotopes of *Sphagnum* and vascular plants in a peat core reveal climate change in Northern Japan over the past 2,000 years. *Geochemistry, Geophysics, Geosystems, 22*(9), 1-16.

Sauer, P. E., Miller, G. H., & Overpeck, J. T. (2001). Oxygen isotope ratios of organic matter in arctic lakes as a paleoclimate proxy: field and laboratory investigations. *Journal of Paleolimnology, 25*, 43-64.

Saurer, M., Borella, S., & Leuenberger, M. (1997). $\delta^{18}O$ of tree rings of beech (*Fagus silvatica*) as a record of $\delta^{18}O$ of the growing season precipitation. *Tellus B: Chemical and Physical Meteorology, 49*(1), 80-92.

Scheidegger, Y., Saurer, M., Bahn, M., & Siegwolf, R. (2000). Linking stable oxygen and carbon isotopes with stomatal conductance and photosynthetic capacity: a conceptual model. *Oecologia, 125*(3), 350-357.

Scheirer, D. C. (1980). Differentiation of bryophyte conducting tissues: structure and histochemistry. *Bulletin of the Torrey Botanical Club, 107*(3), 298-307.

Schleser, G. H., & Jayasekera, R. (1985). $\delta^{13}C$-variations of leaves in forests as an indication of reassimilated CO_2 from the soil. *Oecologia, 65*, 536-545.

Schneider, C. A., Rasband, W. S., & Eliceiri, K. W. (2012). *NIH Image to ImageJ: 25 years of image analysis*.

Schneider, D. P., Steig, E. J., van Ommen, T. D., Dixon, D. A., Mayewski, P. A., Jones, J. M., & Bitz, C. M. (2006). Antarctic temperatures over the past two centuries from ice cores. *Geophysical Research Letters, 33*(16).

Schofield, W. B. (1981). Ecological significance of morphological characters in the moss gametophyte. *The Bryologist, 84*(2), 149-165.

Schubert, B. A., & Jahren, A. H. (2012). The effect of atmospheric CO_2 concentration on carbon isotope fractionation in C_3 land plants. *Geochimica et Cosmochimica Acta, 96*, 29-43.

Seel, W. E., Baker, N. R., & Lee, J. A. (1992). Analysis of the decrease in photosynthesis on desiccation of mosses from xeric to hydric environments. *Physiologia Plantarum, 86*, 451-458.

Shaw, A. J., Szovenyi, P., & Shaw, B. (2011). Bryophyte diversity and evolution: windows into the early evolution of land plants. *American Journal of Botany, 98*(3), 352-69.

Shaw, J. A., & Renzaglia, K. S. (2004). Phylogeny and diversification of bryophytes. *American Journal of Botany, 91*(10), 1557-1581.

Skrzypek, G., Kaluzny, A., & Jedrysek, M. O. (2007). Carbon stable isotope analyses of mosses-comparisons of bulk organic matter and extracted nitrocellulose. *Journal of the American Society for Mass Spectrometry, 18*(8), 1453-8.

Song, X., Barbour, M. M., Farquhar, G. D., Vann, D. R., & Helliker, B. R. (2013). Transpiration rate relates to within- and across-species variations in effective path length in a leaf water model of oxygen isotope enrichment. *Plant, Cell and Environment, 36*(7), 1338-51.

Stahle, D. W. (1999). Useful strategies for the development of tropical tree-ring chronologies. *IAWA Journal, 20*(3), 249-253.

Sternberg, L., De Niro, M. J., & Savidge, R. A. (1986). Oxygen isotope exchange between metabolites and water during biochemical reactions leading to cellulose synthesis. *Plant Physiologist, 82*, 423-427.

Sternberg, L. (1989). Oxygen and hydrogen isotope ratios in plant cellulose: Mechanisms and applications. In P. W. Rundel, J. R. Ehleringer & K. A. Nagy (Eds.), *Stable Isotopes in Ecological Research* (Vol. 68, Chapter 9, pp. 124-141). New York, NY: Springer.

Sternberg, L., Pinzon, M. C., Anderson, W. T., & Jahren, A. H. (2006). Variation in oxygen isotope fractionation during cellulose synthesis: intramolecular and biosynthetic effects. *Plant, Cell and Environment, 29*(10), 1881-9.

Sternberg, L. (2009). Oxygen stable isotope ratios of tree-ring cellulose: the next phase of understanding. *New Phytologist, 181*(3), 553-62.

Sternberg, L., & Ellsworth, P. F. (2011). Divergent biochemical fractionation, not convergent temperature, explains cellulose oxygen isotope enrichment across latitudes. *PLoS One, 6*(11), e28040.

Street-Perrott, F. A., Holmes, J. A., Robertson, I., Ficken, K. J., Koff, T., Loader, N. J., Marshall, J. D., & Martma, T. (2018). The Holocene isotopic record of aquatic cellulose from Lake Äntu Sinijärv, Estonia: Influence of changing climate and organic-matter sources. *Quaternary Science Reviews, 193*, 68-83.

Thielen, S. M., Gall, C., Ebner, M., Nebel, M., Scholten, T., & Seitz, S. (2021). Water's path from moss to soil: A multi-methodological study on water absorption and evaporation of soil-moss combinations. *Journal of Hydrology and Hydromechanics, 69*(4), 421-435.

Thomas, R. J., Ryder, S. H., Gardner, M. I., Sheetz, J. P., & Nichipor, S. D. (1996). Photosynthetic function of leaf lamellae in *Polytrichum commune*. *American Bryological and Lichenological Society, 99*(1), 6-11.

Tissue, D. T., Barbour, M. M., Hunt, J. E., Turnbull, M. H., Griffin, K. L., Walcroft, A. S., & D., W. (2006). Spatial and temporal scaling of intercellular CO_2 concentration in temperate rain forest dominated by *Dacrydium cupressinum* in New Zealand. *Plant, Cell and Environment, 29*(4), 497-510.

Tolonen, K., Possnert, G., Junger, H., Sonninen, E., & Alm, J. (1992). High resolution C dating of surface peat using the AMS technique. *Suo, 45*(4), 271-275.

Tuittila, E.-S., Vasander, H., & Laine, J. (2004). Sensitivity of C sequestration in reintroduced *Sphagnum* to water-level variation in a cutaway peatland. *Restoration Ecology, 12*, 483-493.

Turberville, C. M., Fuentes-González, J. A., Rogers, S., & Pienaar, J. (2021). Moss phyllid morphology varies systematically with substrate slope. *Plant Ecology and Evolution, 154*(3), 419-431.

Turetsky, M. R., & Wieder, R. K. (2016). Boreal bog *Sphagnum* refixes soil-produced and respired $^{14}CO_2$. *Écoscience, 6*(4), 587-591.

Valanne, N. (1984). Photosynthesis and photosynthetic products in mosses. In A. F. Dyer & J. G. Duckett (Eds.), *The Experimental Biology of Bryophytes* (Chapter 11, pp. 257-273). London: Academic Press.

Verma, S. B. (1996). Surface exchange of water vapour between an open sphagnum fen and atmopshere. *Boundary-layer Meterology, 79*, 243-264.

Vitt, D. H. (1981). Adaptive modes of the moss sporophyte. *The Bryologist, 84*(2), 166-186.

Vogel, J. C. (1980). *Fractionation of the carbon isotopes during photosynthesis*. Presented at the Sitzungsberichte der Heidelberger Akademie der Wissenschaften

Waite, M., & Sack, L. (2010). How does moss photosynthesis relate to leaf and canopy structure? Trait relationships for 10 Hawaiian species of contrasting light habitats. *New Phytologist, 185*(1), 156-72.

Wang, L., Good, S. P., Caylor, K. K., & Cernusak, L. A. (2012). Direct quantification of leaf transpiration isotopic composition. *Agricultural and Forest Meteorology, 154-155*, 127-135.

Wasley, J., Robinson, S. A., Lovelock, C. E., & Popp, M. (2006). Climate change manipulations show Antarctic flora is more strongly affected by elevated nutrients than water. *Global Change Biology, 12*(9), 1800-1812.

Watson, M. A. (1975). Annual periodicity of incremental growth in the moss *Polytrichum commune*. *The Bryologist, 78*(4), 414-422.

Wickham, H. (2016). *ggplot2: Elegant graphics for data analysis*.

Wigley, T. M. L., Jones, P. D., & Briffa, K. R. (1987). Cross-dating methods in dendrochronology. *Journal of Archaeological Science, 14*, 51-64.

Williams, T. G., & Flanagan, L. B. (1996). Effect of changes in water content of photosynthesis, transpiration and discrimination against $^{13}CO^{2}$ and $C^{18}O^{16}O$ in *Pleurozium* and *Sphagnum*. *Oecologia, 108,* 38-46.

Xia, Z., Zheng, Y., Stelling, J. M., Loisel, J., Huang, Y., & Yu, Z. (2020). Environmental controls on the carbon and water (H and O) isotopes in peatland *Sphagnum* mosses. *Geochimica et Cosmochimica Acta, 277*, 265-284.

Yakir, D., De Niro, M. J., & Rundel, P. W. (1989). Isotopic inhomogeneity of leaf water: Evidence and implications for the use of isotopic signals transduced by plants. *Geochemica et Cosmochimica Acta*, *53*, 2769-2773.

Ye, H., & Mather, J. R. (1997). Polar snow cover changes and global warming. *International Journal of Climatology, 17*, 155-162.

Yoshimura, K. (2003). A quantitative analysis of short-term ^{18}O variability with a Rayleigh-type isotope circulation model. *Journal of Geophysical Research, 108*(D20).

Zanazzi, A., & Mora, G. (2005). Paleoclimatic implications of the relationship between oxygen isotope ratios of moss cellulose and source water in wetlands of Lake Superior. *Chemical Geology, 222*(3-4), 281-291.

Appendix

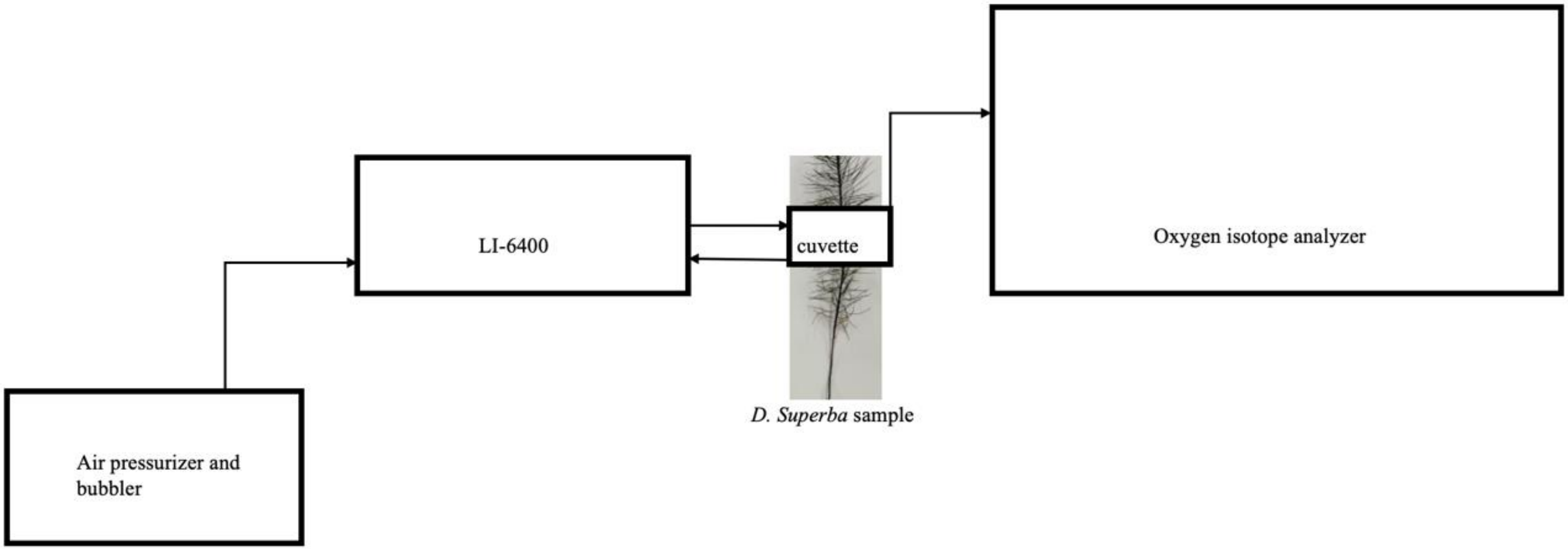

Figure A.1. Systematic diagram of the gas exchange and vapour oxygen isotope analysis for Chapter 2. The arrows represents the direction of air flow.

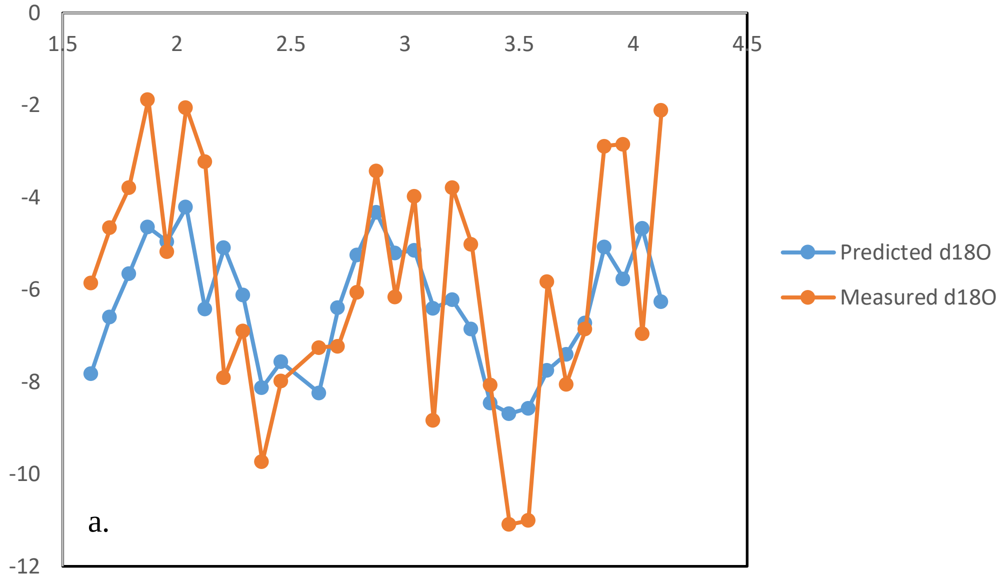
0
-2
-4
-6
-8
-10
-12
1.5
2
2.5
3
3.5
4
4.5
a.
Predicted d18O
Measured d18O

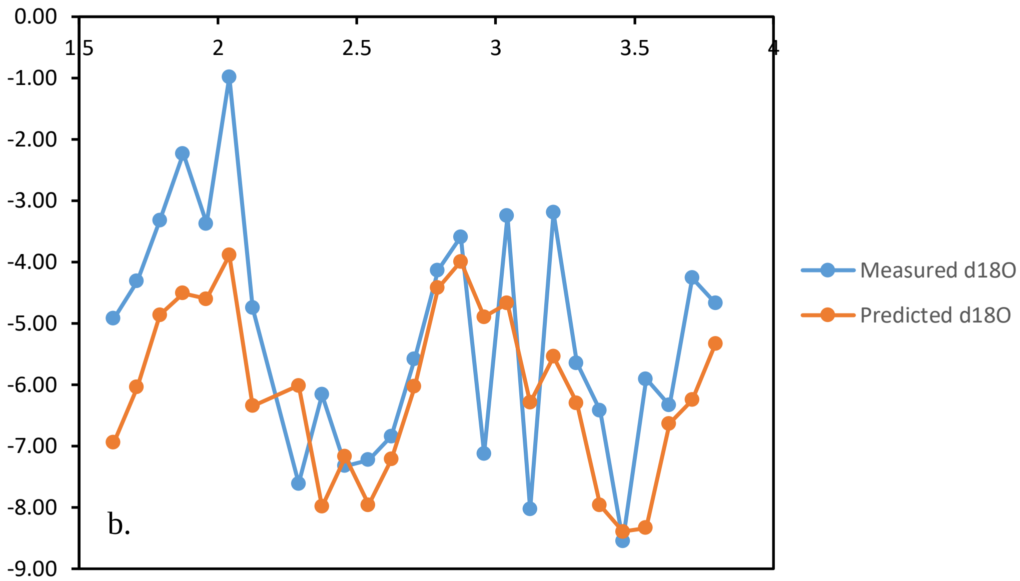
0.00
-1.00
-2.00
-3.00
-4.00
-5.00
-6.00
-7.00
-8.00
-9.00
1.5
2
2.5
3
3.5
4
b.
Measured d18O
Predicted d18O

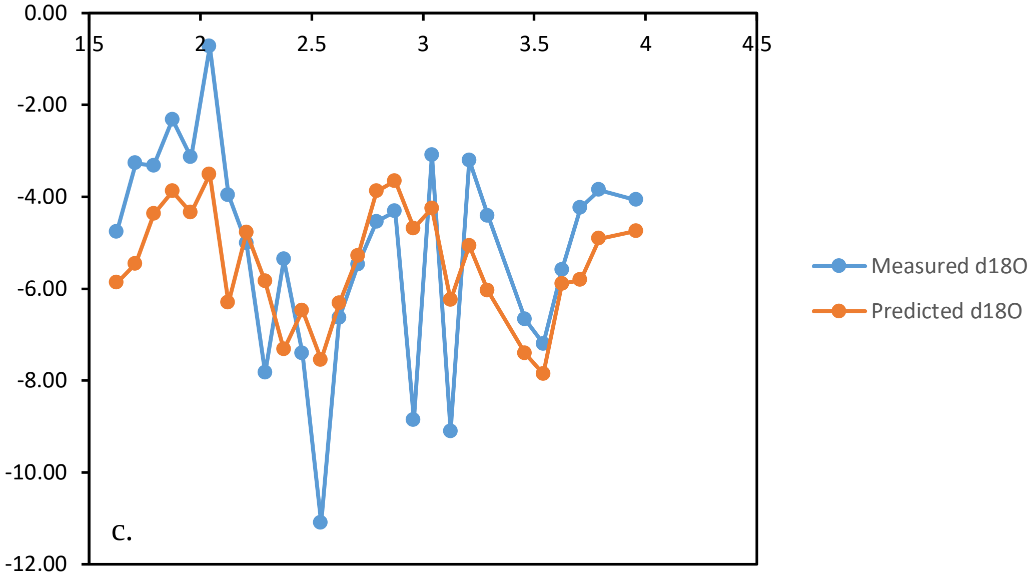
0.00
-2.00
-4.00
-6.00
-8.00
-10.00
-12.00
1.5
2
2.5
3
3.5
4
4.5
c.
Measured d18O
Predicted d18O

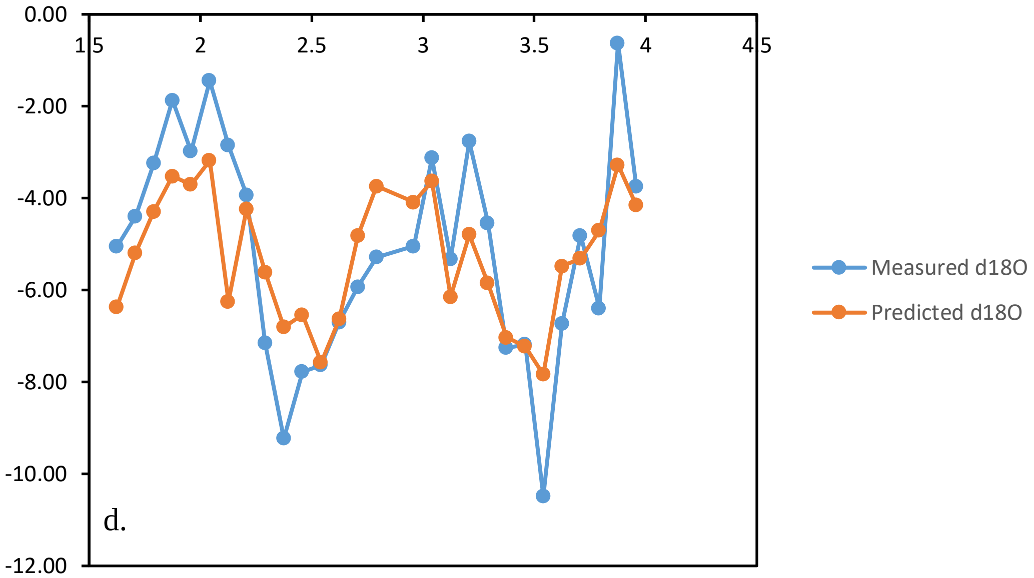
0.00
-2.00
-4.00
-6.00
-8.00
-10.00
-12.00
1.5
2
2.5
3
3.5
4
4.5
d.
Measured d18O
Predicted d18O

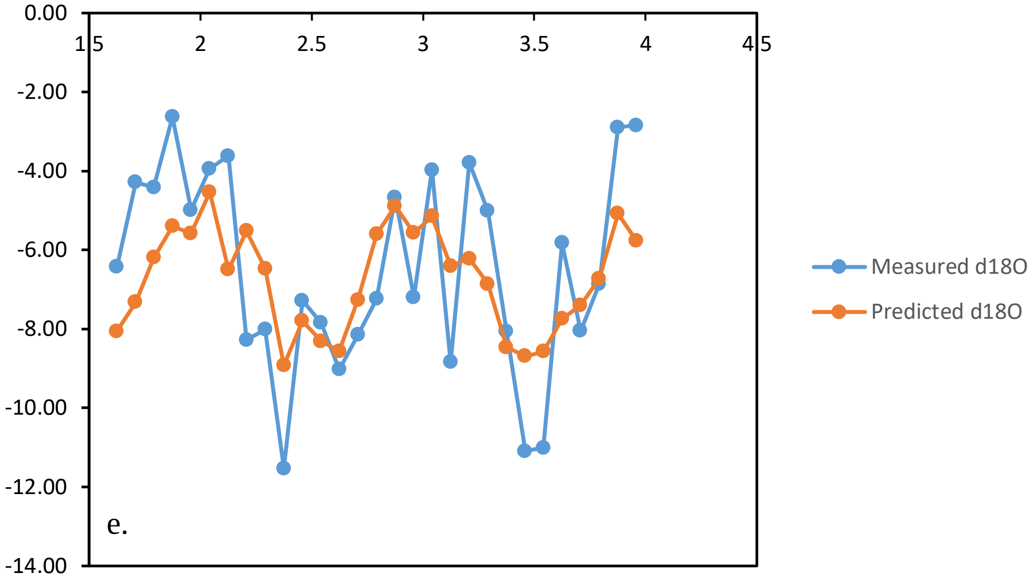

Figure A.2. Scatter graphs of the predicted and measured $\delta^{18}O$ of precipitation at a) Rotorua, b) Hamilton, c), Waikato, d), Tauranga, and e) Taupo. Predictions were made using the monthly equations from the simple linear model of measured $\delta^{18}O$ of precipitation and minimum temperature (°C).

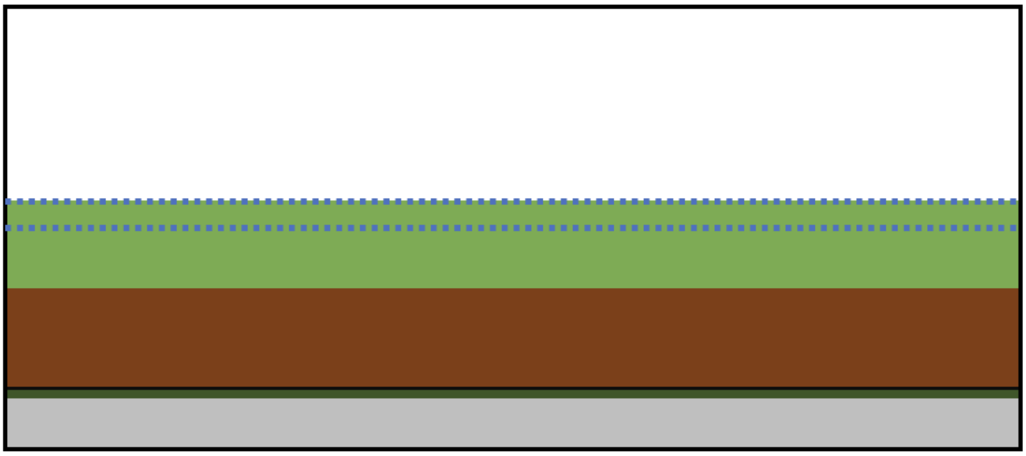

Figure A.3. Illustrative diagram of the growing medium in each growing container. The grey represents the coarse stones used as a drainage system with a sheet of shade cloth on top (dark green). On top of the shade cloth was a thin layer of activated charcoal to minimize algal growth (black line). Live Sphagnum (green) was placed on top of the potting mix with all growing tips towards the top of the container. Two pieces of bird netting (blue dotted line) was placed on top of the growing tip: one piece of the bird netting was used to hold the Sphagnum tips in place while another was placed just above the growing tips so new growth can be differentiated from old growth.

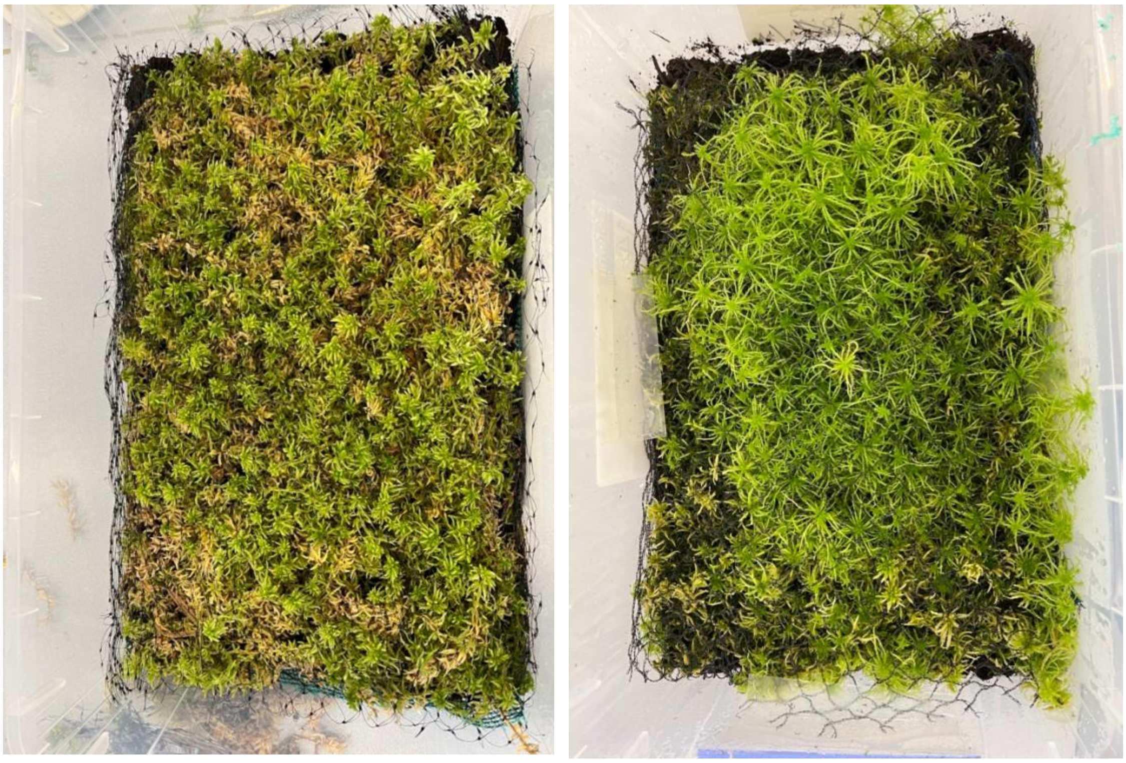

Figure A.4 i). Placement of *Sphagnum cuspidatum* in the growing container. *S. cuspidatum* rinsed with distilled water to remove any terrestrial debris. Stalks of *S. cuspidatum* were placed in containers as close to the neighbouring stalk without overlapping to imitate peat mats. ii). Growth of sphagnum after six months.

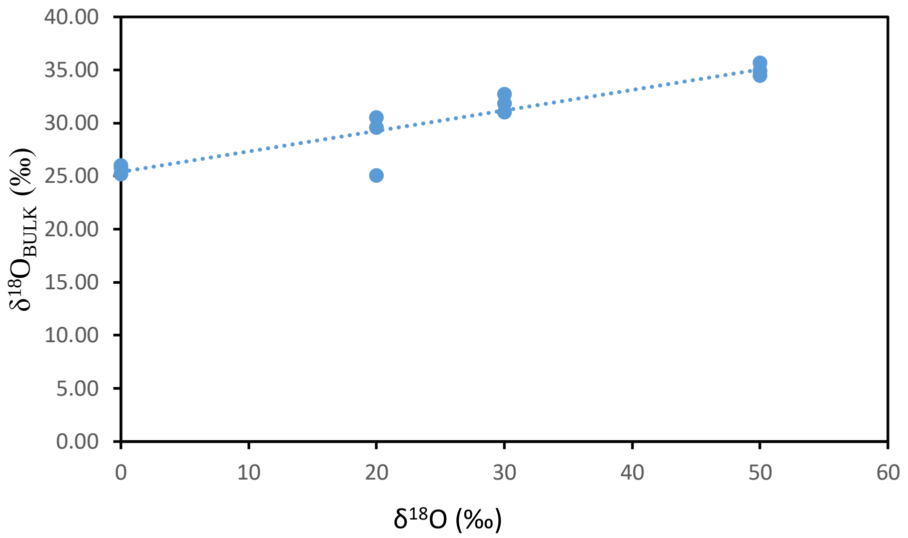

Figure A.5. Relationship between $\delta^{18}O_{BULK}$ and $\delta^{18}O_{SW}$ with all samples included. The blue dotted line represents the line of best fit ($\delta^{18}O_{BULK} = 0.1931\ \delta^{18}O_{SW} + 25.4$, $r^2 = 0.86$).

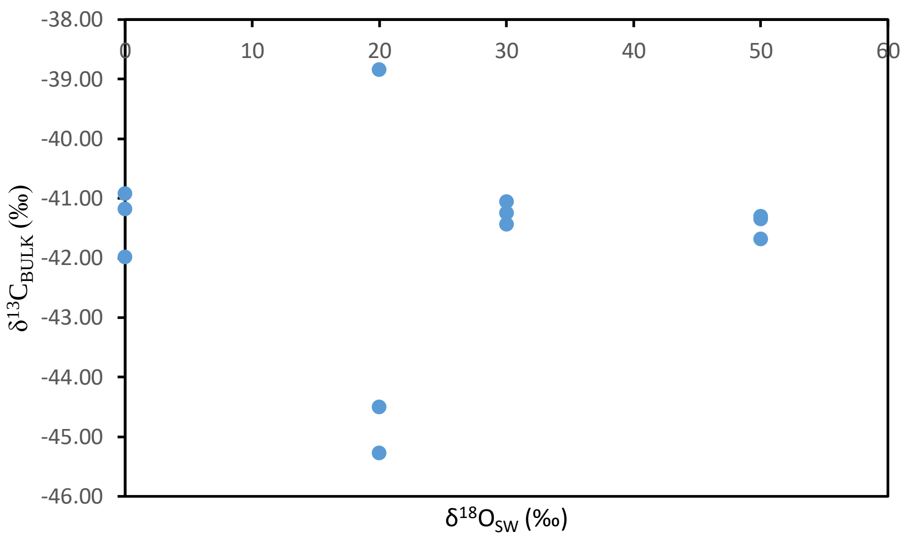

Figure A.6. Scatterplot graph of $\delta^{13}C_{BULK}$ against $\delta^{18}O_{SW}$ with all samples included.